A PHOTODYNAMIC CHARACTERIZATION OF

EXTRINSIC MEMBRANE PROBES

By

DADA SALIM NAJJAR

Bachelor of Science

Oklahoma State University

Stillwater, Oklahoma

1977

Submitted to the Faculty of the
Graduate College of the
Oklahoma State University
in partial fulfillment of
the requirements for
the Degree of
DOCTOR OF PHILOSOPHY
July, 1981

To My Parents

A PHOTODYNAMIC CHARACTERIZATION OF

EXTRINSIC MEMBRANE PROBES

Thesis Approved:

_____
Thesis Adviser

_____

_____

_____

_____
Dean of the Graduate College

ACKNOWLEDGMENTS

This work is the product of four intellectually stimulating years made possible by the intelligent guidance, inspirational dedication to research and cooperation of my competent adviser, Dr. Mark G. Rockley. Without his encourgement this work may not be in the present form. I wish to thank him, not only for his help and patience, but more importantly for his deep care and sincere friendship.

I gratefully acknowledge financial support from the National Institute of Health grant 1R01 GM25355. Appreciation is also expressed to the Oklahoma State University Chemistry Department for financial support in the form of a teaching assistant.

A special thanks is given to Dr. Paul J. Devlin for his help in obtaining Raman Spectra, and to Dr. Horacio A. Mottola for his advice on the critical aspects of the absorbance measurements. I extend my sincere gratitude to Dr. Olin Spivey for loaning, for a time above and beyond the call of duty, of a Hg lamp to start the Xe arc lamp. Thanks are also due to Dr. K Darrell Berlin for supplying some fluorescent probes.

I would like to express my appreciation for the technical help provided by Dr. Betty Hamilton. Special thanks are due to Mr. Heinz Hall and his staff for their

iii

TABLE OF CONTENTS

LIST OF TABLES

LIST OF FIGURES

x

CHAPTER I

FLUORESCENCE SPECTROSCOPY OF BIOLOGICAL
MEMBRANES

Introduction

Until now, many questions about membrane structure and biosynthesis remain unexplained despite the recent upsurge in membrane research. In order to understand the importance and function of membrane phenomena (e.g. diffusion, transport, protection, cell communication, cell recognition etc.), it is necessary to investigate the structure of the membrane and its relation to these functions.

In many studies, artificial membranes are substituted for natural membranes, to partially mimic the real systems and similtaneously to reduce the complexity of such studies.

Membrane Structure

Some years after the discovery and identification of the cell by Robert Hooke in 1665, came the work of Carl Nageli in 1855 who examined the cell boundary, to which the name plasma membrane was given. Later work, carried out by Wilhelm Pfeffer in 1897 and Charles Overton in 1899, laid the foundation for the idea of a lipid membrane surrounding the cell. They discovered that the cell membrane controlled

the rate of entry of substances into the cell. A suggestion by Gorter and Grendel in 1925 that the lipid is in the form of a bilayer was the basis of today's accepted model of membrane structure proposed by Danielli and Davson (1). They postulated that the lipid core of the membrane was sandwiched between two layers of protein. In the early 1960's, following the development of electron microscopy, Robertson promoted the concept of a universal unit membrane based on the Davson-Danielli model. Hence, an asymmetric distribution of protein about the lipid core was suggested by the Davson-Danielli-Robertson model which was supported by both electron microscopic and x-ray diffraction evidence.

In order to account for the facilitated diffusion and active transport across the membrane, Danielli included "pores" or active patches lined with the unrolled protein in the previous model. However, the Danielli-Davson-Robertson model was not satisfactory on thermodynamic grounds, since the continuous unfolded layer of protein would have nonpolar residues exposed to water and would be covering the hydrophobic heads of the lipid molecules. With these facts, and other experimental evidence in hand, Wallach and Singer independently postulated a different model of the protein-lipid structure. This model, the "mosaic" model of membrane structure, involved globular proteins embedded in, and even spanning the lipid bilayer (2). The polar groups of both lipids and proteins would be in direct contact with the aqueous surroundings, while the non-polar regions would

be embedded in the heart of the membrane.

A refinement of the mosaic model led Singer and Nicolson in 1972 to propose what is now widely accepted as best explaining the observed data collected about membranes. The Fluid Mosaic Model (Figure 1) involves globular proteins resembling "icebergs" floating in a sea of lipid bilayer. Added to this are the extrinsic globular proteins, external to the body of the membrane which interact electrostatically with the polar head groups of the lipid bilayer.   This is reasonable since the hydrocarbon chains are highly mobile at physiological temperatures.

However, the current picture of the biological membrane, based on the Fluid Mosaic Model is incomplete. Many observations about membrane structure and biosynthesis are still unexplained.   For instance, the roles played by water and inorganic cations have not been accounted for yet, although the removal of either can cause membrane disruption (3, 4).   The reason for the unequal distribution of phospholipids in the membrane remains to be specified (5). Another important question involving the exact basis for transport mechanism achieved by the intrinsic membrane proteins is still to be unravelled (6, 7).   Finally an important question arises, as to how well a membrane is biosynthesized for both growing and non-growing cells (6).

A major function of the membrane is that of protection, insuring the maintenance of a constant internal environment within the cell.   While the membrane is protecting the cell,

it must allow for selective communication with the exterior. It acts, therefore, as a selective permeable boundary, allowing the passage of water and certain nutrients while preventing the passage of other chemicals. Hence, selective movement across the membrane may be dependent only on concentration gradients (passive transport) or may require an energy supply (active transport). Some other functions include compartmentalization, cell fusion, communication, cell recognition as well as control of the membrane-bound enzyme activities. Hence, the cell membrane provides an identity to its cell.
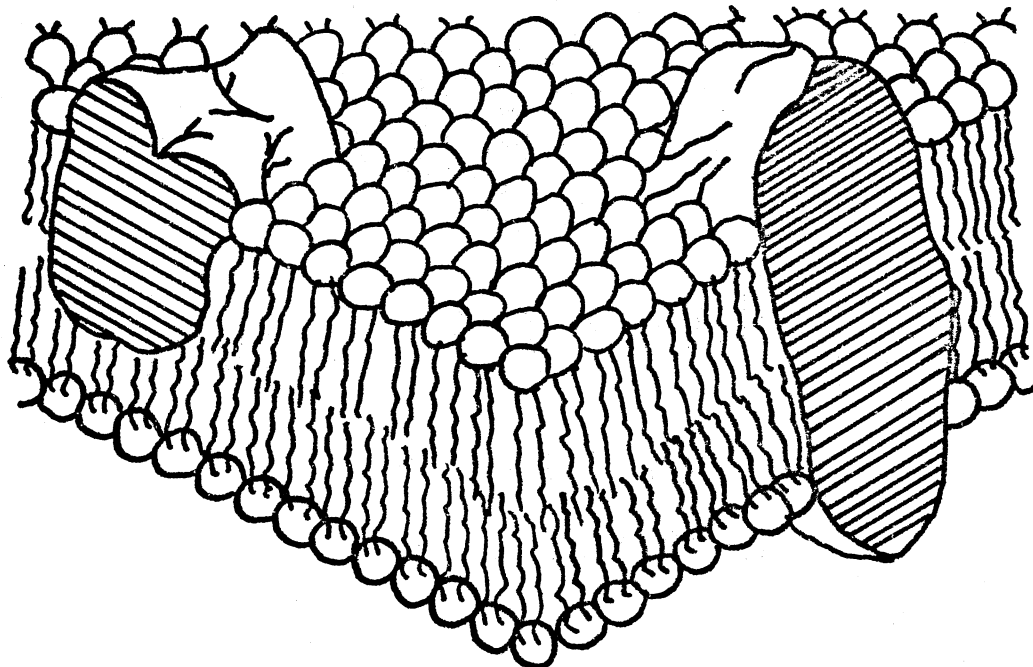
Figure 1. Fluid Mosaic Model

Although the membrane composition varies with the source, it generally consists of approximately 40% by dry weight as lipids and 60% as proteins. In addition, membranes contain about 20% of their weight as water, which is essential to the maintenance of their structure (7). The interaction of such components defines the important role played by the membrane. For example, although proteins are essential in a membrane, their functions are dependent on the properties of the particular phospholipid bilayer. Typically there are more than 30 phospholipid molecules present for every protein molecule. Therefore, it is not surprising that most models of biological membranes are based on the presence of a lipid bilayer. A comprehensive discussion of the properties of the lipid bilayer is therefore necessary for a complete picture of membrane structure and function.

The Phospholipid Bilayer

The physical properties of a bilayer are dependent on its lipid components and their interactions. Biological membranes contain mixtures of these lipids in different proportions (Table I). Phospholipids (phosphoglycerides) which are amphipathic lipids constitute the major components of cell membranes. These possess polar heads in addition to the non-polar hydrocarbon tails (Figure 2). Phosholipids differ in size, shape and electric charge depending on their polar head groups (Table II).

TABLE I

PERCENTAGE LIPID COMPOSITION OF ANIMAL AND BACTERIAL MEMBRANES (8)

	Myelin	Erythro-cyte	Mito-chondria	Micro-some	Azoto-bacter agilis	Escheri-chia coli*
Cholesterol	25	25	5	6	0	0
Phosphatidylethanolamine	14	20	28	17	100	100
Phosphatidylserine	7	11	0	0	0	0
Phosphatidylcholine	11	23	48	64	0	0
Phosphatidylinositol	0	2	8	11	0	0
Phosphatidylglycerol	0	0	1	2	0	0
Cardiolipin	0	0	11	0	0	0
Sphingomyelin	6	18	0	0	0	0
Cerebroside	21	0	0	0	0	0
Cerebroside sulphate	4	0	0	0	0	0
Ceramide	1	0	0	0	0	0
Lysylphosphatidylglycerol	0	0	0	0	0	0
Unknown or other	12	2	0	0	0	0

*Approximate values, ignore minor components.

TABLE II

POLAR HEAD GROUPS OF THE PHOSPHOLIPIDS

Phosphatidylethanolamine   Phosphatidylcholine   Phosphatidylserine   Phosphatidylinositol

Phosphatidylglycerol   3'-O-Lysylphosphatidylglycerol   Cardiolipin (diphosphatidylglycerol)
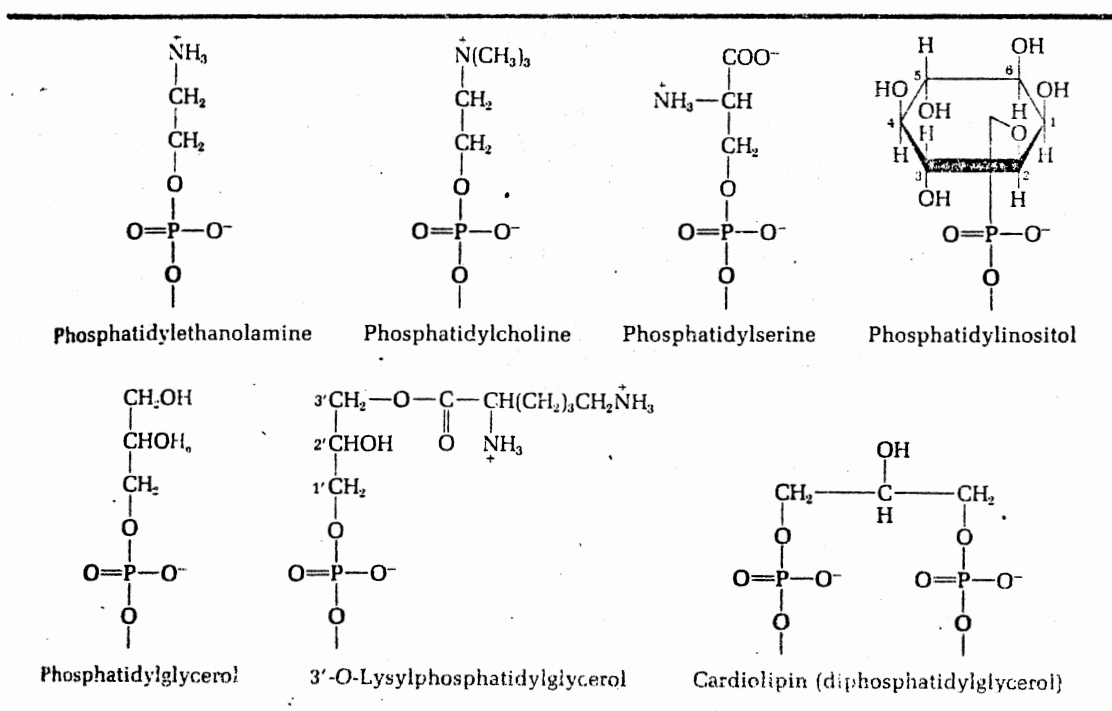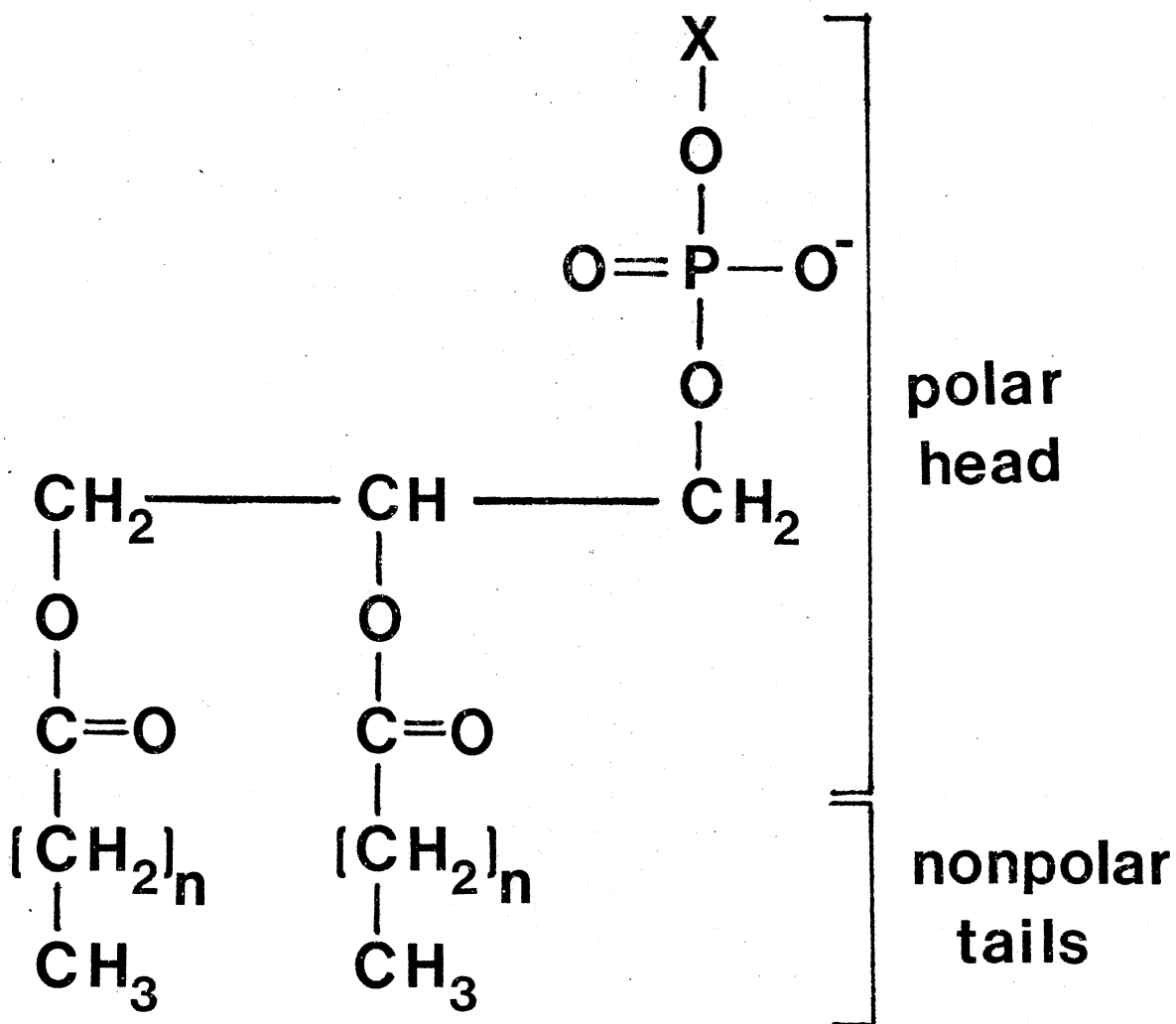
Figure 2. Phospholipid Structure

The fatty acids associated with these lipids range in chain length and unsaturation. For example, stearic (18:0), palmitic (16:0), and myristic (14:0) acids are common among the saturated acids, while oleic (18:1) and linoleic (18:2) are common among the unsaturated acids. Membrane components are held together by noncovalent forces; for example, acyl

chains of phospholipids interact with each other and with proteins by vander Waals interactions. By contrast, the polar groups at the interface of the biological membrane and its surrounding fluids interact mainly by coulombic and hydrogen-bonding forces.

Molecular structures of the membrane have been probed by different non-disruptive techniques, such as Raman Spectroscopy (9, 10), Nuclear Magnetic Resonance (11-13), Electron Spin Resonance (14, 15) etc. Such studies have shown that lipids are in constant dynamic activity. Lipid molecules can migrate or diffuse from one part of the membrane to another, they can even "flip over" from the outside to the inside of the bilayer and vice versa. The rates of such phospholipid flipping are much more rapid in real membranes, a matter of minutes as opposed to the rates of the order of hours in synthetic lipid vesicles (16, 17). Lipid molecules undergo a variety of motions including:

1. Rotational motion which is along the axis perpendicular to the interface.

2. Trans-gauche conformational change in the acyl chains which usually pack in a highly ordered all-trans conformation at low temperatures.

3. Lateral diffusion (movement) of the components in the plane of the membrane. The molecular motion within the bilayer is referred to as "fluidity" and it is this process which imparts viscous properties to the hydrocarbon portion of the membrane. Such properties are detected by techniques

such as N.M.R, E.S.R and fluorescence spectroscopy.

The fluorescent probe 1,6-diphenylhexatriene (DPH), for example

has been widely used for the measurement of microviscosities of natural and artifical biological membranes. Fluorescence polarization measurements of the probe are related to the probe's lifetime in the excited state and to the viscosity of the membrane medium. The reciprocal of the viscosity is called the "fluidity". In lipid bilayers, the term microviscosity was introduced as the geometrical mean of the different viscosities along each axis of symmetry, since the true viscosity is far from being isotropic (18).

Viscosity measurements are used to estimate the degree of order of biological membranes through the equation:

$$\eta = A\, e^{\Delta E/RT} \qquad \qquad \text{Equation (1)}$$

where η is the viscosity and ΔE is the flow activation energy required to overcome the intermolecular forces that oppose the flow. This energy increases with the number of degrees of freedom for intermolecular interactions and also with the chain length. Hence ΔE serves as a criterion for the degree of order of the hydrocarbon in lipid bilayers, where an

increase in order will result in a decreased value of ΔE (19). Another approach for such an estimate is based on the ratio of in-plane and out of-plane rotational diffusion constants of a fluorophore. This dependence was confirmed experimentally with perylene (20, 21). It was found that lysolecithin micelles have an isotropic, unordered structure in spite of having higher internal viscosity as compared to cationic micelles of varying aliphatic hydrocarbon chains. Although the results obtained from such studies are semi-quantitative in nature, they do provide a good estimate of the extent of order in a system when compared with the rates of a standard isotropic solution.

Rates of lateral-transport of fluorescent-labelled particles on the surface of individual cells have been measured using Fluorescence Photo- Bleach Recovery (FPR) and Fluorescence Correlation Spectroscopy (FCS) techniques (22). Cholesterol in the lipid bilayer was found to reduce the lateral diffusion coefficient below the lipid phase transition, while retained solvent increased these coefficients both below and above the phase transition (23). Similar results (15) were obtained using Electron Spin Resonance measurements of spin-labelled lipids.

Any variations in the head groups, chain lengths and degrees of unsaturation of phospholipids are known to affect the membrane rigidity and permeability. However, the lipid bilayer is usually in a "fluid" condition (24) except in the presence of protein (25), Cholestrol (26) or both, where the

lipid tends to be in a relatively immobile phase. Such a presence is marked by changes in the phase transition altering the chain packing from a crystalline to a fluid state. Studies of the phase transition have attracted much attention among researchers (27-29), because of the two types of transitions known to take place in pure phospholipid bilayers:

1. Gel-liquid crystalline transition.

2. Lateral phase transition.

The first type is a result of the tight crystal like packing of the hydrocarbon chains of phospholipids being expanded to produce a less ordered structure. Lipid bilayers behave as solids at low temperatures (gel), while at temperatures above a transition point the hydrocarbon chains begin to move (liquid), even though the bilayer continues to hold together (31).

^{31}P NMR studies were used to follow such changes in vesicles (32), where the rotational motion of the lipids was found to be hindered below the phase transition temperature resulting in a large NMR line width. Also the presence of cations and anions tends to shift the lipid transition temperatures (33).

"Pre-transitions" have been reported in several systems. However in a recent study (34), it was shown that the pre-transition was removed upon association of dipalmitoyl lecithin with a hydrophobic polypeptide, Gramidicin A, acting as a model for intrinsic proteins which

span the whole cell membrane. This was an experimental indication that small amounts of polypeptides affect the organization of the lipid chains and that generalizations of results obtained with model systems to the case of real membranes should be made with caution.

The second type of diffusion, lateral phase seperation occurs when the difference between the transition temperatures of two lipids is too large to allow co-crystallization of the fatty acid chains in the mixture. A broadening and shift of the phase transition then occurs due to interactions between the two lipids. This was observed (35) in a study of a mixture of dipalmitoyl and dilauroyl phosphatidylcholines using the fluorescence probe 12-(9-anthroyloxy)stearic acid (12-AS). The probe was found to be sensitive to only one of the phase transitions, hence indicating it's location in the vicinity of that specific microviscosity. Moreover, some of the properties of the lipid membrane, are expected to be affected by the structural changes occuring at the phase transition. Among these structural changes (31) are:

1. Changes in the polar head group structure. Such changes might affect the binding of ligands to the membrane surface.

2. Structural changes in the hydrocarbon chains. These might affect the interaction between the lipid molecules and other constituents such as cholesterol or proteins.

3. Membrane permeability is expected to be different below and above the phase transitions (36). For example, liposomes of lecithin are extremely permeable to water and non-electrolytes when above the phase transition, while below the melting temperatures the permeability decreases some thousand times (31). Thermally-induced phase transitions are not expected to play a role in living systems, since living systems are usually at constant temperatures. However, there is good evidence that the gel-liquid crystalline phase transition can be triggered by other parameters, such as changes in the ionic environment, pH or by attachment of certain ligands to the membrane surface.

Although phospholipids are one of the major components of membrane lipids and contribute the most to the membrane structure and functions, other classes of lipids are also found in membranes. Among these is the sterol class, of which cholesterol is the most abundant in animal tissues. Cholesterol varies in concentration from one membrane to the other. Although it is insoluble in water, phospholipids usually solubilize it in the membrane. The exact function of cholesterol in the membrane is still unknown. However, studies have shown that it affects the hydrocarbon chains while leaving the polar groups of phospholipids unmodified in membranes (37).

The effect of cholesterol added to phospholipid bilayers has been examined using both proton and ^{13}C NMR

(11). Results showed that cholesterol was associating with the middle section of the fatty acid chains, hence leading to immobilization of these chains. Permeability and fluorescence polarization studies (38) indicate that cholesterol abolishes the phase transition of phospholipids, producing a rather rigid membrane over a wide temperature range.

The effect of cholesterol on biological membranes can be summarized by two phenomena:

1. A broadening of the phase transition as measured by thermal effects (39) and by Raman Spectroscopy (40). The conclusion is that it tends to regulate the degree of order and mobility of the acyl chains of lipids.

2. A dual effect on the fluidity of membranes, i.e., rigidizing effect in the liquid crystalline phase (41-43) and fluidizing effect on the gel phase (9).

It has been suggested that the main biological function of cholesterol is concerned with the stability of the membrane as a barrier (44). Furthermore, cholesterol has been a factor in recent studies on the modulation of lipid fluidity of cell membranes. Other factors affecting the lipid fluidity involve nutritional and thermal manipulations, drugs, as well as hydrogenation of double bonds of lipid molecules using homogeneous catalysis.

Due to the variety of lipid structures and composition in biological membranes, a whole variety of chemical and physical interactions might take place in the bilayer. In

order to study such interactions, certain reporter molecules with spectroscopic signals are often employed. These are usually designed to probe specific sites of interest within the bilayer. Recently, Azzi (45) has reviewed the design and use of fluorescent probes for membrane studies.

Fluorescent Probes

The application of fluorescence spectroscopy to biological membranes requires the presence of a fluorescent probe at a suitable location. These probes may be either intrinsic to the membrane such as tryptophan and tyrosine in proteins, or extrinsic, in which case a fluorescent molecule is introduced into the membrane. Extrinsic probes are of special interest, since they can be designed to have certain fluorescence properties, and to locate at certain sites within the membrane. These fluorescent probes can also be attached to macromolecules either covalently or non-covalently, where covalent labelling has the advantage that the site of attachment can be determined by chemical methods involving degradation of the binding protein. In the design of these probes, it should be understood that not all molecules which absorb light fluoresce with high yields. Competitive processes such as quenching, internal conversion, energy transfer, and many others remove the excitation energy, thus competing with the radiative process. Molecules containing bromo-, iodo-, nitro-, and azo- groups, for example, show little fluorescence because

of enhanced intersystem crossing. Other molecules containing linkages with bond strengths lower than the energy required for electronic excitation will tend to pre-dissociate before fluorescene would occur.

Various fluorescent probes have been designed by investigators to suit their particular membrane and lipid bilayer studies. Following is a list of a few of the more commonly used fluorescent probes (Table III).

Fluorescence Spectroscopy in

Membrane Studies

For a molecule excited by light, the transition to an upper excited state is very rapid. Such a transition is essentially instantaneous (10^{-15} s) compared to the time necessary for any change in the nuclear position to occur (10^{-12} s). The transition probability is determined by the Frank-Condom principle illustrated by the potential energy diagram for a diatomic molecule in Figure 3. Transitions occuring from the equilibrium position of the internuclear separation have the highest probability. Such transitions are indicated by vertical lines in Figure 3. At room temperature, most of the molecules are in the lowest vibrational levels of the ground electronic state S_0 (Figure 4). Each electronic state (e.g. S_0, S_1, S_2, T_1) has internal vibrational levels which are in turn split into a series of closely spaced rotational levels.

TABLE III

COMMON FLUORESCENT PROBES

PROBES	REFERENCES
1-anilino-8-naphthalene sulfonate	(46-48)
1,6-diphenylhexatriene	(49-54)
2-p-Toluidinylnaphthalene 6-sulfonate	(55-56)
1-dimethylaminonaphthalene 5-sulfonate and derivatives (dansyl chloride)	(57-60)
2,7-diamino-10-ethyl-9-phenylphenan-thidinium bromide (ethidium bromide)	(61-62)
1-pyrenebutyric acid	(63)
4-dimethylaminostilbene isothiocyanate	(64-65)
N-N'-di(octadecyl)oxacarbocyanine	(66)
n-(9-anthroyloxy)stearic acids n=6,9,12	(66-72)
n-(9-anthroyloxy)palmitic acids n=2,16	(69-72)
methyl-9-anthroate	(70)
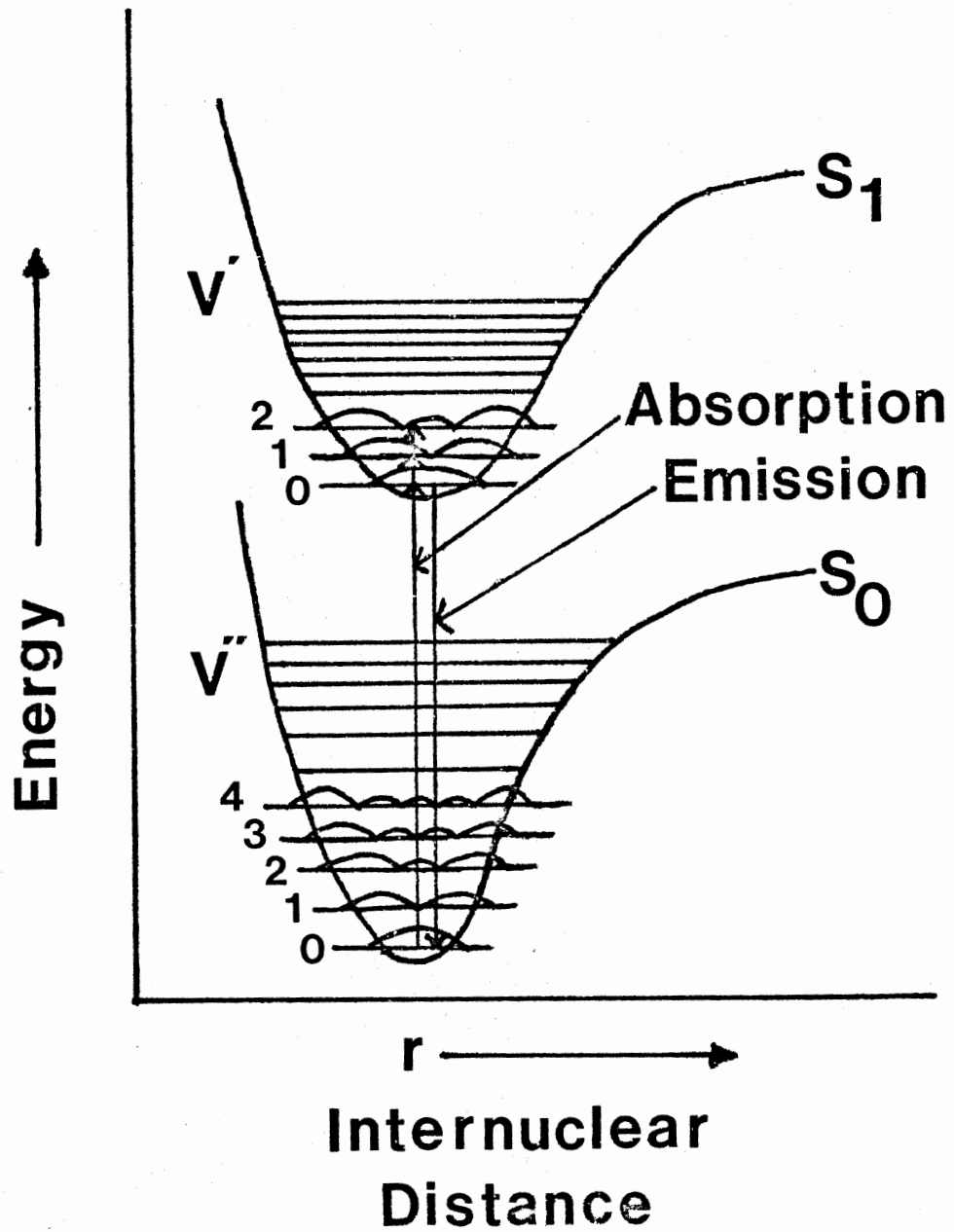
Figure 3. Potential Energy Diagram

Only the rotational levels in the lowest vibrational level of the ground electronic state are shown in Figure 4. This figure is a stylized Jablonski diagram representing the system for just one generalized coordinate. <u>Absorption</u> of light results on the excitation of molecules to higher vibrational levels of upper electronic states S_1, S_2 (Figure 4 a,b). These molecules rapidly loose their excess vibrational energy in the form of heat through collisions with the surrounding solvent molecules and by vibrational redistribution. Such a process is known as a <u>radiationless process</u> and is indicated by wavy lines in Figure 4. The excited molecules may undergo a process known as <u>internal conversion</u> (radiationless transition, 10^{-12} s) as shown in Figure 4d, whereby a molecule passes from a low vibrational level of an upper electronic excited state to a high vibrational level of a lower electronic state within the same spin manifold. The excess vibrational energy is lost by exchange with solvent molecules, leading to the zero vibrational level of S_1. From this resultant level, the molecule can return to the ground state either by spontanteous emission (<u>fluorescence</u>) ($10^{-6} - 10^{-9}$ s) in which the emitted light is incoherent (Figure 4c), by <u>stimulated emission</u> (generally of low probability), or by <u>radiationless transitions</u> such as internal conversion and non-radiative quenching reactions (Figure 4g).
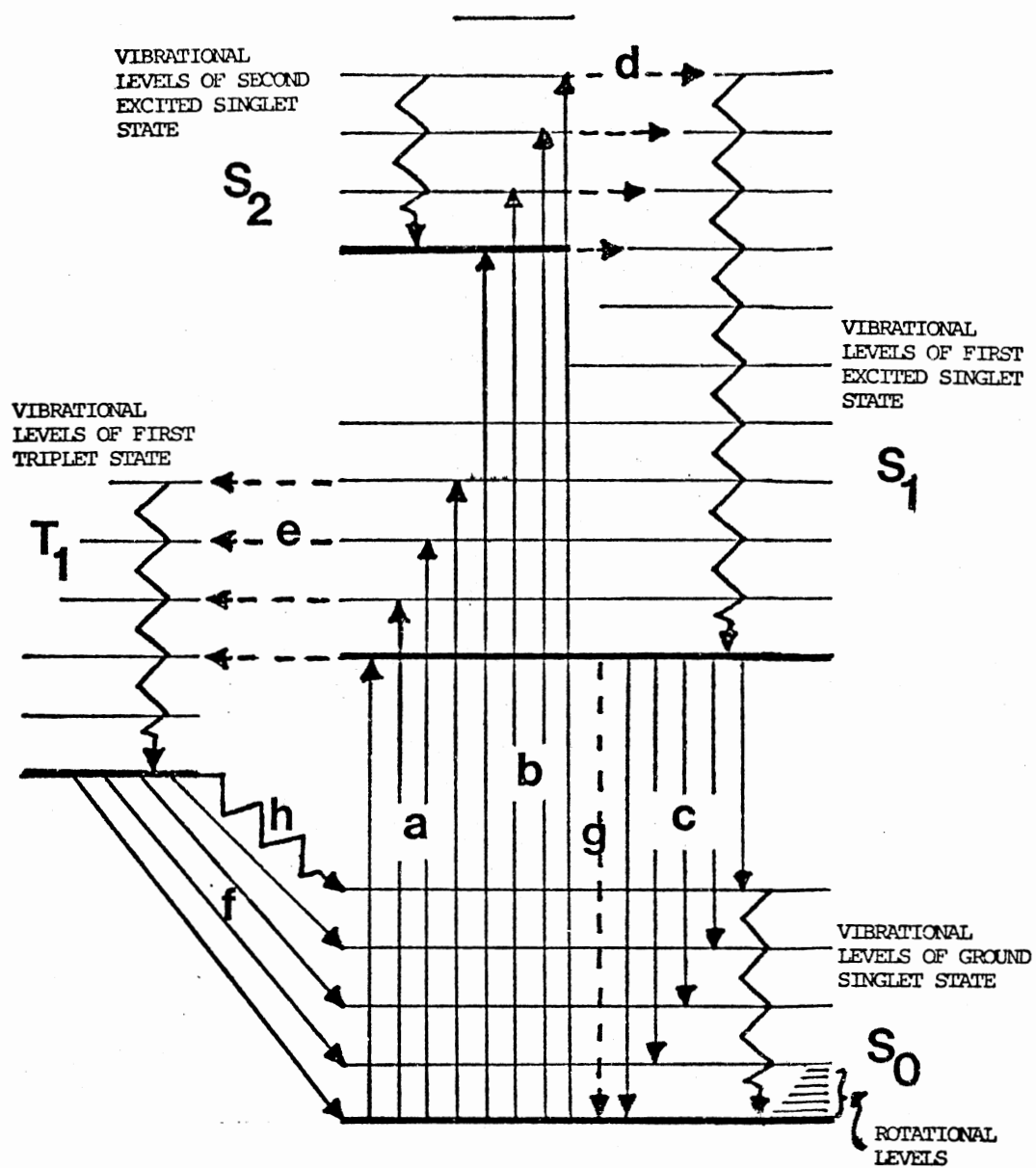
Figure 4.   Simplified Jablonski Diagram

Hence fluorescence is a radiative process that takes place between two states of the same multiplicity, i.e. singlet to singlet or triplet to triplet. Although radiative transitions between states of different multiplicities are theoretically forbidden, spin-orbit coupling introduces "allowedness" into these transitions. The resulting radiative transition is referred to as phosphorescence (10^{-4} - 10^2 s) as shown in Figure 4f; however, the bulk of such transitions (T_1 to S_0) are radiationless (Figure 4h). An indirect way of populating the triplet state is via the singlet state involving a process called intersystem-crossing (10^{-9} s) as shown in Figure 4e, in which molecules cross from a low vibrational level of an excited singlet state to a high vibrational level of a lower triplet state. This is another radiationless transition which can depopulate S_1 and which is sensitive to the environment of the chromophore.

Following is a discussion of the different techniques involving fluorescence spectroscopy, used in the study of model and biological membranes. In each case, it will be noticed that a particular aspect of the fluorescence process has been used to generate information concerning the environment of the fluorescent probe.

Quantum Yield of Fluorescence

The fluorescence quantum yield or efficiency (Φ_F), is defined as the ratio of the number of quanta emitted to the

number of quanta absorbed by the chromophore. The larger
the value of Φ_F, the greater is the fluorescence of the
compound. Φ_F has an upper limit of one and a lower limit of
zero. Thus

$$\Phi_F = \frac{k_R}{k_R + \sum_{i=0}^{n} k_{NR}} = \frac{\text{\# of photons emitted}}{\text{\# of photons absorbed}} \qquad \text{Equation (2)}$$

where k_R and k_{NR} are the rate constants for the radiative
and the non-radiative processes respectively. The term k_R
also relates to the mean natural radiative lifetime of the
excited state τ_0:

$$k_R = 1 / \tau_0 \qquad \text{Equation (3)}$$

The fluorescence efficiency is a function of several
processes, among which radiationless emission and
intersystem crossing play a role. These processes are
affected by factors such as temperature and solvent nature
in case of radiationless process, and by the energy gap
between the singlet and triplet states in case of
intersystem crossing.

For the majority of molecules in the liquid phase, the
fluorescence efficiency is found to be independent of the
exciting wavelength. However, the fluorescence efficiency
of a variety of aromatic compounds is found to be enhanced
by lowering the temperature (73). The fluorescence
intensity is related to the temperature and viscosity of the

system by the equation (74):

$$I = \frac{I_0\,(\eta/T)}{\alpha + \beta\,(\eta/T)}$$ Equation (4)

where I_0 is the absorbed intensity, α and β are constants and η and T are the viscosity and absolute temperature of the medium respectively. Hence, the dependence of the fluorescence intensity on the value η of the medium provides a convenient means for measuring the viscosity, where measurements by conventional methods are rather difficult to carry out. The fluorescent probes auramine O (74) and aurovertin (75) have been shown to have viscosity-dependent quantum yields, making them suitable probes for microviscosity measurements. However, ANS-type probes (76) exhibit an increase in the fluorescence quantum yield when dissolved in deuterium as opposed to water. Radda (77) has employed this effect to assess the water availability to probe binding sites.

Furthermore, the interaction between solvent and solute molecules influences the quantum yield. Hence a correlation between quantum yield and solvent polarity parameter can be drawn through plots of Φ_F vs. $f(\xi)$ where (78)

$$f(\xi) = \frac{\xi - 1}{2\xi + 1}$$ Equation (5)

ξ is the dielectric constant of the solvent. A decrease in

the solvent polarity (i.e. solvent dielectric constant) was found (78) to lead to an increase in the fluorescence quantum yield of 2-toluidinylnapthalene-6-sulfonate (TNS). A similar increase was found when increasing the solvent viscosity. However, the effect of the viscosity was smaller than that produced by varying the dielectric constants of the solvents, confirming that (TNS) is a suitable hydrophobic probe.

Moreover, quantum yields are also affected by several other mechanisms. For instance, the decrease in fluorescence efficiency caused by fluorescence quenching has been used to study the accessibility of oxygen to certain regions of macromolecules (79). Novasad et al. (80) were able to study the translational diffusion of pyrene in reconstituted plasma lipoprotein by measuring the relative quantum efficiencies of excimer fluorescence.

Finally, a decrease in the fluorescence quantum yield of a chromophore caused by energy transfer may be used to assess the presence of other acceptor molecules in its vicinity (81). Fluorescence quantum yield measurements are therefore proving to be of value in the structural characterization of membranes.

Fluorescence Polarization

Polarized fluorescence is one of the most widely used applications of fluorescence spectroscopy in biological systems. It is used to establish the size, shape and

flexibility of macromolecules in solutions and to determine the orientations and motions of molecules in membranes.

Steady-State Measurements

These measurements reflect the orientational constraints imposed on a molecule by its neighboring molecules. The degree of polarization is defined as:

$$P = \frac{I_{VV} - C\, I_{VH}}{I_{VV} + C\, I_{VH}} \qquad \text{Equation (6)}$$

where C stands for the correction factor of the emission monochromator while I_{VV} and I_{VH} refer to the measured emitted intensities when the polarizer is positioned parallel and perpendicular to the direction of polarization of the exciting light. When $P = 0$, the light is unpolarized, for $P = \pm 1$, it is completely polarized, whereas with P values between these extremes, the light is partially polarized.

The probability of absorption is proportional to $\cos^2 \alpha$, where α is the angle between the dipole and the electric vector. Hence maximum absorption of light ocurrs when the absorption dipole is parallel to the electric vector of the light. However, the probability of emission in the horizontal direction is proportional to $\sin^2 \gamma$, while that in the vertical direction is proportional to $\cos^2 \gamma$. γ stands here for the angle between the emission dipole and the electric vector. According to Perrin (82), for randomly

oriented but rigidly held molecules, P takes the limiting value P_0 given by:

$$P_0 = \frac{3 \cos^2 \theta - 1}{\cos^2 \theta + 1}$$
Equation (7)

where θ is the angle between the absorbing and emitting dipoles. The term P_0 is the polarization of the molecule in the absence of any depolarization (randomization of the electric vector) due to Brownian motion or intermolecular process. It is only a function of the polarization due to the absorption of light and of the angle of transfer between the absorption or emission dipoles. If the molecule is excited by polarized light, P_0 ranges in value between

$$- 1/3 \leqslant P_0 \leqslant 1/2$$
Equation (8)

while it range from

$$- 1/7 \leqslant P_0 \leqslant 1/3$$
Equation (9)

for excitation by unpolarized light. In general, the limiting values of P_0 for any systems are:

$$- 0.33 \leqslant P_0 \leqslant 0.5$$
Equation (10)

If the molecule is not rigidly held and is in a medium of low viscosity, then its Brownian motion (translational and rotational movements) will tend to remove the polarization imposed on the system by the polarized

excitation. This will occur if the lifetime of the excited molecules is long enough compared with the time required for rotational diffusion. This is predicted by Perrin's equation (82):

$$\left(\frac{1}{P} \pm \frac{1}{3}\right) = \left(\frac{1}{P_0} \pm \frac{1}{3}\right)\left(1 \pm \frac{3\tau}{\rho}\right) \qquad \text{Equation (11)}$$

The positive signs apply to excitation with unpolarized light (natural), while the negative signs apply to the use of polarized exciting light. τ is the excited state lifetime, while ρ is the rotational relaxation time given for a spherical molecule by:

$$\rho = \frac{3\ V\ \eta}{R\ T} \qquad \text{Equation (12)}$$

where V is the molar volume of the molecule, η is the viscosity of the medium, T is the temperature and R is the gas constant. Analysis of the above equation, makes the following measurements possible. A plot of 1/P vs T/η yields P_0 from the intercept and V or ρ from the slope, if τ is known. Parameters such as temperature, pH, time, concentrations of fluorescent material, concentration of various salts and quenchers, etc., when varied will affect the system; hence plots of 1/P vs the "parameter" will indicate changes in viscosity, ρ , τ ,P_0 or V.

Furthermore, an analysis of the absorption spectra is possible by a plot of P vs. the wavelength of excitation

yielding P_0 values if the measurement is done in a highly viscous medium. If the polarization remains constant with wavelengt, then it can be assumed that only one absorption band is present. However if changes occur in the plot, then the presence of another absorption band is indicated under what would have appeared as a broad absorption spectrum in an ordinary spectrophotometer. Hence, it is possible to use polarization spectra to show the presence of different overlapping electronic transitions. Such a careful study, if applied to biological membranes would determine any perturbation effects on the individual bands caused by the chromophore's environment. This is only true for highly viscous solutions, where the Brownian motion is neglected; hence depolarization will be from the intramolecular depolarization, assuming the energy transfer is negligible.

The degree of polarization (anisotropy) of a fluorophore when applied to natural and artifical membranes, has permitted the calculation of fluidity or (microviscosity) parameters. An increase in microviscosity of liposomes was observed due to an increase in cholesterol to phospholipid ratio. Furthermore, an increase in protein mobility detected with the increasing viscosity, was attributed to the maintainence of dynamic balance in the membrane (83, 84). Changes in membrane structure and release of fragments from the E. Coli outer membrane into the surrounding media, due to peptide antibiotic EM 4G were detected by polarization studies (85). Engelhand et al.(86)

studied the effects of the modification of fibroblast membrane composition by fatty acid supplementation, in relation to hormone stimulation and adenylate cyclase activity. Shatill and Cooper (87) observed the increased sensitivity exhibited by cholesterol rich platelets to epinephrine aggregation by studying the rotational diffusion of DPH. Fluorescence depolarization of DPH was also used (88, 89) to study phase transition and fluidity of single and multilamellar phospholipid bilayers. Differences observed in the thermotropic properties were attributed to the different radii of curvature of these liposomes.

However, such steady state measurements are tedious, requiring the determination of polarized intensities at different temperatures or viscosities before any structural parameters such as constraint and molecular organization are derived. Moreover, care must be exercised when interpreting these results, due to any conformational changes which might result when temperature and viscosity are changed. Another approach to the determination of anisotropic motion of probes involves the measurement of time-dependent nanosecond fluorescence polarization (90, 91), but this is not included in the present study.

Edge Excitation Red Shift

Fluorescence and phosphorescence of some organic molecules exhibit red shifts when excitation is achieved at the long wavelength edge of the first absorption (92). This

process has been referred to as the B shift (93), bathochromic luminescence (94), Red Edge Shift (95) and lastly the term which seemed to describe the phenomena most appropriately "Edge Excitation Red Shift" which is abbreviated as EERS (96).

An important feature of EERS, besides the shift in the emission band, is that there is no change in the spectral shape. In there are such changes, then the phenomena is excluded from the category of EERS. Klopffer (97) attributed EERS effects to phosphorescence occuring from two connected singlet levels. These reasons along with the actual phenomena of EERS point to a deviation from Kasha's rule, which states that luminescence of organic molecules in the condensed phase occurs only from the lowest excited electronic state of a given multiplicity (98). The rule also implies that both fluorescence and phosphorescence do not depend on the excitation energy.

It was noticed for quinine and its related compounds that EERS was exhibited both for the room temperature fluorescence and the low temperature (77 K) fluorescence and phosphorescence (96). Several mechanisms have been suggested for this process. Chen (92) assumed two close-lying excited states. However, Fletcher suggested that it is due to emission from a single energy level from a molecule in either of two or (more) different "average" geometrical conformations due to a rotatable auxochrome (chromophore) group of the compound (93). Later on, Galley

ascribed the dependence of the phenomena to both the excited-state lifetime of the chromophore and the degree of rigidity of the medium (99).

Itoh and Azumi (100) have proposed perhaps the most plausible model stating that not all the solute molecules are identically solvated. The distribution of these solvated species in the ground state (Ground State Distribution) would be similar to that in the excited state (Franck-Condom Excited State Distribution) if fast intramolecular relaxation processes occur. However, a relaxation of the excited state through solvent dielectric relaxation would occur if there exists a large change in the dipole moment of the dye upon excitation. Such a relaxation would lead to an equilibrium excited state distribution. In this proposed mechanism, EERS is prominent if the solvent reorientation relaxation time τ_R is large compared with the fluorescence lifetime τ_F, and if the Franck-Condom solvation energy is reasonably large. That is, the excitation process must be accompanied by a large change in dipole moment. Their suggestion that hydrogen bonding and protonation are important in the solvent reorientation relaxation process was supported by Gangola et al. (101, 102).

The dependence of EERS on the molecular structure of the dye, solvent polarity or acidity, temperature, solvent deuteration, solute concentration, solute excited state lifetime and solvent viscosity suggest the possibility that

the EERS process could be an important tool if applied to biological systems. Since it will reflect the polarity and viscosity of the medium surrounding the chromophore, hence indicating the location of the probe inside the biological membrane. To date, no such studies have been reported.

Activation of Energy of Incorporation

Fluorescence spectroscopy has also been used to study the interaction of fluorescent probes with real and model biological membranes. The interaction is monitored by following the (increase/decrease) with time, immediately after the addition of a fluorescent probe to a membrane. The incorporation curve obtained reflects the process of the penetration of the dye molecule into the lipid membrane matrix. The observed differences of the fluorescent intensities are mainly due to a change in the solvent environment of the dye molecule. The fluorescence spectrum and efficiency are known to be affected by different solvents in a variety of ways. These include polarization and hydrogen bonding, viscosity effects, compound formation and photo-reaction (103). The rate of permeation of a probe across the membrane depends on the transport of the probe between the polar head group region and the hydrocarbon region. It is also highly dependent on the membrane viscosity.

The incorporation of the probe 1-anilino-8-naphthalene sulfonate (ANS) by membranes and vesicles has been

extensively studied in the last several years due to its spectral simplicity and sensitivity to the surrounding environment. In a study by Freedman (104), a biphasic interaction of ANS with erythrocyte membranes, was attributed to the presence of "fast" and "slow" sets of binding sites in these membranes. These two observed different rate constants corresponded to interactions at the outside and diffusions into the membrane. Such interactions were noticed to be pH-dependent and sensitive to changes in ionic strength. Further investigations of ANS with erythrocyte ghosts, at room temperature, indicated a similarity in the ANS binding sites on the molecular level (105). However, the fast ANS response was due to the site on the outer side of the membrane; whereas the second response depended on the state of the membrane. Later work showed that the slow process had a half-time of about 8 minutes (106), in contrast with the rate of interaction of ANS with erythrocyte ghosts under similar conditions where equilibrium was reached within few seconds (104, 105). Fortes (106) found that ANS was a potent inhibitor of anion permeability in red cells. These inhibitory effects indicated that ANS and related compounds are not inert in their interactions with membranes. Hence, extreme care must be exercised when interpreting observations made in the presence of a probe where the probe itself alters the characteristics of the membrane. These perturbations need to be looked for when extending the use of newly synthesized

probes to the study of real membranes.

Nuclear Magnetic Resonance studies showed that the rate of entry of ANS into liposomes was slow, taking up to an hour for completion (107). However, kinetic studies of ANS⁻ transport across phospholipid vesicles conducted using a stopped-flow rapid kinetic technique, indicated that the binding on ANS⁻ on the outside surface occured in a time shorter than 100 μsec (108). While the process involving the permeation occured in a time range of 5-100 second. A partition coefficient was estimated between the polar head group region and the hydrocarbon chain region corresponding to about 4 Kcal of free energy. That value was small when compared with the values of electrostatic free energy necessary for moving an ion from an aqueous environment to a hydrocarbon region (109). Photography has been employed in such studies to observe the different steps and time it takes for the interaction of a probe with cell membranes (110). These steps included the approach of the probe to the cell, its contact and sticking, the local entry of fluorescence from the probe into the cell membrane and finally the lateral spread of the fluorescent probe throughout the cell membrane. It was observed that the steps of "sticking" and "entry" are slower at low temperatures, but once entry has occured, fluorescence spread through the cell was fast, both at high and low temperatures. Using this technique, Kosower et al. (110) were able to differentiate between normal

mitogen-transformed and malignant cell membranes.

Lang studied the interaction of the fluorescent probe 12-(9-anthroyloxy)stearic acid (12-AS) with microsomes at different temperatures (111). 1,6-diphenyl hexatriene (DPH) is another probe that has been extensively used in labelling membranes (112). Apparent activation energies of 7.7 and 8.7 Kcal/mole for its incorporation were reported for choline and ethanolamine-supplemented cells.

Quenching studies of aromatic hydrocarbons have been exploited to obtain information about the permeability of membrane-like systems (112-116). Apparent activation energies of 240 Kcal/mole and -96 Kcal/mole for ANS incorporation in dimyristoyl-L-α-Lecithin (DML) were reported in the first and second halves of the transition, over the time scale of 60 sec (117). The negative activation energy seems to be strange. However, the author attributed that value to the non-reproducibility of the results due to the slow fusion of the vesicles.

Thus, contradictions as to the time of incorporation and the activation energies for these processes are apparent, and further elaboration of the above studies is needed in the near future. Such incorporation studies are important in providing information as to the final location of the probe within the bilayer (118). These incorporation techniques may also be used to obtain data on the occlusion of membrane surfaces by glycoproteins. Such information can not be obtained by fluorescence depolarization studies.

CHAPTER II

EXPERIMENTAL PROCEDURES

Materials

Chemicals

Dipalmitoyl phosphatidylcholine was obtained from Sigma
Chemical Company. It was used without any further
purification. The fluorescent probes,
2-(9-anthroyloxy)stearic acid, 12-(9-anthroyloxy)stearic
acid, 2-(9-anthroyloxy)palmitic acid,
16-(9-anthroyloxy)palmitic acid were purchased from
Molecular Probes. 1,6-diphenylhexatriene was obtained from
Aldrich Chemical Company. All the fluorescent probes used
were commercially available (e.g. Gold Label). They were
used as obtained with no further purification.

Solvents

Spectral grade solvents like methanol, ethanol, heptane
and tetrahydrofuran were used to prepare stock solutions of
the fluorescent dyes. These solvents were also employed to
clean up the glassware used in the preparation of the
samples. Water for the buffer solutions was distilled
twice, deionized, charcoal filtered and millipore filtered

as well. The purity of the solvents was checked by running
its absorption, excitation and emission spectra over the
entire spectral range employed. Absence of absorption and
emission was the criterion of purity.

Procedures

Glassware

Extreme care was exercised in cleaning all glassware,
including fluorescence and absorption cuvettes. Cleaning
was done by soaking the glassware in an acidic solution of
approximately 10% nitric acid, for about an hour. They were
then rinsed successively with distilled water, ethanol,
tetrahydrofuran and heptane. The cleaning process was
repeated many times to make sure that any polar as well as
non-polar fluorescent impurities present were removed. The
final rinse was done with the solvent employed for that
specific solution.

Ultrasonic Cleaner

A Cole-Parmer ultrasonic cleaner was used at first to
clean all the glassware including the fluorescence cuvettes.
However, it was later abandoned because of the cracks caused
along the sides of the cuvettes. The cracks caused were due
to inperfections in the quartz and mainly to stresses and
strains introduced in the manufacturing of the cuvettes.
Later on, the ultrasonic cleaner was found to be very
helpful in dissolving dyes, while preparing dye stock

solutions. The dye solution container was immersed in the ultrasonic cleaner filled with distilled water.

Temperature Measurements

In all polarization measurements, temperature was controlled with a thermostatted heater (Thermomix 1460). It had a temperature range of $-20^{\circ}C$ to $200^{\circ}C$, with external cooling. Distilled water was used in the heating bath. The heater had a built-in temperature sensor, with a powerful circulating pump to insure good mixing. All the parts of the heater, in contact with the bath liquid were made of stainless steel. A peristalic pump (Unified Masterflex, Cole-Parmer) was used to circulate water around the sample holder. The flow rate was adjusted by a speed control knob. Silicone tubing of I.D.=0.063" and O.D.=0.192" was used with the pump head (7014). In order to avoid the rupture of the silicone tubing, caused by compression from the head rollers, the tubing section in the pump head was changed occasionally. A Bailey Instrument Co. digital thermocouple was used for direct temperature measurements. The microprobe sensor had a teflon sheath with a diameter of 0.025". The tip sensitive thermocouple was immersed into the sample through a hole in the cuvette cover for accurate temperature measurements. The jacket was thermostatically controlled sufficiently well that the maximum temperature excursion of the sample over the course of an individual incorporation experiment did not exceed $\pm 0.1^{\circ}C$. Due to the

heating of the sample above ambient temperatures, convection currents were created which gave rise to temperature gradients. In addition to that, membranes tend to settle down in the cuvette if left unstirred for a while. These problems were circumvented by constant stirring of the vesicle suspension at approximately 5 Hz with a teflon coated stirrer. The magnetic stirrer was contained underneath the sample compartment of the fluorometer. Stirring of the sample was found to be essential for measuring reproducible data. In order to study any effects of lipid binding to the teflon stirrer, control experiments were conducted in which glass stirrers were used instead of teflon stirrers. These gave similar results. It was concluded that teflon stirrers introduced no errors in the measurements.

pH Measurements

A Fisher pH meter, model 610 Accumet was used. The manufacturer claims an accuracy of $\pm$ 0.02 pH units, and a repeatability of $\pm$ 0.01 pH units. The model was equipped with a glass-body combination electrode that incorporated both reference and indicator elements. The pH meter was standardized with buffer solutions of known pH values, prior to each use.

Phosphate Buffer

A phosphate buffer solution of pH=7.4, was used to

prepare the model biological membranes. This was prepared by dissolving the salts listed in Table IV, in one liter of distilled water. At times a more concentrated solution (5X) was prepared as a stock. This stock was diluted to the usual (1X) concentration before use. These salts were dissolved in the solution by using a magnetic stirrer. The pH was adjusted to 7.4 by adding either an acidic solution (0.1 N HCl), or a basic solution of 30% NaOH (30g/100mL). The buffer was kept refrigerated at all times to avoid the growth of bacteria. Buffer was discarded when white suspensions or algae growth were observed in the solutions.

TABLE IV

SALT CONCENTRATIONS USED IN PREPARATION
OF THE PHOSPHATE BUFFER

CHEMICALS	CONCENTRATION	FORMULA WEIGHT	(1X) g/L	(5X) g/L
$NaH_2PO_4 \cdot H_2O$	12mM	138.0	1.66	8.28
$Na_2HPO_4 \cdot 7H_2O$	19mM	268.1	5.10	25.49
NaCl	50mM	58.5	2.93	14.63
KCl	50mM	74.5	3.73	18.63

Vesicle Preparation

Model biological membranes consist of aqueous dispersions of lipid bilayers surrounding an internal aqueous compartment. These membranes, referred to as vesicles, can be prepared by several methods which can be reduced to four basic procedures:

1. Ultrasonic irradiation of phospholipids are dispersed in an aqueous medium (119). Lipid vesicles can be prepared following the procedure by Huang (120). This method was not used for these experiments because high-energy sonication often causes degradation of phospholipids (121). Furthermore, titanium particles usually erode from the probe causing contamination of the sample.

2. Another procedure uses lecithin dispersions solubilized with sodium cholate (122). The detergent is removed by gel-filtration on sephadex G-50 (medium) at 4°C. The vesicles formed are then subjected to molecular sieve chromatography on a sepharose 4B column (2.5 by 50 cm) at 4°C. Dynamic light scattering experiments of the isolated vesicle fractions give a size distribution ranging from 1500 $\overset{\circ}{A}$ to 2000 $\overset{\circ}{A}$. This method does not give reliable results, as has been indicated elsewhere (120, 123), because of the many variables that have to be controlled while running the column chromatographic separation.

3. Dilution of an organic solvent containing

phospholipid in an aqueous buffer either by blowing off the solvent with an inert gas like nitrogen (124), or by rapid injection of the phospholipid solution into the aqueous system (125).

4. The injection method has no degrading effect on the phospholipids and is very simple to follow (123). The procedure used is indicated below.

Aqueous lipid vesicles were prepared by injecting 250 μl of an ethanolic solution of lipid, through a Hamilton syringe, into 10 ml of a magnetically stirred phosphate buffer solution (pH=7.4). The same syringe was used for all vesicle preparations, to insure no change in the vesicle sizes. The buffer solution was contained in a test tube, and the actual injection took place about 2.5 cm below the buffer surface. Stirring was accomplished by a standard magnetic stirrer. During injection, the temperature was kept well above the phase transition of the lipid in use. For example, the temperature was kept above 41°C in the case of dipalmitoyl phosphatidylcholine. This was achieved by inserting the test tube into a hot water bath during the preparation. The injection velocity was kept steady and slow, around 0.025 ml/min. Once the injection was over, the vesicle suspension was left to cool to room temperature before being used. The vesicles were kept refrigerated when not in use. The final vesicle suspension consisted of 1.7×10^{-4} M phospholipid in a phosphate buffer of pH 7.4.

Electron Microscopy

The lipid vesicles were characterized by transmission electron microscopy using a Phillips 200 electron microscope. Negative staining of the samples was done with 2.5% aqueous uranyl acetate. Samples were dried onto copper grids that were coated with parlodion and carbon. The vesicle diameters were found to range from 200 to 700 Å. The bilayer thickness, found to be around 50 Å, was measured using freeze-etch techniques. Sizes were corrected for any instrumental and artifical artifacts by comparison to known latex sphere diameters. Electron microscopy of different vesicle preparations gave the same size distribution. A preparation of phospholipid vesicles was kept refrigerated and was examined under the electron microscope every other day for a time interval of 20 days. The size distribution of the prepared sample seemed to be constant over that period, indicating the absence of any vesicle fusion. However, vesicles were freshly prepared for each experiment and used within 3 hours.

Membrane Labelling

Stock solutions of fluorescent dyes were prepared by dissolving these in organic solvents (e.g. tetrahydrofuran). The stock concentrations of each dye were such that, when added to the vesicles an optical density of 0.04 cm^{-1} for the chromophore was obtained. This low optical density eliminates concern about the inner-filter effect (103).

Small volumes (1.5 µl) of the fluorescent probes were added to 2.5 ml of a phosphate buffer solution of lipid vesicles contained in a cuvette. Microliter pipettes (Rainin, models P-20D and P-200D) equipped with disposable tips were used for addition of these microliter quantities. The P-20D model had a range of 0-20 µl in increments of 0.1 µl, with an accuracy to within less than 0.1 µl. While the P-200D model had a range of 0-200 µl in increments of 1.0 µl, with a relative accuracy of 0.5 µl. Labelling was followed by monitoring the change (increase/decrease) in fluorescent intensity as the dye incorporated into the membrane. Fluorescence labelling was complete once the change in intensity had levelled off. The incorporation time was different for each probe. It took about 3 hours, for 1,6-diphenylhexatriene to fully incorporate into the membrane compared to about 20 minutes for 2-(9-anthroyloxy) palmitic acid.

Only for those experiments involving the measurement of the critical probe/lipid concentration was the incorporation process different. In these experiments the incorporation of the probe into the vesicles was done at temperatures above the phase transition of the lipid.

Absorption Spectroscopy

Absorption measurements were made on a Perkin-Elmer spectrophotometer, model 552 equipped with a chart recorder model 561. It was a double-beam, ratio recording,

UV-Visible spectrophotometer with microcomputer electronics, a keyboard entry and digital ordinate and abscissa displays. It had a wavelength range from 190 to 900 nm. The recorder was operated and controlled by the microcomputer. The instrument was modified by inserting a magnetic stirrer below the sample chamber. The baseline was automatically corrected to within $\pm$ 0.002 A units once the machine was turned on. This feature was used by placing the cuvettes filled either with lipid vesicles or solvents in both sample and reference chambers, depending upon the specific experiment, before turning the machine on. Failure to obtain a flat baseline was an indication of impurity in the sample or on the walls of the cuvettes. A straight baseline obtained over the spectral range of 850 to 210 nm was the usual starting point for any experiment involving absorption measurements.

Fluorescence Spectroscopy

Fluorescence measurements were made on a home-built fluorometer. An arrangement of the spectrofluorometer is shown in Figure 5. A xenon arc lamp (450 Watt) was used as a source of continuous uv-visible light. A high voltage power supply, model 301 (Photochemical Research Associates, Canada) was modified by adjusting the spark gap to 19mm, and disconnecting the wiring to the amperage meter. The power supply was unusable as received from the manufacturers. Much difficulty was encountered in igniting the lamp.
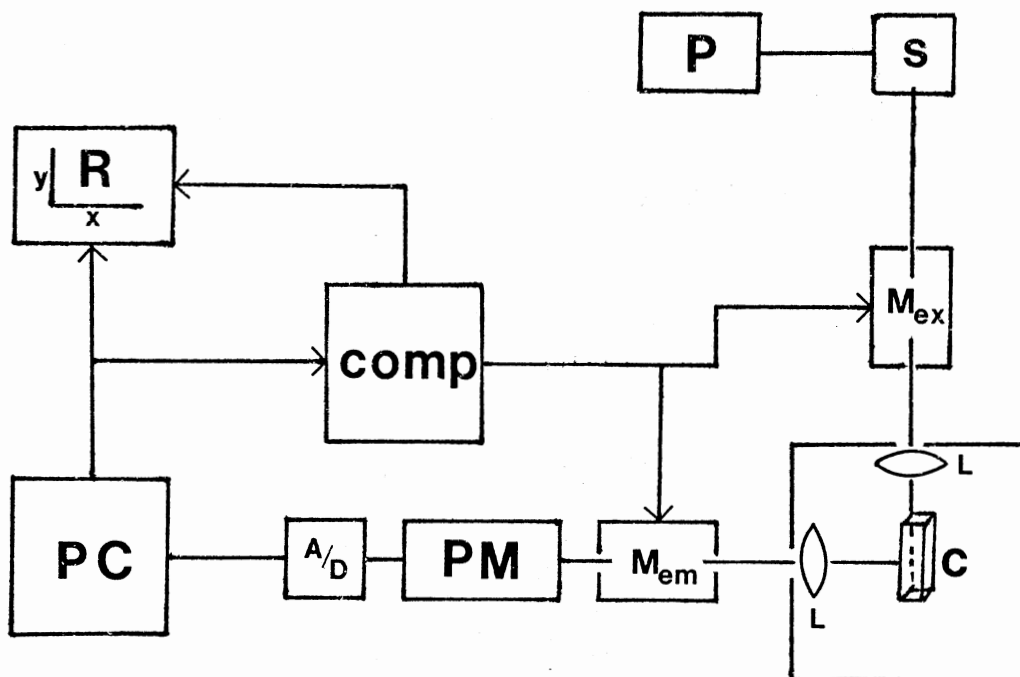
Figure 5. Schematic Diagram of the Spectrofluoro-
meter Arrangement. P Represents the
Power Supply; S the Light Source; M_{ex}
and M_{em} the Excitation and Emission
Monochromators Respectively; L the
Condensing Lens; C the Sample Holder
(Cuvette); PM the Photomultiplier; A/D
the Amplifier and Discriminator; PC
the Photon Counter; R the Recorder;
and COMP the Apple Computer.

Therefore, a Hg lamp was used to photo-ionize the Xe molecules prior to pulsing the lamp with the company's ignitor. While starting the lamp, the current supply was turned down. Once the lamp ignited, the current was increased so that the power did not exceed that required for the xenon lamp. The xenon lamp was cleaned with ethanol and extreme care was exercised in the process of installing it.

A 0.45 meter monochromator (McKee-Pedersen Instruments, model MP-1018B) of Czerny-Turner configuration was used to select the required wavelength for excitation. It had a reciprocal linear dispersion of 9 $\overset{\circ}{A}$/mm , a grating blazed at 2700 $\overset{\circ}{A}$ and ruled with 2360 lines/mm. It had a wavelength range up to 500 nm. A solar cell was placed in the excitation monochromator to monitor the intensity of the xenon arc lamp.

The sample chamber contained a condensing lens of diameter=1" and focal length=4", a sample holder with a set of thin film polarizers from Melles Griot Optics for polarization measurements, and another condensing lens in between the sample and the emission monochromator. The emission monochromator had a diffraction grating of 1180 lines/mm blazed at 3000 $\overset{\circ}{A}$ and had a spectral range of 200-1000 nm with a reciprocal linear dispersion of 18 $\overset{\circ}{A}$/mm. A photomultiplier, Centronic 4249 QB, enclosed in a tube housing model 62 (Pacific Precision) was mounted on the exit port of the emission monochromator. The output of the photomultiplier was processed by photon counting, using a

quantum photometer model 9511 (Ortec Brookdeal), the output of which was passed into an apple II Plus computer as well as an Omniscribe recorder (Houston Instruments). The sensitivity of the photon counter was selected by proper setting of both the range switch and the %rms deviation. A decrease in the %rms deviation led to an increase in the time constant. While scanning the excitation or emission spectra the time constants were chosen by the formula:

$$\text{time constant} \leq \frac{\text{band pass (Å)}}{6 \times \text{scan speed (Å/min)}}$$
Equation (13)

The excitation spectra were not corrected for variation in lamp intensity with wavelength. However, the lamp intensity was always monitored using a solar cell installed in the excitation monochromator. All polarization measurements were made by manual rotation of the polarizers. The grating correction factor of the emission monochromator was calculated at each emission wavelength and was included in the polarization calculations (126). Polarization values were calculated using the following equation:

$$P = \frac{I_{VV} - C\, I_{VH}}{I_{VV} + C\, I_{VH}}$$
Equation (14)

where $C = \dfrac{I_{HV}}{I_{HH}}$ is the correction factor

I_{VV} and I_{VH} stand for the measured emitted intensities when

the polarizers are positioned parallel and perpendicular to the direction of the vertically polarized exciting light. While I_{HV} and I_{HH} represent the emitted intensities when the polarizers are positioned perpendicular and parallel to the direction of the horizontally polarized exciting light.

The entire fluorometer was automated using an Apple II Plus microcomputer. Programs were written to run excitaion and emission spectra. Different scan and recorder speeds as well as repetitive runs were controlled by the programs. A list of the actual scan speeds of the excitation monochromator are shown in Table V, while those of the emission monochromator are shown in Table VI. Other programs were written to control the polarization measurements and correction factor calculations. Each data point reported in such calculations was the result of an average of at least a hundred calculations. A listing of these programs is given in Appendix A.

TABLE V

SCAN SPEEDS OF EXCITATION MONOCHROMATOR

Number entered into the computer program (1-220)	Actual speed (Å/min)
128	50
166	100
194	200
220	571

TABLE VI

SCAN SPEEDS OF EMISSION MONOCHROMATOR

Number entered into the computer program (1-220)	Actual speed (Å/min)
75	50
128	100
166	200
194	400
220	1125

CHAPTER III

THE ACTIVATION ENERGY OF PROBE

INCOROPORATION IN MODEL

MEMBRANES

Introduction

Extrinsic fluorescent probes have been extensively used in the study of biological membranes. The incorporation of these probes is still an ill-defined process. Fluorescent probes are known to locate in an environment dictated by their polarity. Hydrophobic dyes are usually designed to probe the inside of the bilayer, like 1,6-diphenylhexatriene. Hydrophillic probes are employed in the study of the outer membrane surface. Recently, fluorescent probes like n-(9-anthroyloxy) fatty acids have been designed to mimic the phospholipids by possessing both polar and non-polar regions. These probes span one half of the bilayer depending on the length of their fatty acid chains as shown in Figure 6. A study of the activation energies of incorporation of these lipid-mimic fluorescent dyes into model membranes is detailed below. The results reveal much about the energetics of the incorporation process, and sheds some light on the exact location of the probes.

51
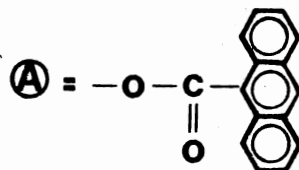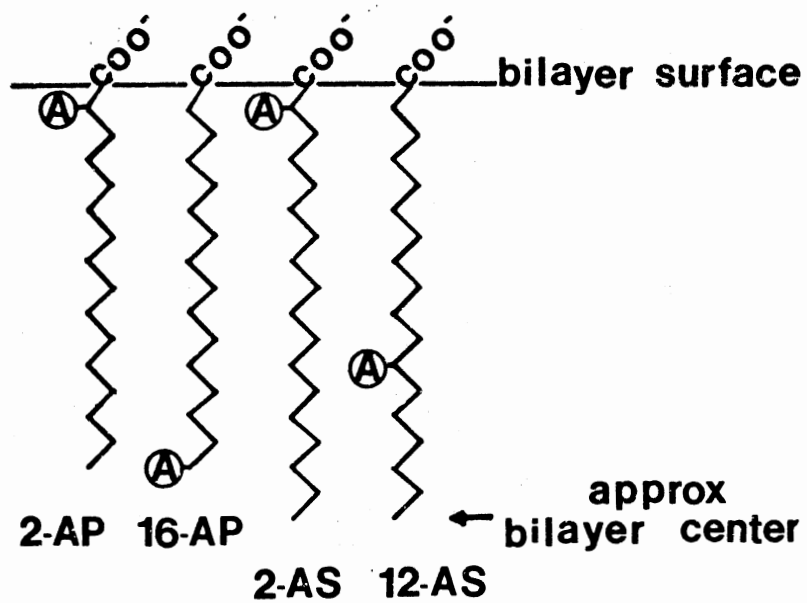
Figure 6.   The Set of n-(9-Anthroyloxy)
            Fatty Acid Fluorescent
            Probes as Located in a
            Biological Membrane.

Results And Discussion

Experimental

Fluorescence spectroscopy was employed in the study of the activation energy of incorporation. In all the activation energy studies, dipalmitoyl phosphatidylcholine vesicles were employed. These were prepared freshly the same day as they were used. The final lipid vesicle suspension consisted of 1.7×10^{-4} M phospholipid in a phosphate buffer of pH=7.4. The housing of the sample compartment was thermostatically controlled over the course of each experiment. The maximum temperature excursion of the sample did not exceed $\pm 0.1^{\circ}$C, over the period of an individual incorporation measurement. The temperature was monitored by a thermocouple immersed into the sample through the cuvette cover. Care was exercised to avoid placing the thermocouple in the path of the exciting beam. Once a constant temperature was achieved, the probe was added to the sample.

To 2.5 ml of vesicle suspension, a small aliquot (1.5 μl) of an organic dye solution in tetrahydrofuran was added giving a final absorption of 0.04. The incorporation process was timed from the point the dye was added. A disposable pipette was used to mix the sample to achieve an even distribution of the dye in the vesicle suspension. It took about three minutes after probe addition for the sample to be positioned properly in the sample chamber and for the

stirrer to be adjusted for uniform stirring speed. A
uniform stirring of the sample was needed to minimize the
noise level in the incorporation curves and to achieve
reproducible data.

The rate of incorporation of the probes by the vesicles
was monitored by following the change (increase/decrease) in
the fluorescence intensity. This change was recorded by a
photon-counting fluorometer as a function of time using a
strip chart recorder.

Wavelength Settings

The wavelength settings of the excitation and emission
monochromators are listed in Table VII.

TABLE VII

WAVELENGTH SETTINGS OF FLUOROMETER
FOR DIFFERENT PROBES

Probe	Excitation(nm)	Emission(nm)
2-AP	363.5	442.5
16-AP	366	439
2-AS	362	446
12-AS	367	458
DPH	355	450

These wavelengths were carefully chosen to obtain a maximum fluorescence intensity with no interference from Raman bands. The Raman bands associated with the lipid vesicles were avoided by using a dilute solution of lipid vesicle suspension. However, the Raman bands of H_2O solvent were unavoidable. Raman emission seemed to distort both the excitation and emission spectra especially at low emission intensities. It was soon apparent that the use of emission filters was not selective enough in such studies. Raman scattering (inelastic light scattering) corresponds to a shift in the original frequency of the emergent light by a quantum of energy corresponding to a vibrational transition of the sample. Raman bands were assigned by measuring the shifts in the wavelengths of the emission maxima while varying the exciting wavelength as shown in equation (15).

$$\bar{\nu}(cm^{-1}) = \frac{1}{\lambda_{exc}(cm)} - \frac{1}{\lambda_{em}(cm)} \qquad \text{Equation (15)}$$

The most intense detected Raman bands of the system used were those of water in the region of 3200 - 3600 cm^{-1}. The other water bands near 1640, 800, 450 and 175 cm^{-1} were extremely weak. The Raman bands of the dipalmitoyl phosphatidylcholine lipid were detected at 2884, 2849, 1130, 1089 and 1064 cm^{-1}.

The band pass of the emission monochromator was typically 3 nm while that of the excitation monochromatar was typically 2.5 nm. The fluorescence intensity of the

chromophore emission was low compared to that of the Raman scattering. This was due to the low probe concentration employed in each experiment. Concentrations were chosen so that the maximum absorption at λ_{max} was less than 0.04 per cm to avoid problems associated with the inner filter effect (103).

Inner Filter Effect

Incorrect interpretation of fluorescent results frequently arises due to the confusion between solute quenching and inner filter effects. Luminescence quenching includes all processes that cause a reduction in the fluorescence or phosphorescence quantum efficiencies. These include internal conversion, intersystem crossing, energy transfer as well as collisions with other solute molecules. Hence, luminescence quenching is a fundamental effect characteristic of the system under consideration. On the other hand, inner filter effects are instrumental artifacts which have no consequence on the primary process of emission. However, these effects reduce the observed fluorescence intensity by either an excessive absorption of the exciting light or by absorption of the emitted luminescence.

Inner filter effects can be minimized by employing a proper geometrical arrangement of the beam of exciting light and the direction of viewing the fluorescence light in relation to the sample. For right angle illumination, the

exciting light passes through the sample in a direction perpendicular to that along which the emitted light is monitored. The cell compartment is constructed in such a way that the photomultiplier sees only the illuminated sample and not the illuminated cell walls. Hence, interferences by stray light arising from reflections off the cuvette faces or fluorescence of the cuvette itself is minimized. The effective intensity reaching the photomultiplier is usually reduced by a factor equal to 10^{-Dd}. D is the total optical density per cm of the sample at the wavelength used for excitation and d is the distance travelled by the exciting light through the sample up to the region viewed by the photomultiplier. According to Parker, this illumination arrangement is suitable for weakly absorbing solutions (103). If Dd is less than 0.02, which amounts to 4.6% absorption, then no correction is necessary for the observed fluorescence intensity. Absorbances of 0.04 per cm were employed in all the activation energy experiments. Since the emission was sampled from the middle of the cuvette, this corresponded to a Dd value of 0.02.

Incorporation Curves

The fluorescence intensity increased with time as the incorporation process took place. This was observed for the n-(9-anthroyloxy) fatty acid probes as well as 1,6-diphenylhexatriene. The increase was exponential and levelled off at long times. All the incorporation curves

for the different probes were similar in their exponential rise. Some typical incorporation curves are shown in Figure 7, for 12-(9-anthroyloxy)stearic acid, measured at different temperatures of incorporation into the lipid vesicles, as a function of time. At temperatures above the phase transition of the lipid, the incorporation of all the probes was essentially instantaneous for the time scale of these experiments. After the incorporation was over, emission and excitation spectra of the different incorporated probes were taken. These spectra are shown in Appendix B.

Data Analysis

The linear fluorescence intensity, reached at long times, was extrapolated back to earlier times. A fluorescence intensity difference, extrapolated minus observed, was obtained from this straight line. When plotted against time, logarithmic incorporation curves were attained as shown in Figure 8. It was clear that the incorporation processes of these probes into the lipid vesicles, on a time scale larger than 1 min, were first order or pseudo-first order. The data is not shown for times less than 5 minutes, due to the time it took the sample to stabilize after the probe addition. Turbulence was noted immediately after probe addition. The rate constants of the incorporation processes were obtained from the slopes of the semi-logarithmic plots of the fluorescence intensity differences according to the equation (16):
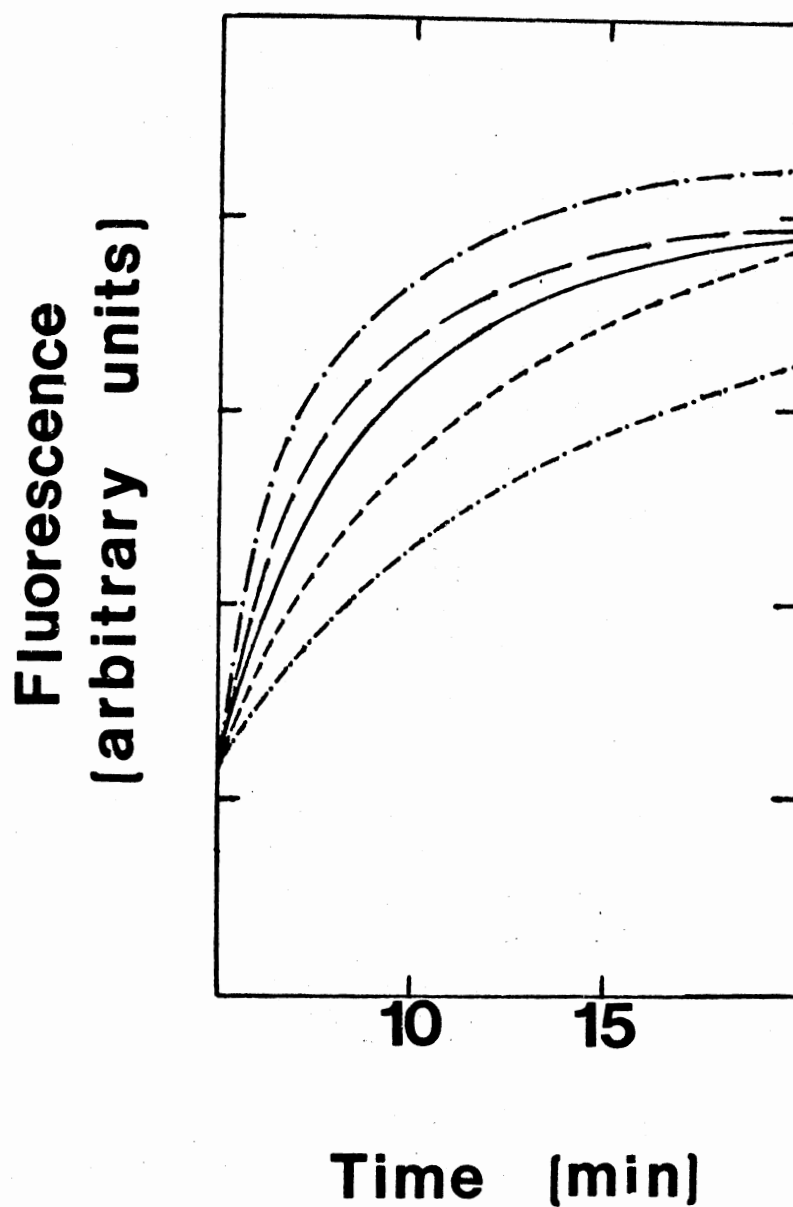
Figure 7. The Relative Fluorescent
Intensity of 12-AS,
Measured at Different
Temperatures of Incorpor-
ation into DPPC
Vesicles, as a Function of
Time.   -.-.-, Temp=20°C;
-----, Temp=25°C; ———,
Temp=35°C; — — —,
Temp=38.5^{o}C; —.—.—,
Temp=40.5^{o}C.
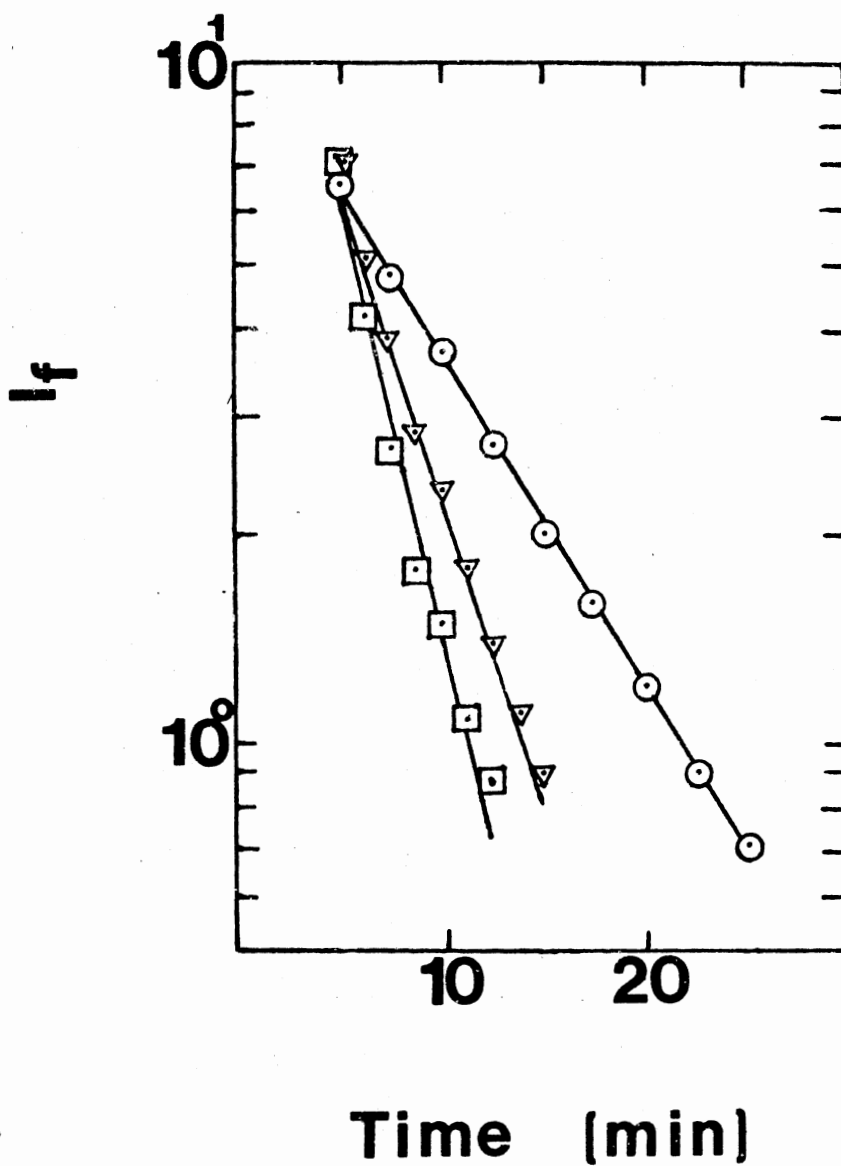
Figure 8. Semi-Logarithmic Plots of the
Fluorescent Intensity Differ-
ence for the Case of 12-AS
Incorporated into DPPC
Vesicles at Different Tempera-
tures, as a Function of
Incorporation Time.
⊙----⊙, Temp=20°C;
▽----▽, Temp=35°C;
▣--▣ , Temp=40.5°C.

$$\ln (I_f - I_t) = - kt \qquad \text{Equation (16)}$$

where I_f is the final fluorescence intensity attained as a plateau in the incorporation curves; I_t is the fluorescent intensity at any time t, and k is the rate constant for incorporation.

Activation Energies

The rate constants are related to the activation energies of incorporation according to the formula:

$$k = A \times e^{(-E_{act}/RT)} \qquad \text{Equation (17)}$$

Where E_{act} is the Arrhenius activation energy, A is the preexponential factor and k is the rate constant for incorporation. T stands for the absolute temperature of the system while R is the gas constant. From the Arrhenius plots of the rate constants for incorporation, activation energies were calculated from the relative slopes, Table VIII. Some of these Arrhenius plots are shown in Figure 9. The error limits were calculated from the standard deviation of the rate constants for one set of measurements. The preexponential factors A, measured from the intercepts of the Arrhenius plots, are listed for all the probes in Table IX. These preexponential factors, also known as the frequency factors, correspond to the collision frequencies between the fluorescent dyes and the lipid vesicles and to the orientation factors of the molecules during the collision process.

TABLE VIII

CALCULATED ACTIVATION ENERGIES

Probe	E_{act}(Kcal)
2-AP	2.6 ± 0.3
16-AP	12 ± 1
2-AS	5 ± 1
12-AS	10 ± 1
DPH	23 ± 2

Table IX

CALCULATED PREEXPONENTIAL FACTORS

Probe	$A(cm^3 \ mol^{-1} \ s^{-1})$
2-AP	16
16-AP	4×10^7
2-AS	6×10^3
12-AS	2×10^6
DPH	2.5×10^{15}
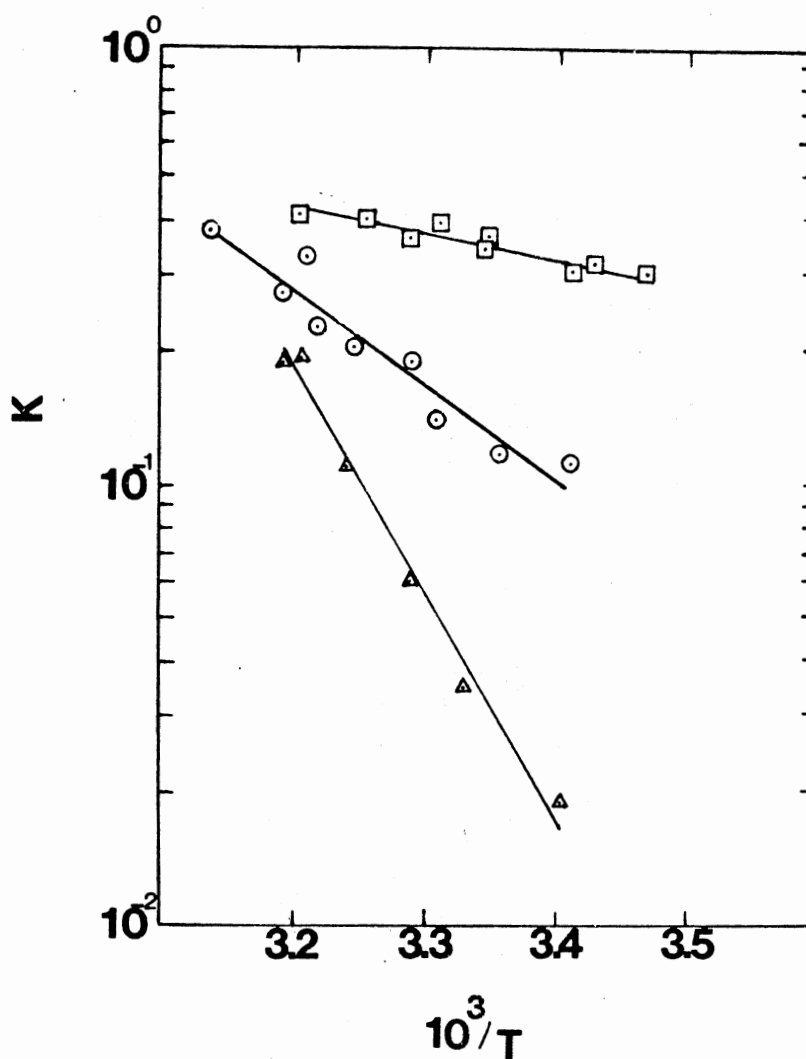
Figure 9. Arrhenius Plots of the Rate
Constants for Incorporation
of 2-(9-Anthroyloxy)Palmitic
Acid (□---------□); 12-(9-
Anthroyloxy)Stearic Acid
(⊙---------⊙);
and 1,6-Diphenylhexatriene
(△---------△) into Dipal-
mitoyl Phosphatidylcholine
Vesicles.

Controls

Anthracene was used in the hope that it would be a good control for the n-(9-anthroyloxy)fatty acids, since they all share the same fluorescent moiety, an anthryl group. However, difficulties were encountered in obtaining reproducible data for its incorporation. A relative activation energy of (11.5 ± 1) Kcal was obtained. A decrease in fluorescence intensity was observed for anthracene's incorporation as opposed to the increase observed using the other probes. Excitation was at $\lambda_{exc} = 374$ nm while the emission was monitored at $\lambda_{em} = 401$ nm. The non-reproducibilty of the anthracene data may be attributed to the different binding sites occupied by the probe inside the membrane.

Control experiments were conducted for all the fluorescent probes employed. These involved a repetition of the experiments with no vesicles present. Hence, the probe was added to the phosphate buffer instead. The mixing of the tetrahydrofuran, used as a probe solvent, with the phosphate buffer led to some increase in the fluorescence intensity. Rate constants were obtained, at different temperatures, following the same procedure as before. The calculated rate constants, for all the probe controls, seemed to be independent of temperature as shown in Table X, for an example purpose. Arrhenius plots of these control rate constants gave slopes of approximately 0 K, indicating no activation energies.

TABLE X

RATE CONSTANTS FOR THE PROBE 12-(9-ANTH-ROYLOXY)STEARIC ACID AS A FUNCTION OF TEMPERATURE

Temperature(^{o}C)	Rate Constant
48	0.0688
43	0.0687
37	0.0758
32.9	0.0935
32.6	0.0757
32.3	0.0831
29	0.0962
23.4	0.0873

Discussion

Examination of the calculated activation energies listed in Table VIII, reflect a great deal of information about the process of probe incorporation as well as the membrane itself. An enhancement in the fluorescence intensity was due to an increase in the fluorescence quantum yields of the probes as they were transferred from an aqueous medium (buffer) into a hydrophobic environment. Such studies showed that binding of all the probes were dependent on the incubation temperature in agreement with Lang et al. (111).

The insertion energy was found to be lowest when the chromophore moiety (anthracene) was nearest the polar end of the probe. Thus, the insertion energies for 2-(9-anthroyloxy)stearic acid and 2-(9-anthroyloxy)palmitic acid (5 and 2.6 Kcal, respectively) are much lower than the insertion energies for probes in which the chromophore is well removed from the polar head group, as in 16-(9-anthroyloxy)palmitic acid and 12-(9-anthroyloxy)steatric acid. The insertion energies for these probes were 12 and 10 Kcal respectively. This gives implicit credibility to the idea that the n-(9-anthroyloxy)fatty acids align themselves with the lipids in the bilayer. Such results agree with the information derived from the structure of these probes, as to their expected location in a biological membrane. As further confirmation of the above, it is noteworthy that the insertion energy for 12-(9-anthroyloxy)stearic acid is lower than that for 16-(9-anthroyloxy)palmitic acid, although by only 2 Kcal.

From this data it can be concluded that moving the chromophore 14 carbons down the lipid chain (16 vs. 2)-(9-anthroyloxy)palmitic acids increases the insertion energy by about 0.7 Kcal per carbon. The same trend is seen when comparing the insertion energies for 12 and 2-(9-anthroyloxy) stearic acids. In that case, the energy increases by 0.5 Kcal per carbon. The two figures are well within experimental error of each other giving an average

insertion energy of 0.6 kcal per carbon.

There remains a difference in insertion energies between 2-(9-anthroyloxy) palmitic acid (2.6 Kcal) and 2-(9-anthroyloxy)stearic acid (5 kcal) to be explained. The probe 2-(9-anthroyloxy)stearic acid has a lipid chain two carbons longer than 2-(9-anthroyloxy)palmitic acid. This fact must account for some of the difference. However, such a comparsion of chain lengths can not be made between the probes 12-(9-anthroyloxy)stearic acid and 16-(9-anthroyloxy)palmitic acid. Since the position of the anthracene chromophore is the dominant cause for the high or low insertion energy.

Finally, the above conditions shed some light on the result obtained for 1,6-diphenylhexatriene. The insertion energy for 1,6-diphenylhexatriene is a factor of 2 greater than that 16-(9-anthroyloxy)palmitic acid. This is consistent with locating 1,6-diphenylhexatriene in the middle of the bilayer, perhaps with the long molecular axis oriented parallel to the plane of the bilayer.

Applications

An induced solid tumor, 13762 rat mammary adenocarcinoma, was adapted for growth of ascites at Mason Research Institute (Tumor Bank Inventory). Three pharmacologically distinct sublines were isolated MAT-A, MAT-B and MAT-C. After several passages in Carraway's laboratory (Oklahoma State University, Biochemistry), the

MAT-B and MAT-C ascites lines became the more stable MAT-B1 and MAT-C1 lines (Rockley, N. L., private communication). Although these ascites were still adenocarcinomas, they both exhibited different surface structures. MAT-C1 cells had an irregular surface covered with branched microvilli, while MAT-B1 cells acquired a more normal appearance as was evidenced by scanning electron microscopy (127). The morphological differences were quite marked between the two cell lines.

In order to study the validity of the incorporation studies, this method was used to obtain data on the occlusion of membrane surfaces by glycoproteins employing these two different cell lines. Fluorescence polarization studies of the probe 1,6-diphenylhexatriene incorporated into these cells showed no differences between the two cell lines. These polarization curves, shown in figures 10 and 11, had the same polarization values both above and below the phase transition, as well as a similar broad phase transition. Such a study was not sensitive enough to differentiate between the two cells, although they were known to have different morphological activities. However, when this method was applied to the incorporation of 1,6-diphenylhexatriene into these cells different activation energies were obtained. In both cases, 1,6-diphenylhexatriene was excited at 355 nm and the fluorescence intensity was monitored at 450 nm. Similar probe and cell membrane concentrations were employed in this

DPH/MEMBRANES
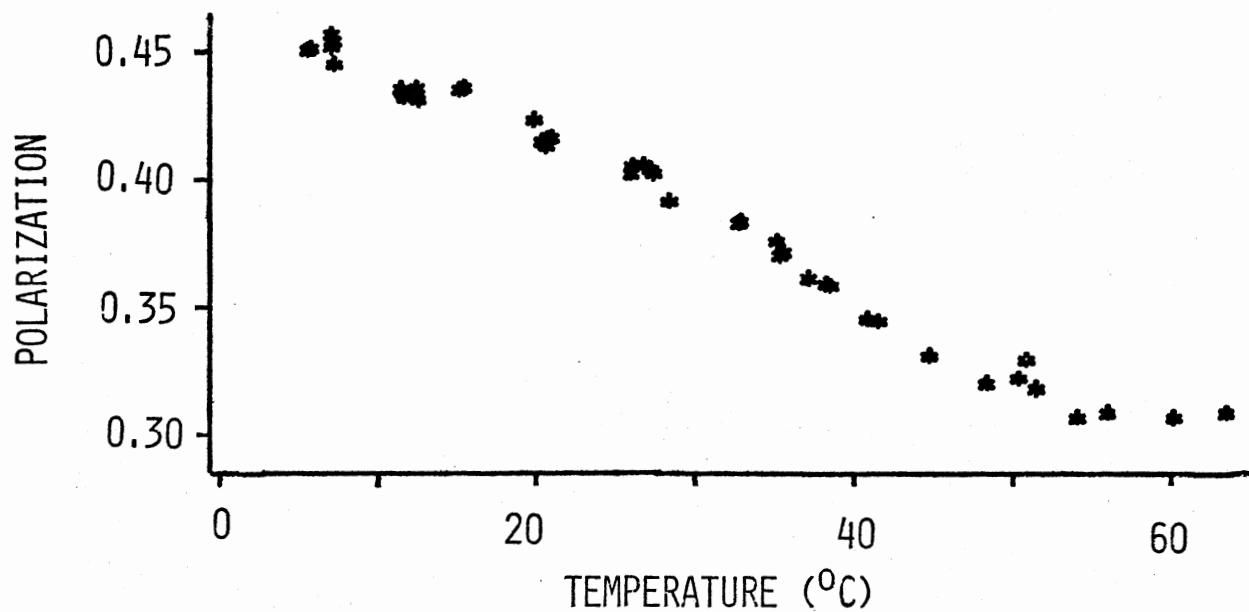
CANCER CELLS B1

Figure 10.   Polarization Values Measured at Different
Temperatures of 1,6-diphenylhexatriene
Incorporated into MAT-B$_1$ Microvilli.
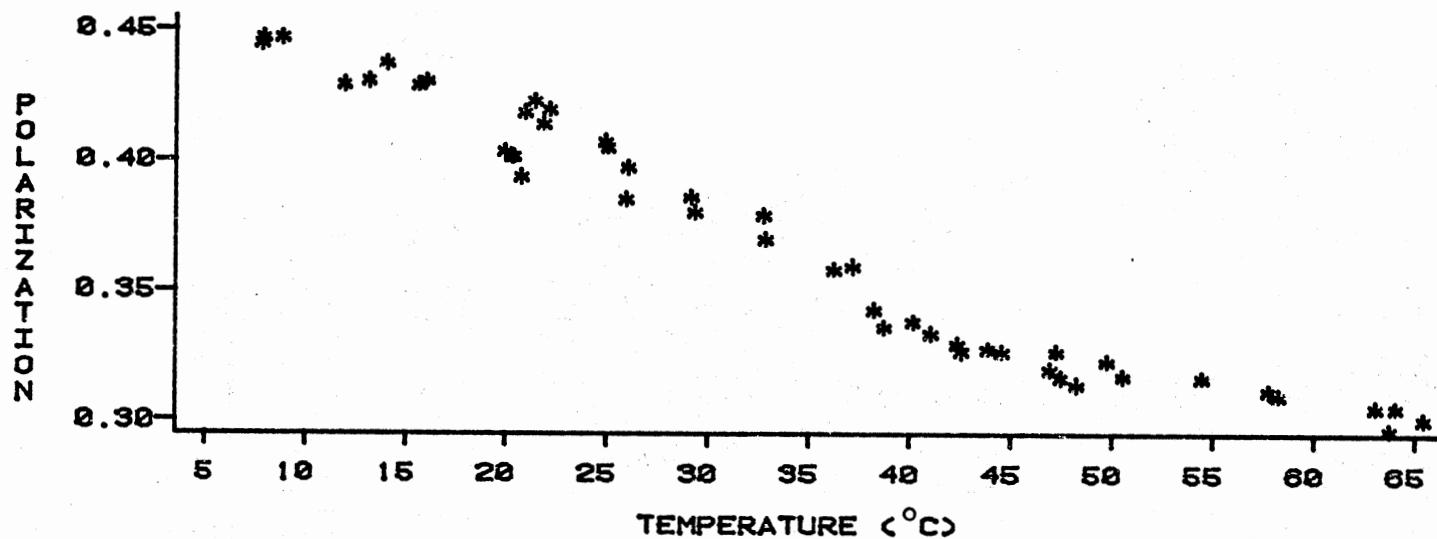
CANCER CELLS C1

Figure 11. Polarization Values Measured at Different
Temperatures of 1,6-diphenylhexatriene
Incorporated into MAT-C_1 Microvilli.

study, for a comparison with the model membrane vesicles. Examination of the calculated activation energies, listed in Table XI, show a difference of about 8 Kcal of insertion. This was attributed to the presence of bulky glycoproteins on the surface of MAT-C_1 membrane surface which blocked the entrance of DPH. Such results were consistent with the biological information collected about these membranes. However, a comparison of the insertion energies of 1,6-diphenylhexatriene in model membranes (23 Kcal) to that of the MAT-B_1 and MAT-C_1 cancerous cells (12 and 18 Kcal, respectively) shows a pronounced difference. The fact that the model membrane vesicles consist only of the lipid dipalmitoyl phosphatidylcholine, as opposed to the presence of many lipids and proteins in case of the real cells, accounts for most of that difference. The model systems are much more ordered and hence much less fluid in the gel phase, thus requiring larger activation energies for the probe.

This method was also used to characterize one of a series of synthesized fluorescent probes (128). The general formula and structure of the compound Methyl 5-(2-Anthryl)pentanoate are shown below.

$$Ar(CH_2)_4CO_2R$$
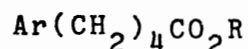
where AR = 2-anthryl and R = CH_3

TABLE XI

ACTIVATION ENERGIES OF DPH IN
DIFFERENT CANCER CELL LINES

Microvilli	E_{act}(Kcal)
MAT-B$_1$	12 ± 1.5
MAT-C$_1$	18 ± 2
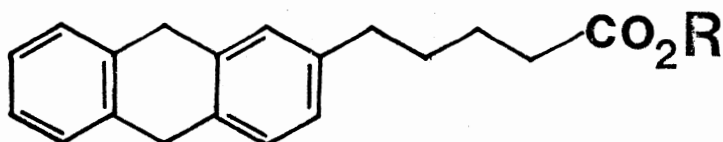
This compound has the acyl and polar head groups attached linearly to the fluorescent anthracene moiety (i.e. at the 2-position, instead of the more usual 9-position) . The fluorescent group in this compound will align itself parallel to the fatty acid chains inside the biological membrane. Thus, a minimum disturbance to the lipid domain is expected. On the other hand, the set of n-(9-anthroyloxy)fatty acid lipid mimic probes position themselves in such a way that the anthracene moiety is perpendicular to the fatty acid chains. This is due to the fact that the fatty acid chains of these lipid-mimic probes are attached at the 9 position on the anthracene. Although the set of n-(9-anthroyloxy) fatty acid probes have proved to be of great importance in membrane studies, they do cause

some perturbation in the membrane (129).

The probe methyl 5-(2-anthryl)pentanoate was excited at 407.5 nm while the emission was monitored at 359 nm. All the probe and membrane concentrations were kept the same as for the previous incorporation studies, for comparison purposes. An activation energy of 10 Kcal was calculated. This is the same insertion energy as was found for 12-(9-anthroyloxy)stearic acid. Both of these probes had to move the chromophore about 12 carbons down into the lipid domain, accounting for the carbons on the anthracene back bone in case of 12-(9-anthroyloxy)stearic acid. It is apparent that the insertion energy is not lowered by the improved configuration of the probe. Polarization studies are required to establish whether or not the bulk lipid structure is less perturbed.

Conclusions

Although these results are very tedious to obtain with any degree of reproducibility, they do provide information that is not available by any other methods. Furthermore, the results reported here verify the binding constant efficiency data obtained in separate studies of the uptake and fluorescence quenching of n-(9-anthroyloxy) fatty acid probes (130, 131).

Such kinetic studies may be used to follow the rate of membrane perturbation as well as the change in the membrane structure during the process of incorporation. A study of

the surface properties of cell membranes, which are essential for the immunological activity of the cell, can also be conducted employing such a method. This research can be further carried on by employing other fluorescent probes of different fatty acid chain lengths and chromophore positions, to elaborate more on this method's validity and it's range of application. These studies should be extended to other lipid model vesicle systems, having different polar heads and fatty acid chains. Once these monolipid system studies are completed, the work should be extended to systems of multilipids and proteins and to multilamellar dispersions.

CHAPTER IV

SATURATION OF BIOLOGICAL MEMBRANES CAUSED
BY FLUORESCENT PROBES

Introduction

The wide use of extrinsic fluorescent probes in the characterization of biological membranes should be treated with care, due to the introduction of external molecules into the membrane (45). However, these extrinsic fluorescent probes are of special interest because they can be designed with certain fluorescent properties and with polarities which dictate their location within the membrane (132). These probes introduce some perturbation to the system as opposed to the use of intrinsic fluorescent probes, like tryptophan and tyrosine in proteins, which are usually inherent in the biological membrane system.

Although extensive research has been conducted in this area, there remains the nagging questions concerning the membrane perturbation caused by the "impurity" nature of these fluorescent dyes, and how much dye can be incorporated into the membrane before saturation can be reached (35, 69, 130, 133-136). The criticism of saturating the membrane with the fluorescent probe has, for example, been raised in a study of the lipid phase transitions of Escherichia Coli

using fluorescent techniques (137). In order to avoid the saturation problem, ideal systems of minimal probe concentrations should be employed. However, an ample amount of the dye is required for any significant fluorescent signal to be observed. To examine this problem more closely, UV/Visible absorption spectra of model lipid vesicles with incorporated fluorescent probes at several concentrations have been measured. A series of n-(9-anthroyloxy)fatty acids which are lipid-mimic fluorescent probes was employed. These probes are known to locate themselves at different depths in the membrane according to a study of activation energies of incorporation (Chapter III). The actual incorporation of these probes was monitored by following their absorption spectra during the incorporation process. Experiments in which the vesicles were titrated with probe concentrations indicated the presence of probe/lipid ratios beyond which the membrane was saturated with the dye.

Solvent Effects on Absorption Spectra

Almost all absorption and emission spectra of fluorescent molecules, when applied to biological membranes, are taken in the liquid phase. Hence, the need to understand the interaction of the different solvents with the fluorescent molecules is essential.

The two types of intermolecular interactions responsible for any spectral changes in a solvent medium are

the universal and the specific interactions (98). The latter corresponds to the formation of hydrogen bonds, complexes and exciplexes resulting from the molecular properties of the solvent and solute. Whereas the universal interaction is due to the influence of the solvent as a dielectric medium, and depends on the dielectric constant and the refractive index of the solvent. A blue wavelength shift in the absorption spectra is usually due to an increase in the energy spacing between the ground and the excited electronic states. This is accomplished by either raising the energy level of the excited electronic state or by lowering the ground electronic level. On the other hand, a red wavelength shift in the absorption spectra corresponds to a lower energy difference between the ground and excited states. This happens by either raising the ground energy level, or by lowering of the excited energy state. Although one of the two processes or both are responsible for each phenomena, it is not always possible to differentiate between them.

The changes in the energy levels are attributed to dipole-dipole interactions between the ground and excited states. Such interactions usually correspond to a shift in the Frank-Condon excited state, resulting in an equilibrium excited state, hence stabilizing the molecule. The solvent interaction with the different fluorescent molecules is used to study the membrane saturation caused by the excessive use of dyes in membrane studies.

Results and Discussions

Controls

Absorption spectrophotometry seemed to be a sensitive method for measurement of membrane saturation caused by fluorescent probes. However, stringent control of the purity of the glassware was essential for getting any reproducible data. The absence of interfering absorptions by impurities adhering to the cuvette walls or present in the solvents was guaranted by running absorption control experiments until a flat baseline (within $\pm$ 0.001 absorbance units) from 850-210 nm was achieved with vesicles but no probe in the sample compartment of the spectrophotometer.

Stirring the sample was also essential for getting reproducible spectra and absorptions. Control experiments indicated that stirring of the vesicles did not alter the rate of probe incorporation into the vesicles and had no consequences on the absorbance measurements.

The saturation experiments were based on observations of any differences in the absorption spectra of the fluorescent probe incorporated inside the vesicles compared with that in the phosphate buffer solution. Hence, measurement of the absorption spectra of the fluorescent probes in different solvent systems was essential. For example, the spectra of the probes in tetrahydrofuran were measured to insure that the spectra of the probes after incorporation were not like that of the fluorescent probes

in the tetrahydrofuran solvent. Also spectra of the fluorescent probes were taken in the phosphate buffer to insure the non-formation of micellar systems upon the addition of the probe. These controls were essential since the probes were added to the vesicle suspension from a stock solution of probe in tetrahydrofuran solvent. Control absorption spectra of the different probes were also taken in non-polar solvents, like heptane, for comparison purposes with those of the incorporated probes.

UV-Visible Absorption

The same set of n-(9-anthroyloxy)fatty acid probes as well as 1,6-diphenylhexatriene were employed in these experiments. The absorbance of these probes seemed to differ with the polarity of the solvent used. Spectral positions and band shapes also varied with the solvents. By utilizing these spectral changes, some idea about the polarity of the probe environment could be inferred. Moreover, by following such spectral changes as a function of incorporation, information as to the rates of probe incorporation could be obtained. Such spectral and absorbance changes were recorded over a range of wavelengths during the progress of probe incorporation.

Analysis of 16-(9-Anthroyloxy)Palmitic
Acid Spectra

An example of the spectrum vs. time of incorporation

for the case of 16-(9-anthroyloxy)palmitic acid is shown in Figure 12. A description of the spectra and figures of the other probes is included in the same chapter, as a separate section (Absorption Spectra).

A change in the spectral shape is noticed in Figure 12 as the probe 16-(9-anthroyloxy)palmitic acid starts to incorporate into the membrane. The absorption spectra of 16-AP in all the polar solvents (e.g. methanol, buffer) were similar. Also a similarity in spectral shape was observed for the probe in all non-polar solvents (e.g. heptane and the inside of the vesicles). This incorporation of the probe was therefore followed by measuring its absorption spectra many times during the incorporation process until there was no further change in the spectral shape and absorbance intensities. Once that point was reached, it was evident that the incorporation process was over. The absorbance spectra of the incorporated probes were very similar to that of the probes in heptane, hence indicating that the final environment of the incorporated probes is hydrophobic in nature. An example of the spectrum of the incorporated probe is shown for the case of 16-(9-anthroyloxy)palmitic acid in Figure 13, while those in heptane and buffer, shown for comparison purposes, are in Figure 14.

Examination of the spectra in Figures 13-16, shows that prior to incorporation the spectrum of the probe is very similar to that of the probe in the phosphate buffer.
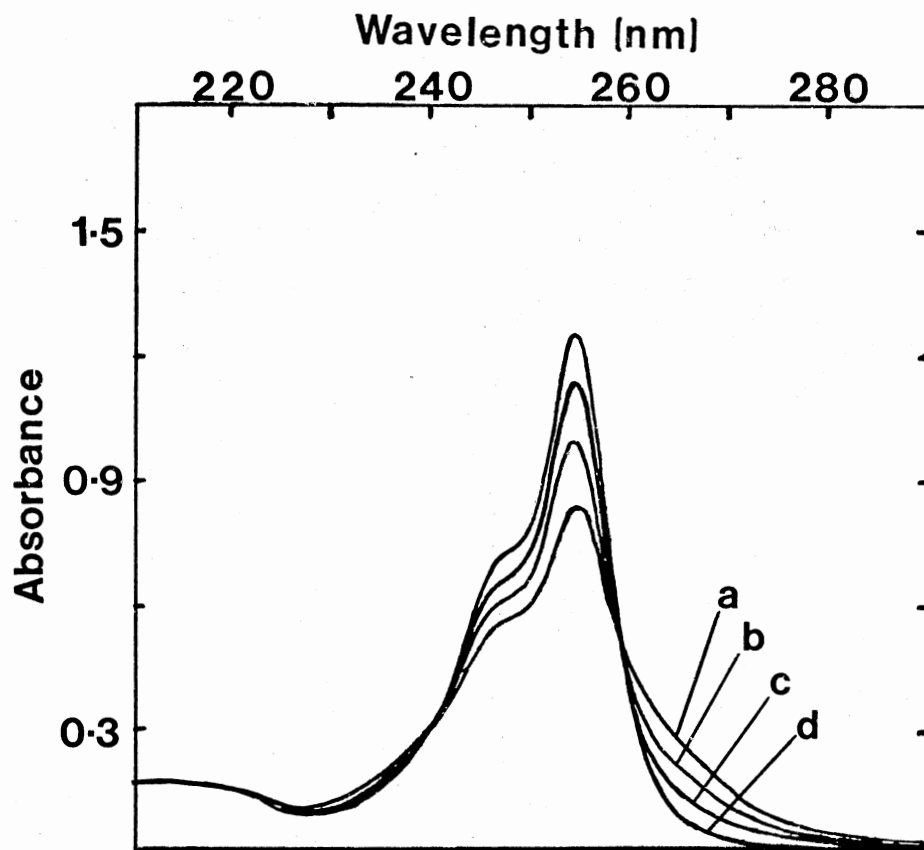
Figure 12. Absorption Spectra Vs. Time of Incorporation for 16-(9-Anthroyloxy) Palmitic Acid. a = 1, b = 2.5, c = 4 and d = 5.5 Minutes After Addition of Probe to the Vesicle Suspension.
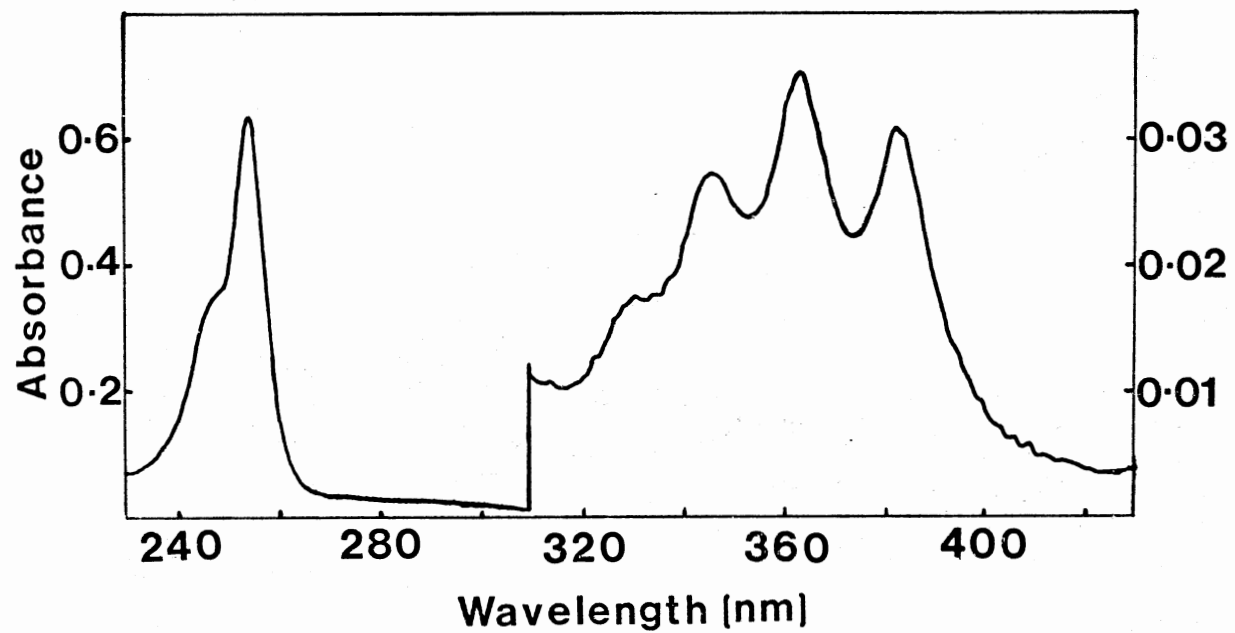
Figure 13.   Absorption Spectrum of 16-(9-Anthroyloxy)Palmitic
Acid in Lipid Vesicles.
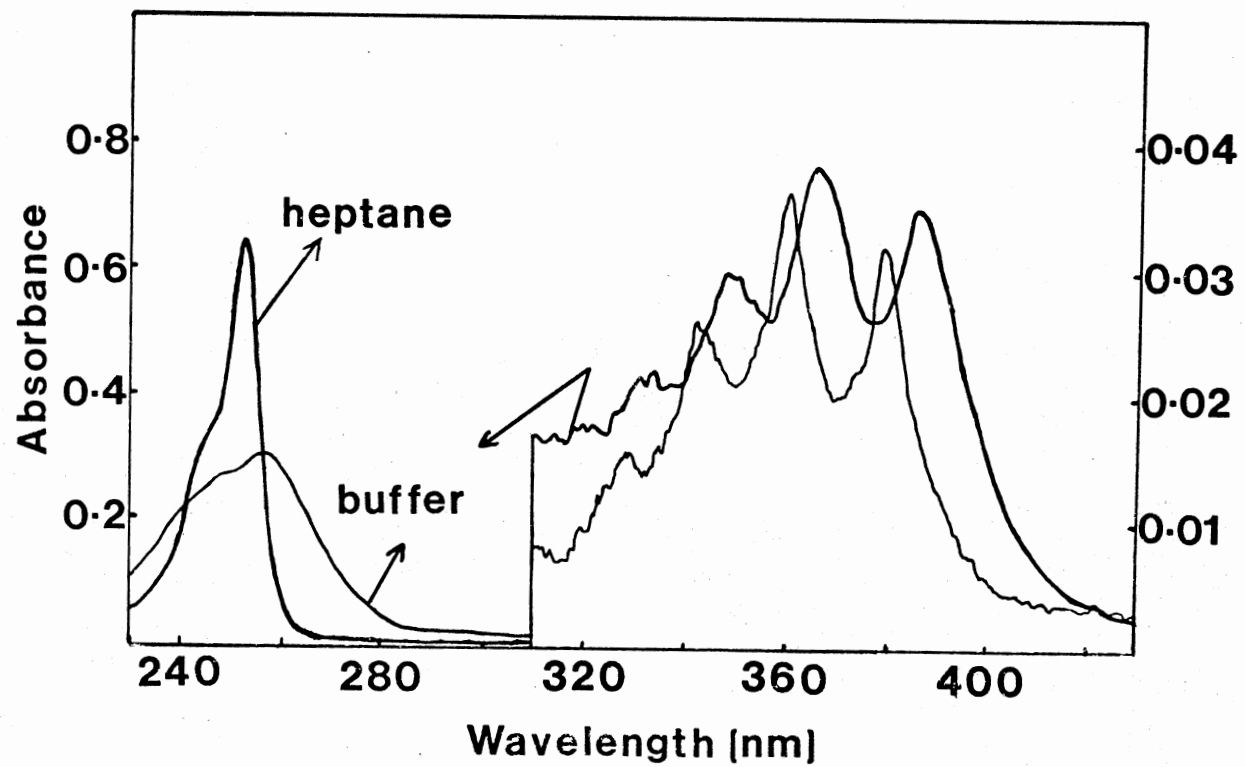
Figure 14. Absorption Spectra of 16-(9-Anthroyloxy)Palmitic Acid in Heptane and in Buffer.
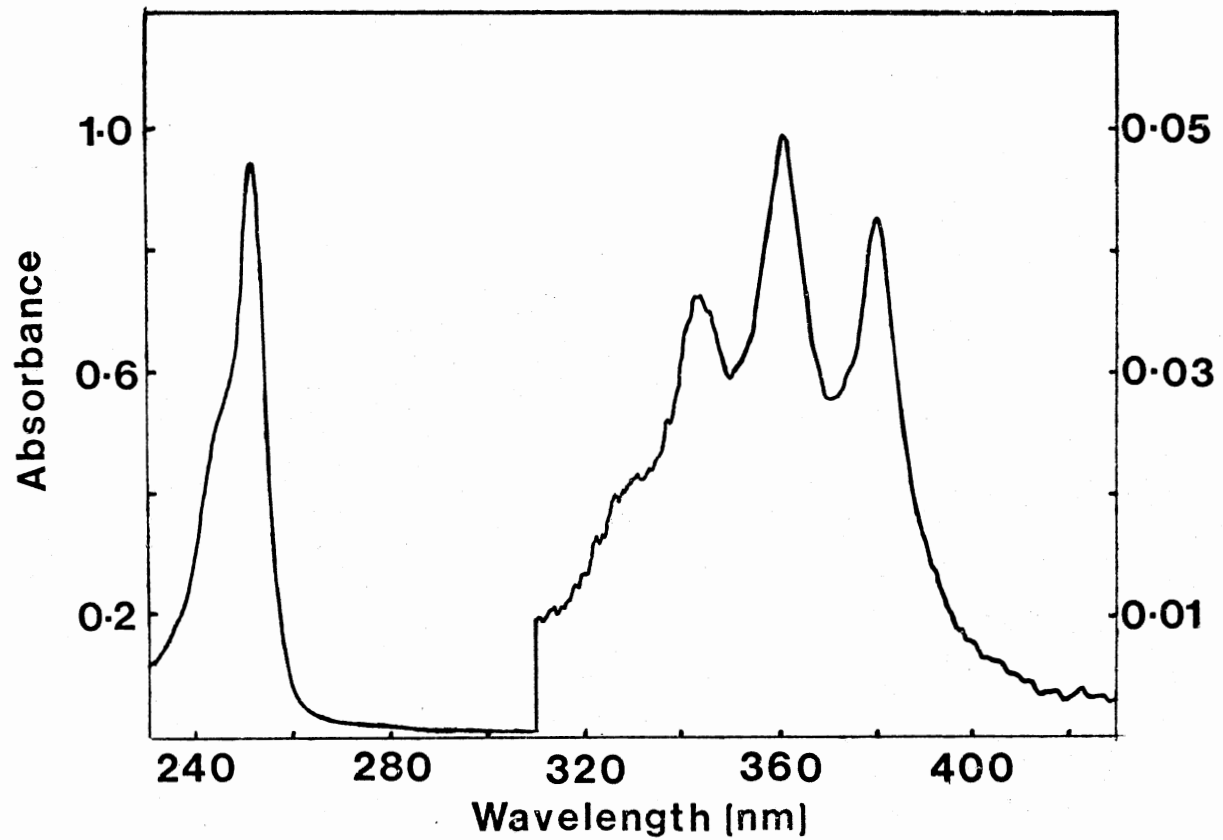
Figure 15. Absorption Spectrum of 16-(9-Anthroyloxy) Palmitic Acid in Methanol.
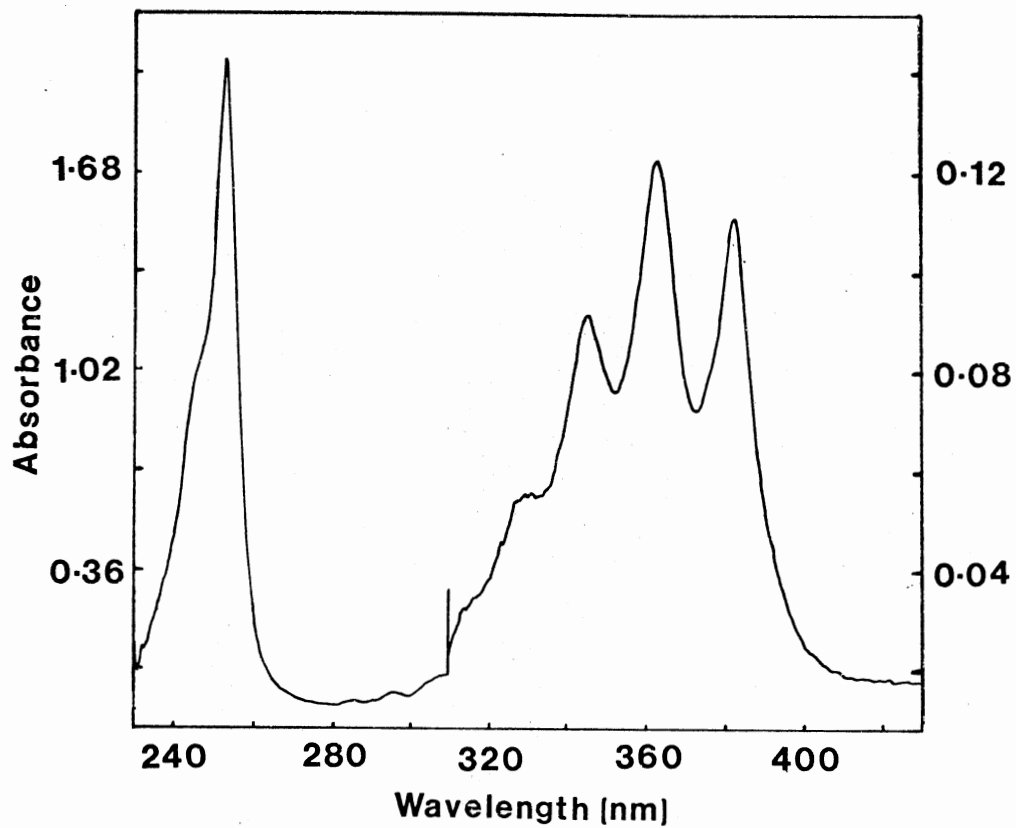
Figure 16. Absorption Spectrum of 16-(9-Anthroyl-
oxy) Palmitic Acid in Tetrahydrofuran.

However, upon incorporation a hypsochromic (shorter) wavelength shift for the absorption at 260 nm, for example, was observed. In addition to that, both hyperchromic (increase) effect for the absorption intensities at 256 and 380 nm, and hypochromic (decrease) effect for the absorptions at 370 and 350 nm, for example purposes, were also evident. These spectral changes were apparent over the entire spectral range.

The presence of a couple of isoabsorptive points in Figure 12, indicates the occurance of at least two different environments in which the probe resides (138). The areas underneath the absorption curves of the incorporated probe and that in the phosphate buffer solution were found to be equal within experimental error.

Saturation Experiments

Saturation of the biological membrane was observed by running an absorbance experiment in which successive small aliquots (μl) of the probe solution were added to the same vesicle suspension volume. Once the probe was completely incorporated, absorbance measurements were taken at different wavelengths. The fact that the incorporation of certain fluorescent probes takes a long period of time, (over 3 hrs for the case of 1,6-diphenylhexatriene) makes each saturating experiment very time consuming. In addition, the fact that the auto-zeroing of the machine is an important factor in the absorbance measurements makes

keeping the machine on for a long period of time (2 days) unfavorable. Hence, for those experiments involving only the measurement of the critical saturating concentration, incorporation of the probes into the vesicles were conducted at temperatures above the phase transition of the lipid. Such observation of maximum rate of incorporation at these temperatures has been reported previously (118). Once the incorporation was over, the sample was cooled down to room temperature, before any measurements were taken. Experiments were repeated several times to prove the reproducibility of the results.

Data Analysis

Beer's law plots of the data obtained from the control studies, showed a linearity over the concentration range used. These curves were obtained for almost the entire spectral range. An example of these control plots for the case of 16-(9-anthroyloxy) palmitic acid in methanol is shown in Figures 17 and 18. These controls were performed to indicate the non-formation of any probe dimers or excimers upon the addition of the probe into the lipid vesicle suspension or the solvent system. Any deviation from Beer's law would either indicate the presence of a dimer or the saturation of the membrane.

CONTROL "16AP/METHANOL"
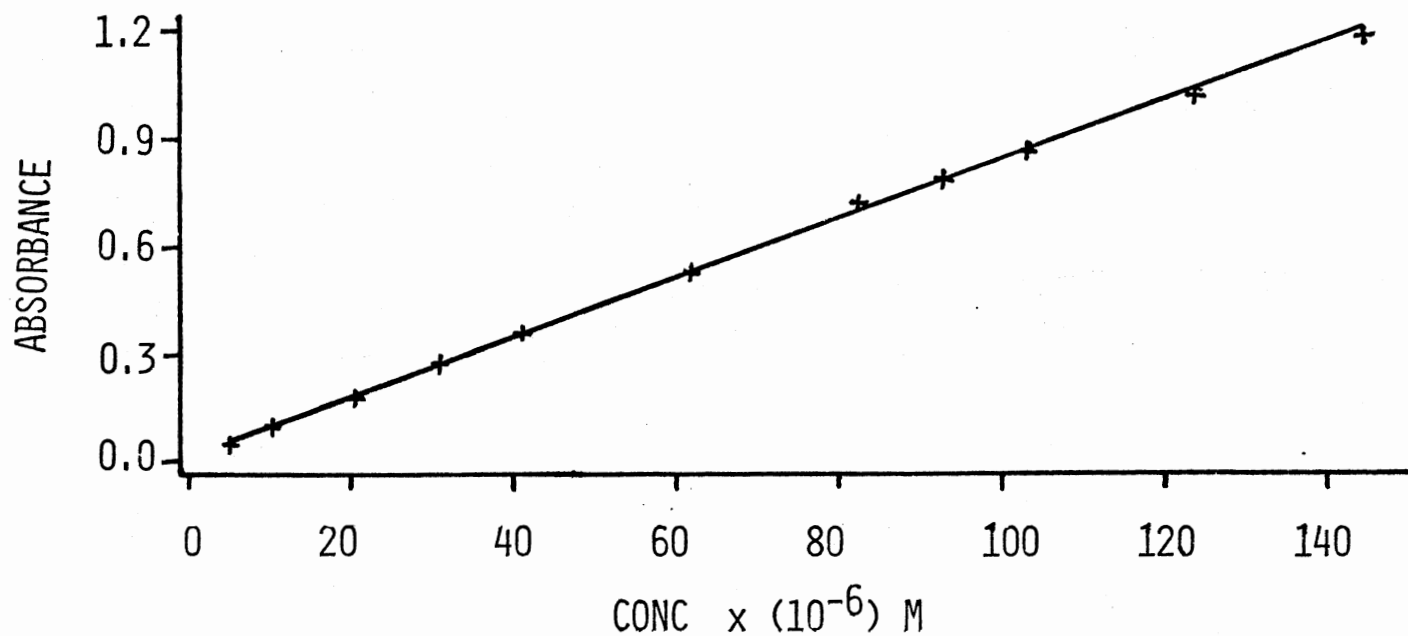
381 NM

Figure 17.   Beer's Law Plot of 16-(9-Anthroyloxy)Palmitic
Acid in Methanol at 381 nm.

CONTROL "16AP/METHANOL"

CONC x (10^{-6}) M
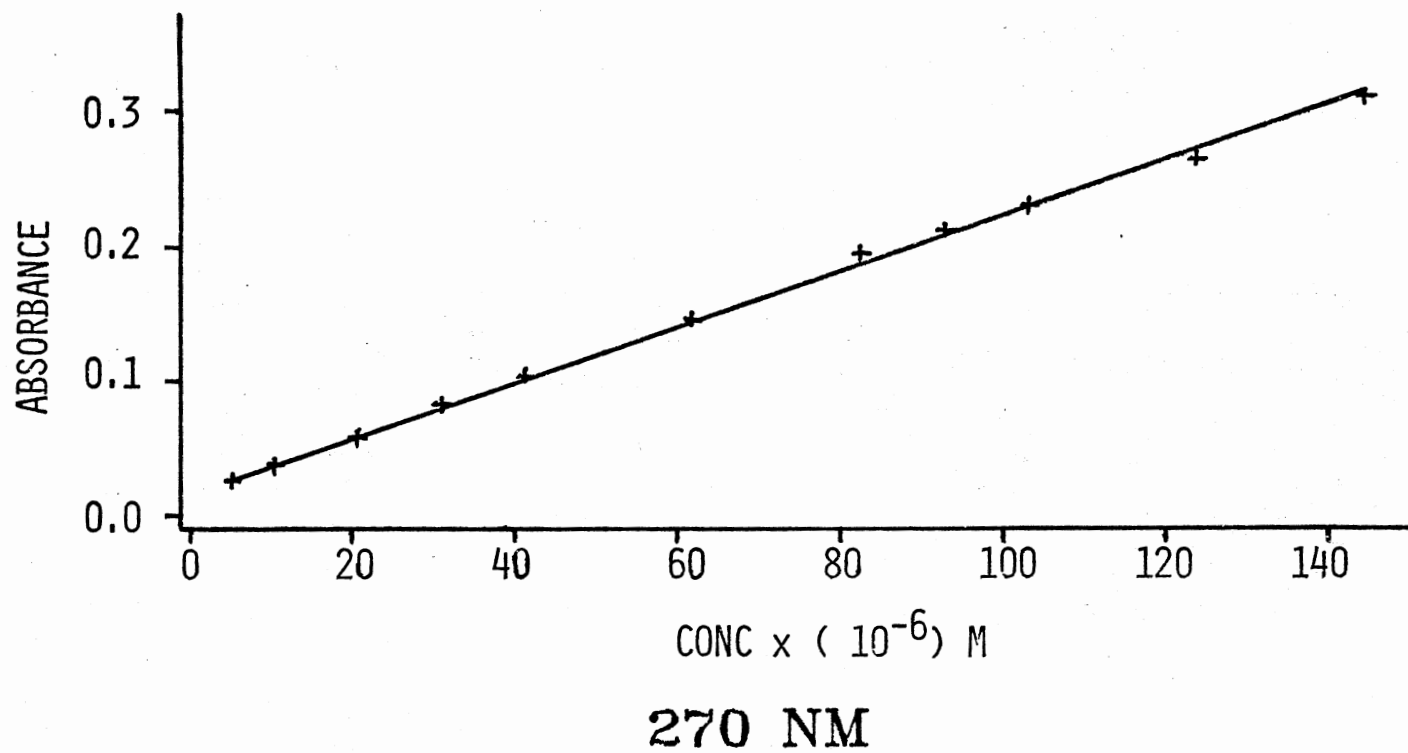
270 NM

Figure 18.   Beer's Law Plot of 16-(9-Anthroyloxy)Palmitic
Acid in Methanol at 270 nm.

During the titration experiments, in which probes were incorporated at successively increasing concentrations into the vesicles, non-linearity in the Beer's plots was observed for all probes. The presence of a clear break in the linearity of these plots was evident above a certain critical probe/lipid ratio. This break was consistent with the appearance of the isoabsorptive points in the absorbance spectra, indicating the presence of two different environments. Below the break point, the absorption spectra of the incorporated probes were consistent with those in non-polar environments, hence stressing the hydrophobic nature of the inside of the membrane and the fact that all of the probe lies inside the membrane. On the other hand, it was clear that above the break point, the probes were present in two different environments indicating the presence of an excess amount of probe floating in the buffer solution outside the vesicles. The relative slopes of the lines below the break points indicate the molar absorptivities of the probes inside the vesicles, while those of the lines above the break points represent a combination of molar absorptivities of the probes inside as well as outside the vesicles. For the case of 16-(9-anthroyloxy)palmitic acid, the break point is clearly evident in Figures 19-21.

For measurements taken at different wavelengths, these plots were similar for the same probe, indicating the presence of a break point at the same critical probe/lipid
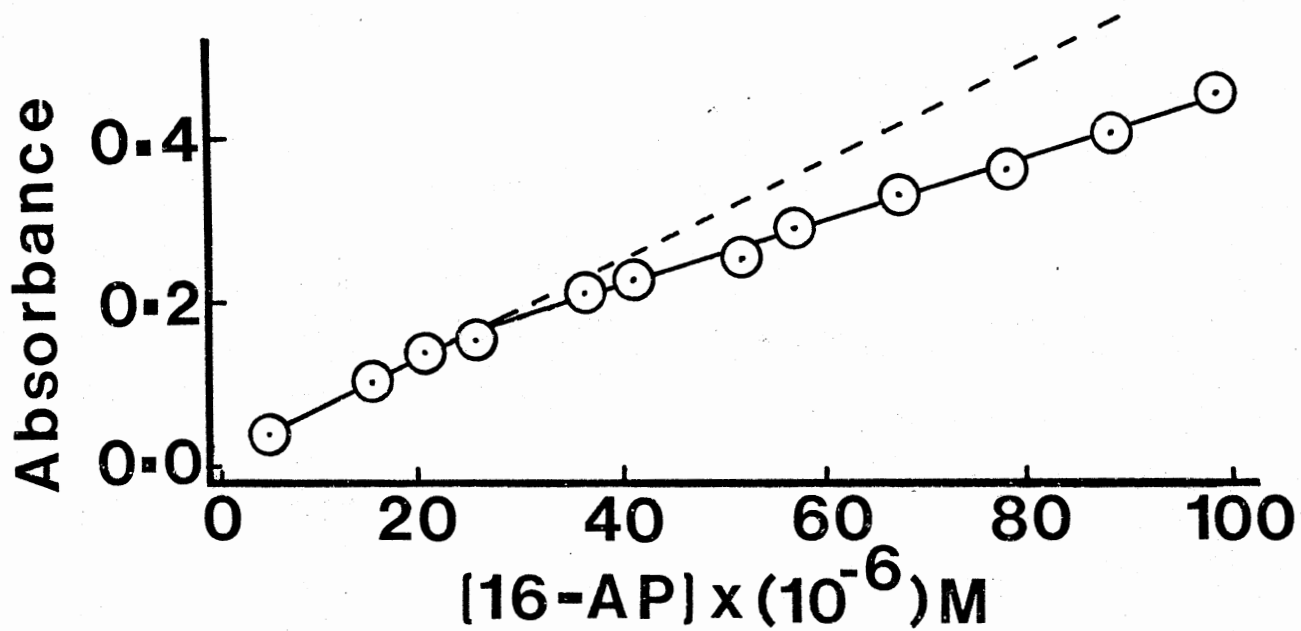
Figure 19. Absorbance of the Incorporated 16-(9-Anthroyl-
oxy)Palmitic Acid at 381 nm as a Function of
Probe Concentration in the 2.5 ml Vesicle
Suspension.

16AP INCORPORATION
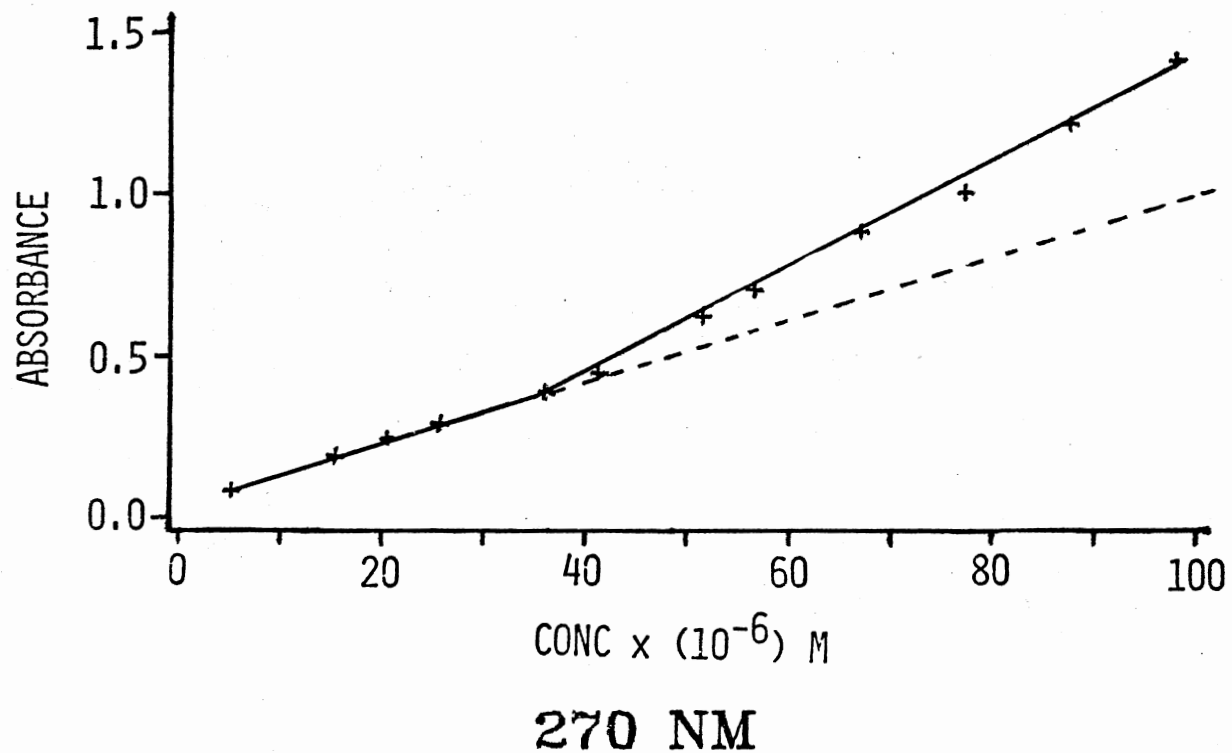
270 NM

Figure 20.   Absorbance of the Incorporated 16-(9-Anthroyl-
oxy)Palmitic Acid at 270 nm as a Function of
Probe Concentration in the 2.5 ml Suspension
of Vesicles in Buffer.

16AP INCORPORATION
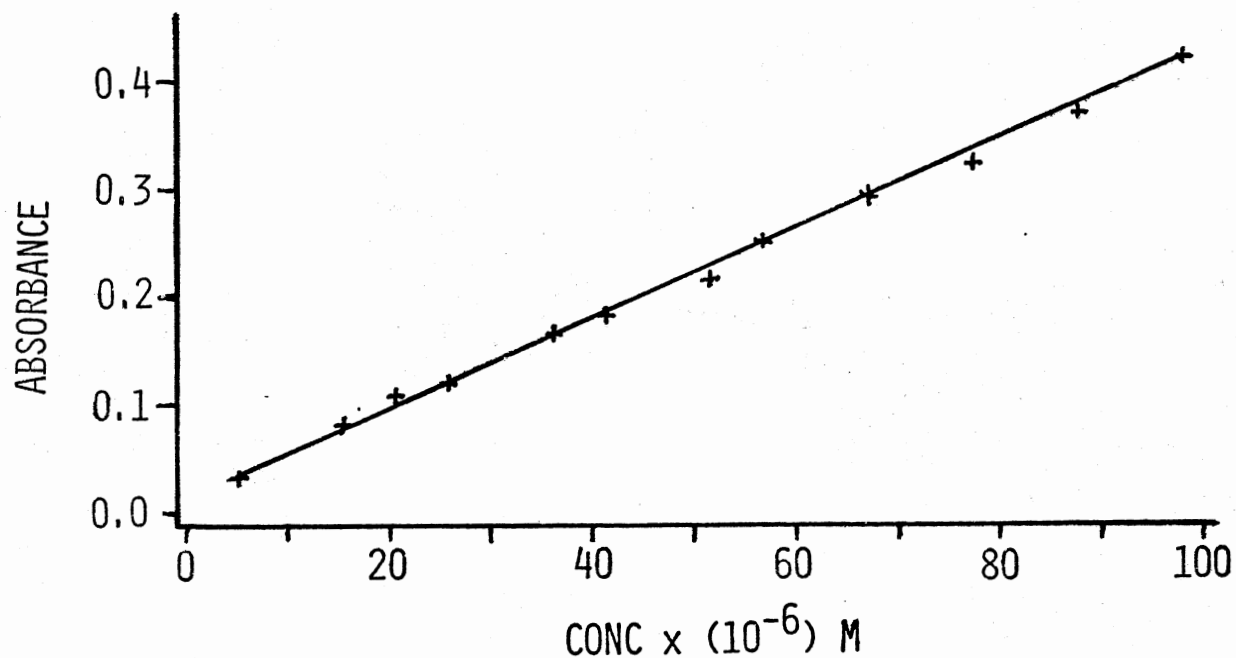
390 NM

Figure 21. Absorbance of the Incorporated 16-(9-Anthroyl-oxy)Palmitic Acid at 390 nm as a Function of Probe Concentration in the 2.5 ml Suspension of Vesicles in Buffer.

ratio. These measurements were taken over the spectral
range 400 to 215 nm for all probes studied. Similar trends
of these plots were obtained for all probes at different
wavelengths, provided the wavelength did not correspond to
that of an isoabsorptive point. The break point obtained
for each probe was different indicating the presence of
different critical probe/lipid ratios in each case, as shown
in Table XII.

TABLE XII

CRITICAL PROBE/LIPID CONCENTRATION RATIOS

PROBE	CRITICAL (PROBE/LIPID) CONCENTRATION RATIO
2-AP	0.23 ± 0.02
2-AS	0.23 ± 0.04
12-AS	0.15 ± 0.02
16-AP	0.18 ± 0.03
DPH	0.016 ± 0.001

Examination of the data reveals the fact that beyond these indicated critical probe/lipid ratios, any concentration employed would lead to a saturation of the membrane. Hence, any lifetime or polarization measurements taken on such a system would be a combination of two different environments instead of one. Saturation occurs more readily with chromophores buried deeper within the bilayer than those located next to the membrane surface. For example, 1,6-diphenylhexatriene saturates the membrane at a probe to lipid ratio one order of magnitude less than that of 2-(9-anthroyloxy)palmitic acid. The lowest ratio was found to correspond to 1,6-diphenylhexatriene, which is located in the middle of the bilayer.

The critical ratios for 2-(9-anthroyloxy)palmitic acid and 2-(9-anthroyloxy)stearic acid were similar in magnitude (0.23). It is important to note that the fluorescent moiety in both probes is located equally far from the bilayer surface. However, the critical ratios for the other probes with their chromophores well removed from the membrane surface were lower. For example, critical ratios of only 0.15 and 0.18 were found for 12-(9-anthroyloxy)stearic acid and 16-(9-anthroyloxy)palmitic acid respectively, where the chromophore is located deeper within the bilayer.

Absorption Spectra

Analysis of 2-(9-Anthroyloxy)Palmitic
Acid Spectra

The fluorescent probe 2-(9-anthroyloxy)palmitic acid is located with the chromophore close to the bilayer surface. The incorporation into the membrane is very fast as evident from the rate constant studies reported in Chapter III. The spectra of this probe in tetrahydrofuran and in vesicles were very similar with maxima at 384, 364, 346 and 256 nm as shown in Figures 22 and 23. According to Birks (98), the absorption spectra of all n-(9-anthroyloxy)fatty acids seem to be similar to that of anthracene. The bands in the spectral range 420-300 nm, correspond to p-bands which are either the $S_1 \leftarrow S_0$ or $S_2 \leftarrow S_0$ absorption bands. Whereas, the (β-bands) occuring at shorter wavelengths around 256 nm, are stronger bands with less vibrational structure.

Examination of the incorporation curve shows a small difference in intensity as the probe incorporates into the membrane (Figure 24). This explains the fact that the break point is not as distinct in the case of 2-(9-anthroyloxy)palmitic acid as compared to that of other probes that go deeper into the membrane (Figure 25). All the saturation studies conducted at different wavelengths, resulted in the same probe/lipid concentration ratio 0.23. As expected, the control studies of the probe in the solvent system tetrahydrofuran showed a linearity in the Beer's law

Figure 22. Absorption Spectrum of 2-(9-Anthroyloxy)Palmitic Acid in Tetrahydrofuran Solvent.

Figure 23. Absorption Spectrum of 2-(9-Anthroyloxy)Palmitic
Acid in Lipid Vesicles.

Figure 24. Absorption Spectra Vs. Time of Incorporation for 2-(9-Anthroyloxy)Palmitic Acid. The Different Spectra Indicate an Increase in Intensity with Incorporation Time.
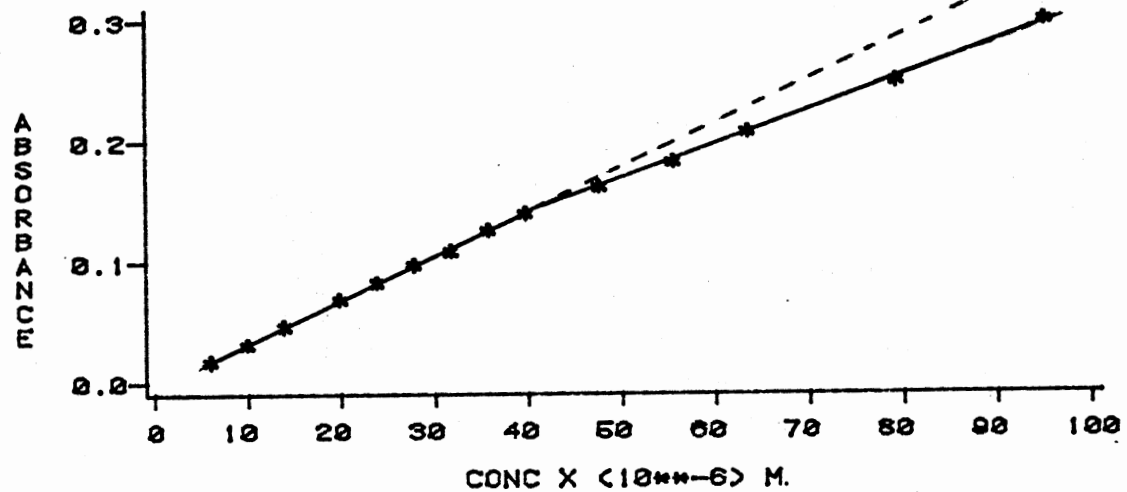
330 NM

Figure 25. Absorbance of the Incorporated 2-(9-Anthroyl-
oxy) Palmitic Acid at 330 nm as a Function
of Probe Concentration in the 2.5 ml
Suspension of Vesicles.

plots over the entire spectral range (Figure 26). The concentrations of the dye used in the control studies were similar to those employed in the lipid. The formation of any dimers was evidenced by the broad absorption bands as opposed to the sharp bands observed for monomers.

Analysis of 2-(9-Anthroyloxy)Stearic Acid Spectra

The fluorescent probe 2-(9-anthroyloxy)stearic acid locates itself at the same position as that of 2-(9-anthroyloxy)palmitic acid. This fact was further stressed by the results obtained from this study. Critical probe/lipid concentration ratios equal to 0.23 were found for both probes and their spectra were similar. A more enhanced difference in the absorption spectra was obtained for this probe upon incorporation as opposed to that of 2-AP, as shown in Figure 27. This led to a more pronounced break point in the saturation curves. The break point was seen to be very sharp at wavelengths where the absorption difference was at a maximum for example at 260 nm, Figure 28, but it started to diminish as it was monitored at 375 nm, Figure 29, and disappeared totally at 340 nm, Figure 30. The control studies of the probe in tetrahydrofuran showed the expected linearity over the entire wavelength range employed, as shown in Figure 31.

330 NM

Figure 26 .   Beer's Law Plot of 2-(9-Anthroyloxy)Palmitic
Acid in Tetrahydrofuran Solvent at 330 nm.

Figure 27. Absorption Spectra Vs. Time of Incor-
poration for 2-(9-Anthroyloxy)Stearic
Acid. The Different Spectra Indicate
an Increase in Intensity with Incor-
poration Time.

2AS INCORPORATION
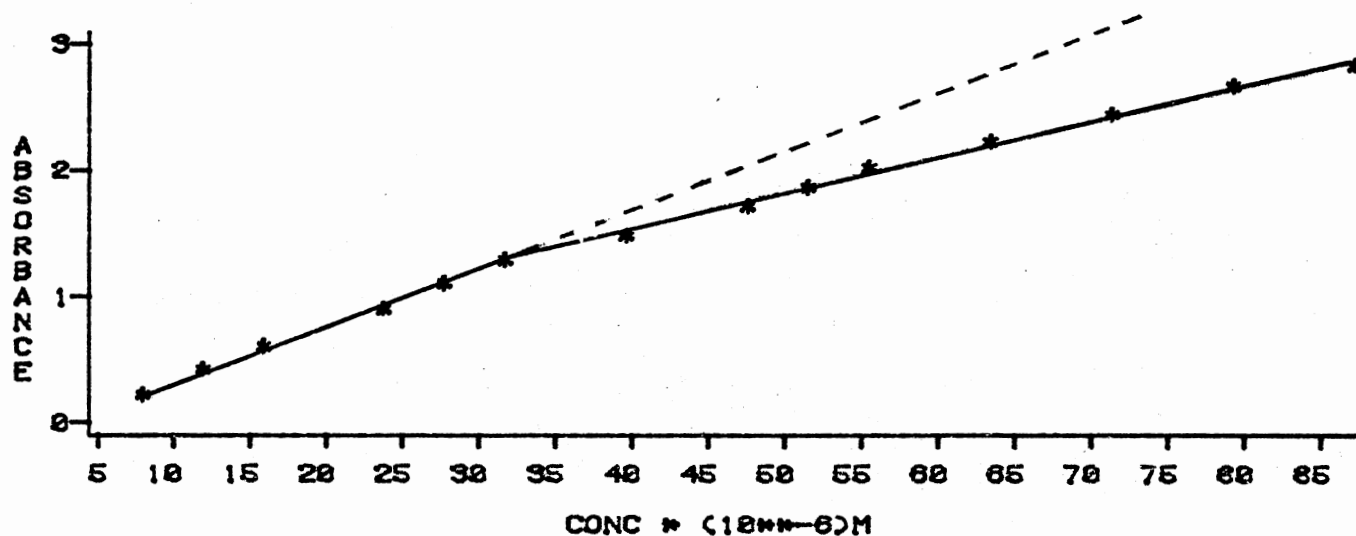
260 NM

Figure 28.   Absorption of the Incorporated 2-(9-Anthroyloxy)
             Stearic Acid at 260 nm as a Function of Probe
             Concentration in the 2.5 ml Suspension of
             Vesicles in Buffer.
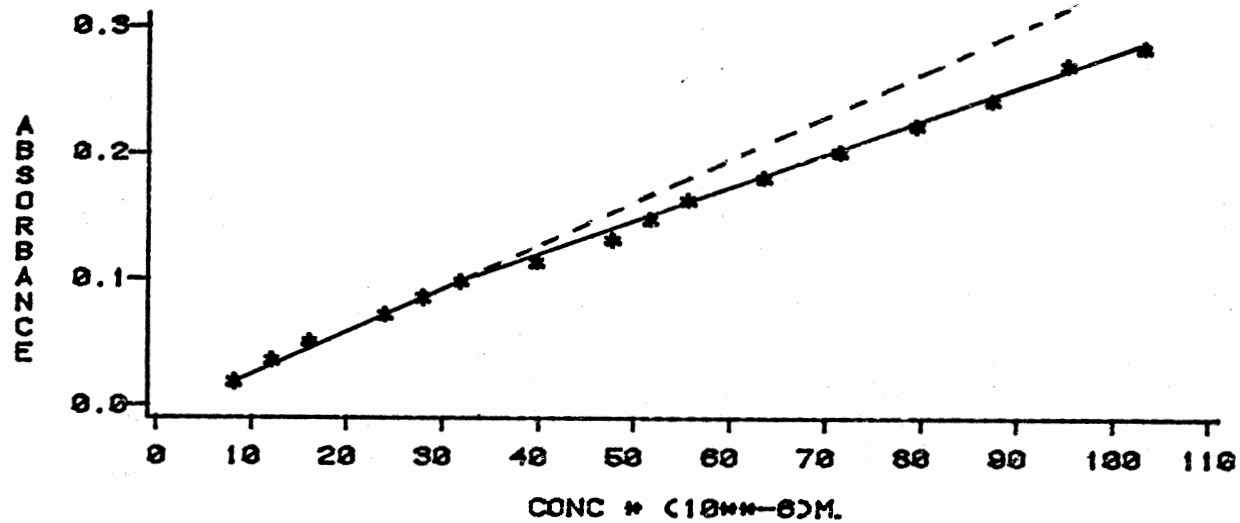
2AS INCORPORATION

375 NM

Figure 29.   Absorption of the Incorporated 2-(9-Anthroyloxy)
Stearic Acid at 375 nm as a Function of Probe
Concentration in the 2.5 ml Suspension of
Vesicles in Buffer.

2AS INCORPORATION

340 NM

Figure 30.   Absorption of the Incorporated 2-(9-Anthroyloxy) Stearic Acid at 340 nm as a Function of Probe Concentration in the 2.5 ml Suspension of Vesicles in Buffer.

CONTROL "2AS/THF"
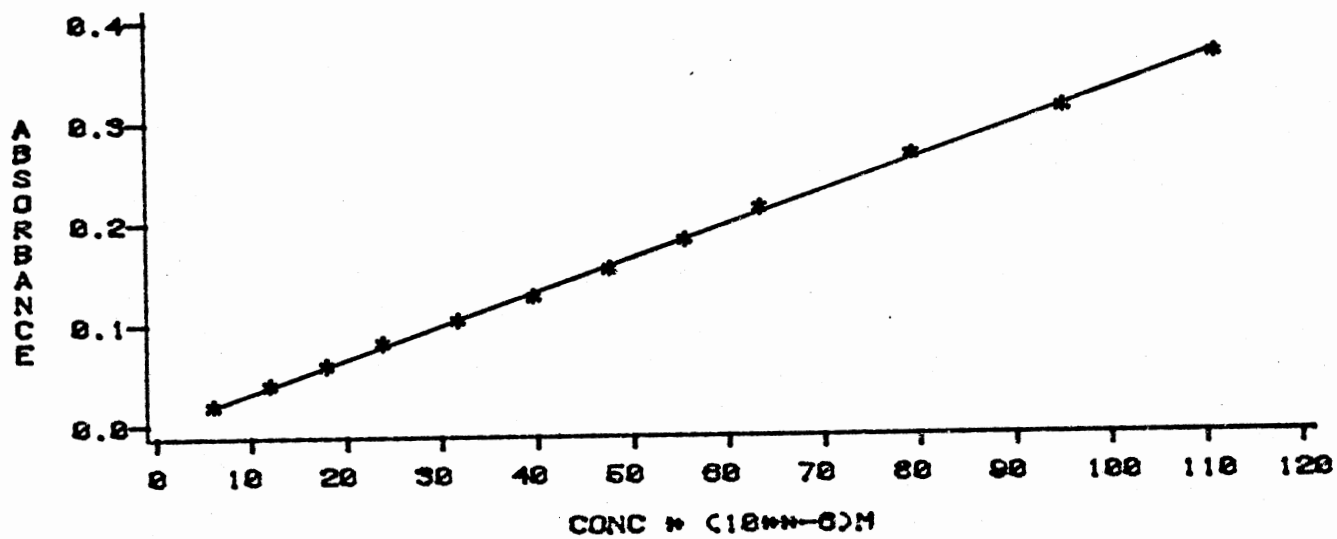
375 NM

Figure 31. Beer's Law Plot of 2-(9-Anthroyloxy)Stearic
Acid in Tetrahydrofuran at 375 nm.

Analysis of 12-(9-Anthroyloxy)Stearic
Acid Spectra

The differences in absorption intensity upon incorporation were more pronounced in the cases of 12-AS and 16-AP as compared to those of 2-AS and 2-AP (Figure 34). Since the chromophores of the probes 12-AS and 16-AP are located far away from the polar head groups, saturation of the biological membrane occurs more readily. The spectra of this probe in different solvents showed similar trends as the other probes (Figures 35 and 36). The break points were observed at all the wavelengths monitored at, except for the isoabsorptive point at 240 nm (Figures 37-39).

Analysis of 1,6-Diphenylhexatriene
Spectra

The absorbance of DPH increased as the probe incorporated into the membrane (Figure 40). It had a higher quantum yield in non-polar solvents as opposed to polar ones. The change in intensity reached a maximum around the absorption peaks 380, 360 and 340 nm. However, at the isoabsorptive point occuring at 320 nm, no change in absorption intensity was observed.

It was noticed that the absorption spectra of the probe during the incorporation process approached that of the probe in a non-polar environment (Figures 41 and 42). Since DPH was difficult to dissolve in polar solvents, absorbance control measurements in those solvents were not taken.
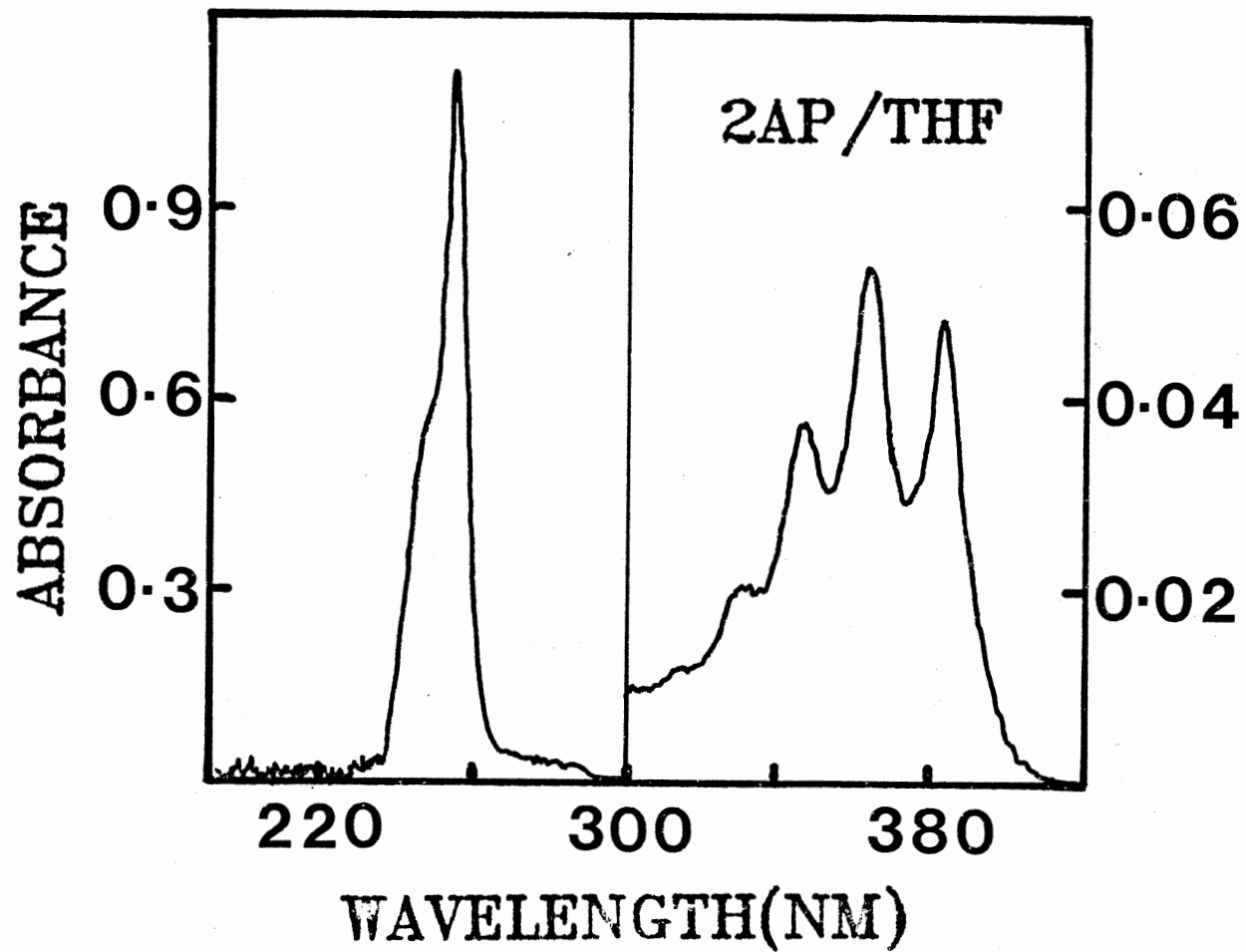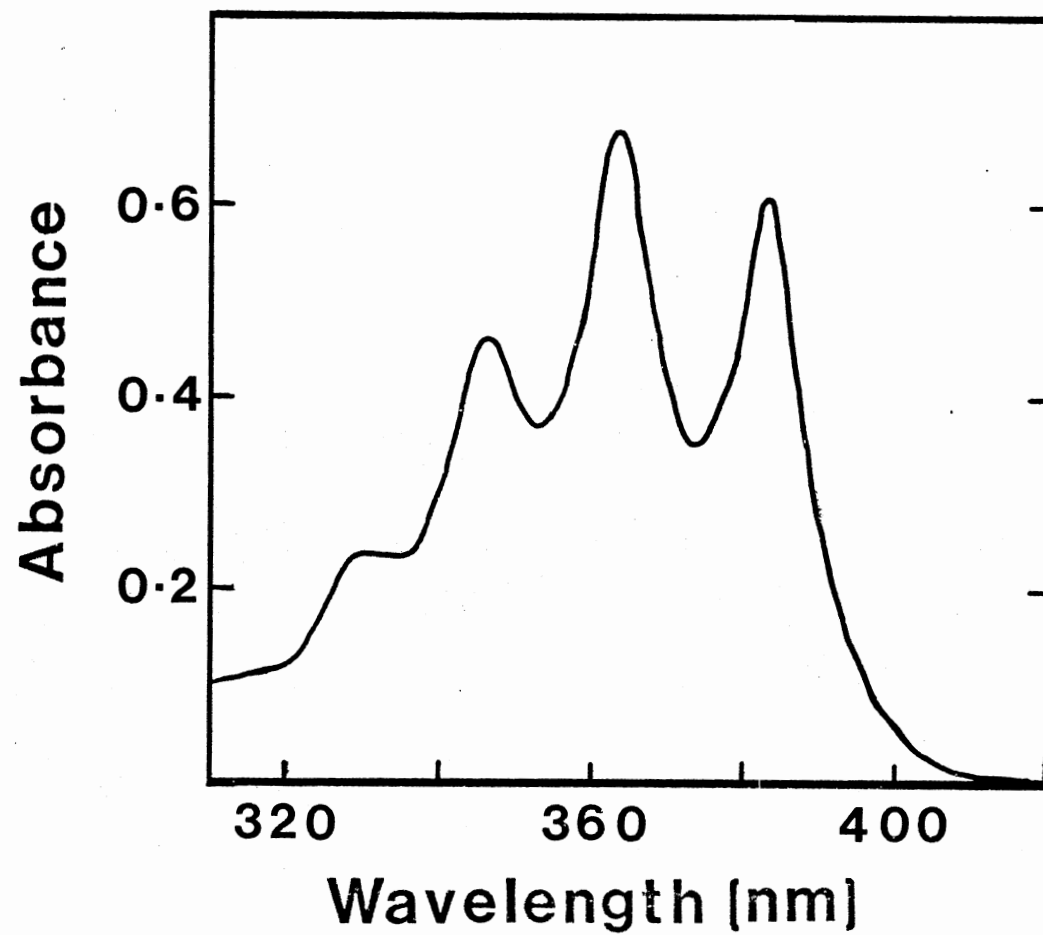
Figure 32. Absorption Spectrum of 2-(9-Anthroyloxy) Stearic Acid in Tetrahydrofuran.
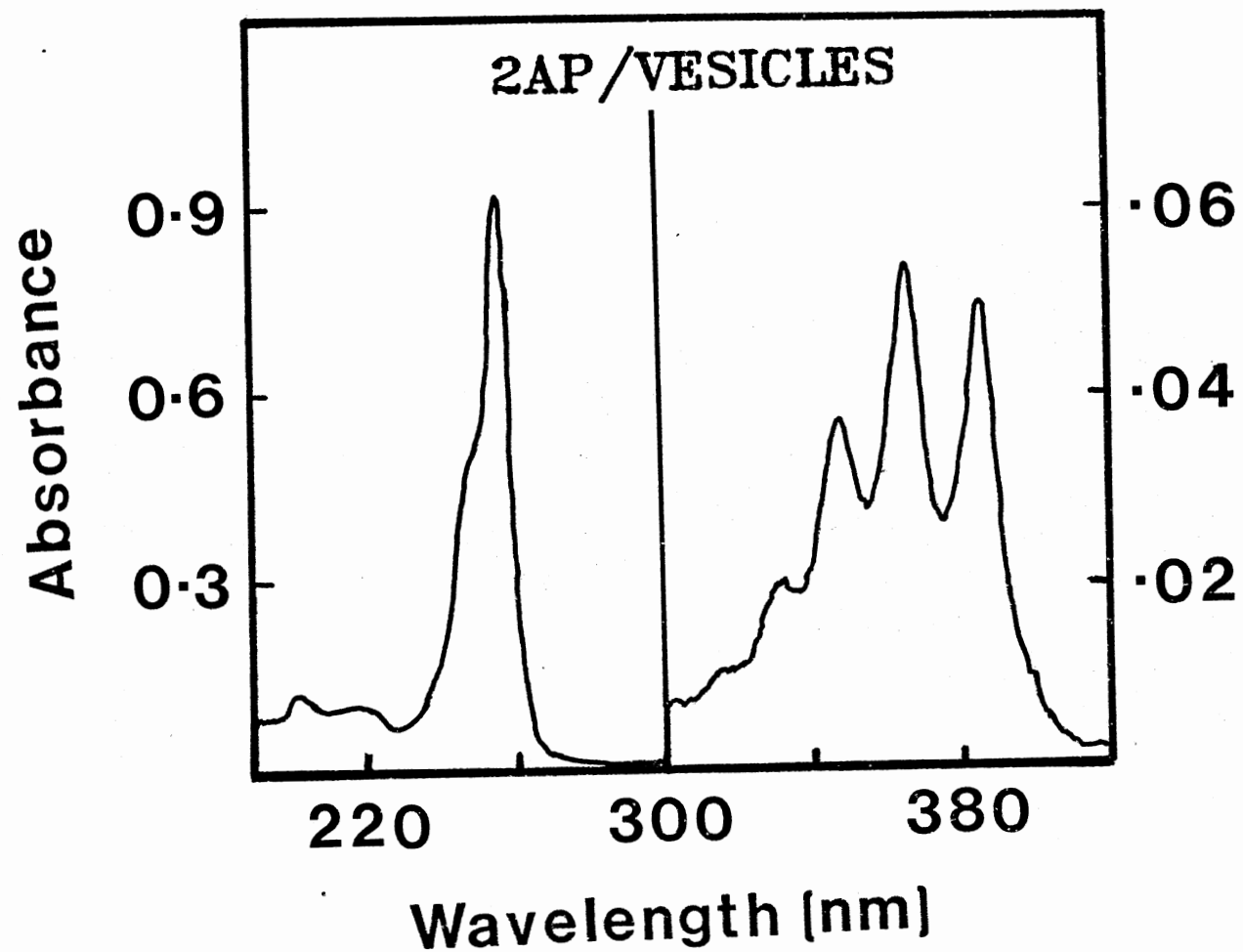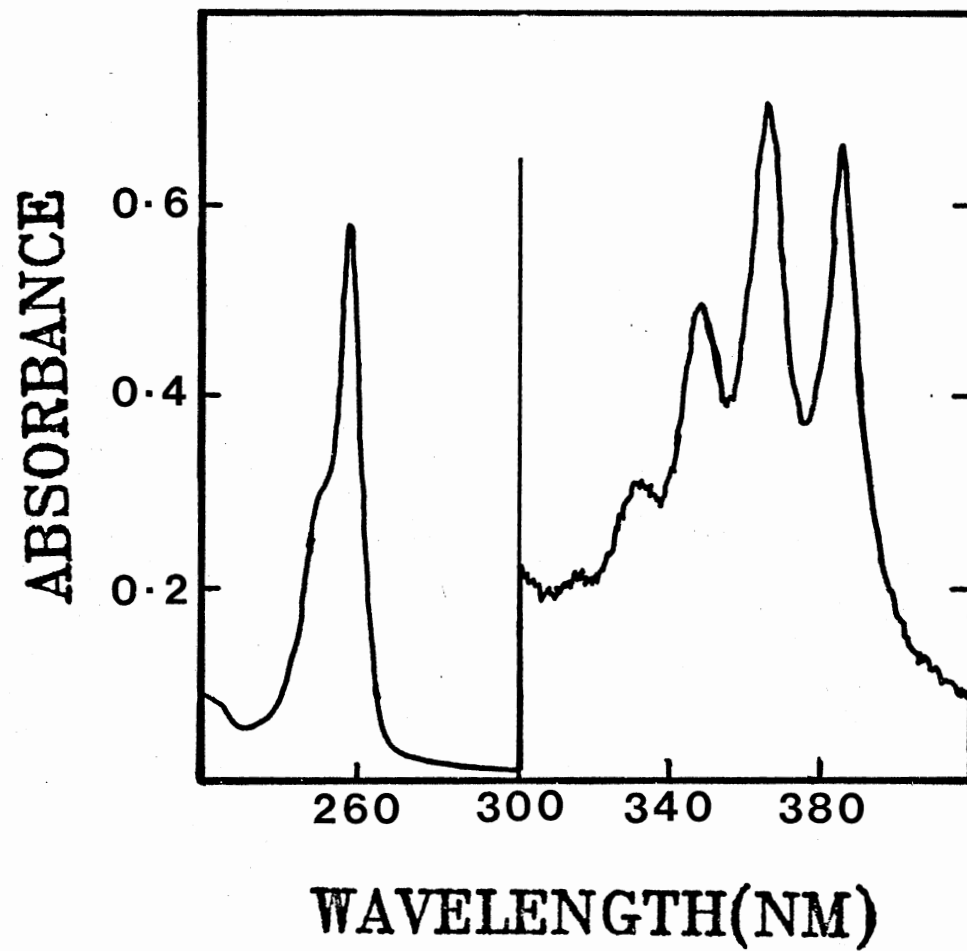
Figure 33.   Absorption Spectrum of 2-(9-Anthroyl-
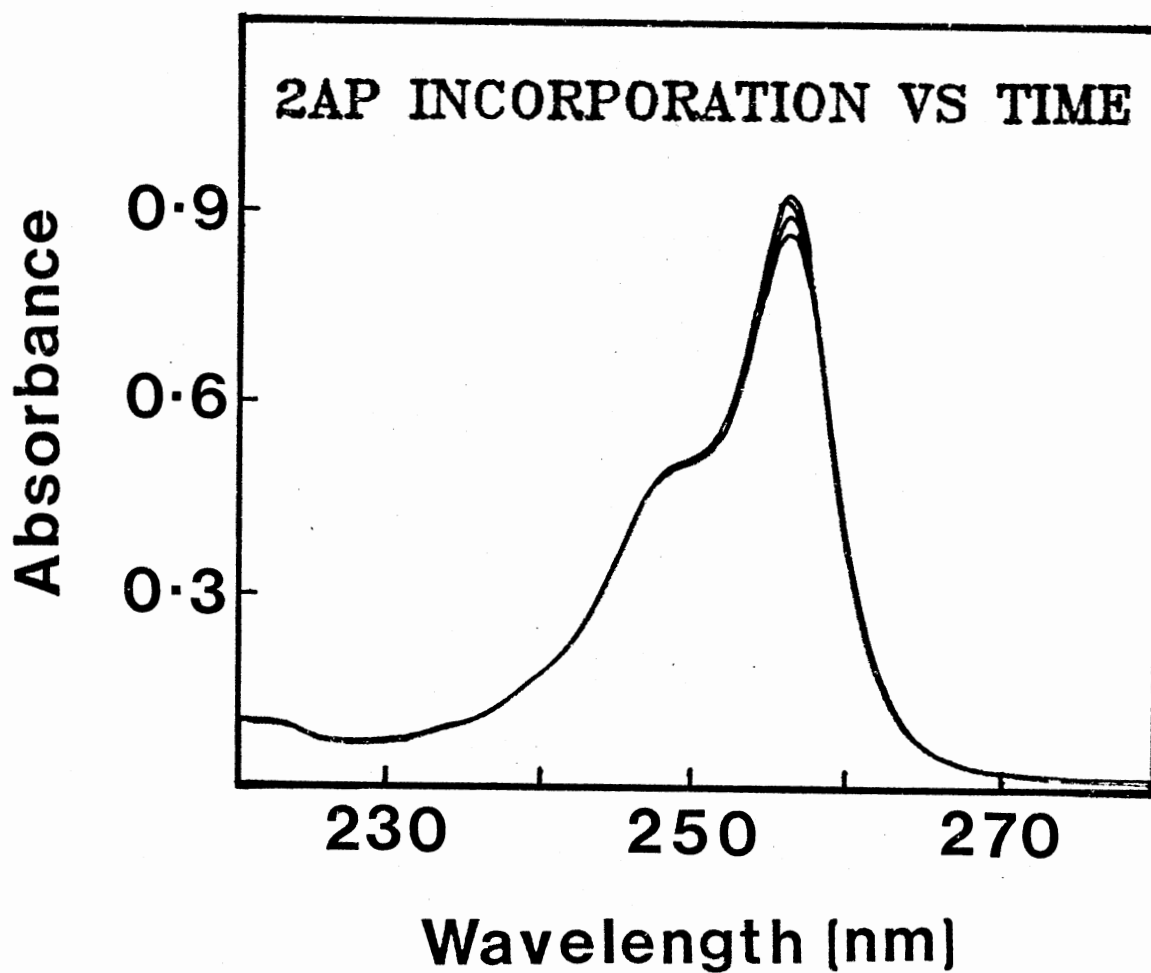oxy)Stearic Acid in Lipid Vesicles.
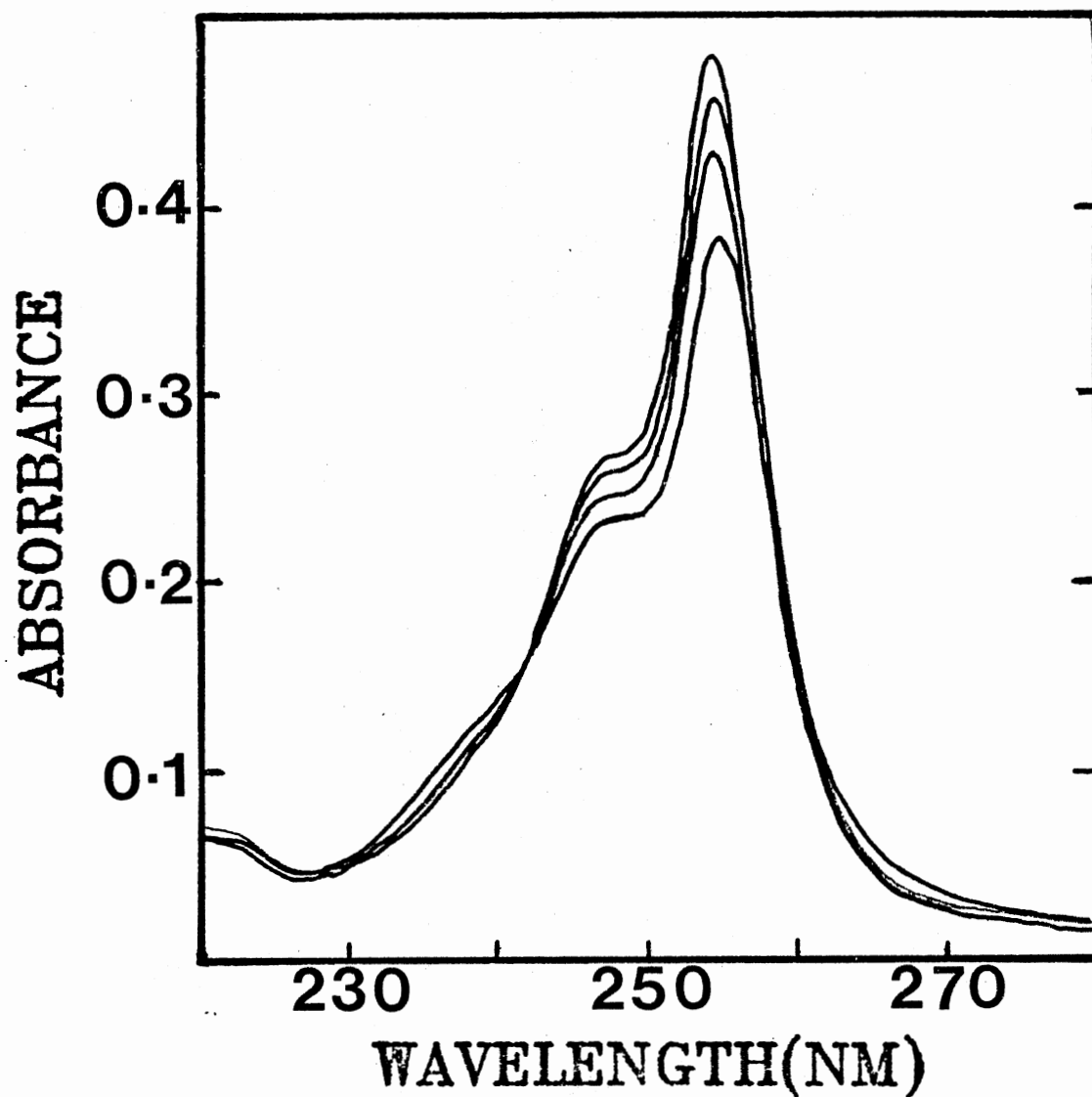
Figure 34. Absorption Spectra vs. Time of Incorporation for 12-(9-Anthroyloxy)Stearic Acid. The Different spectra Indicate an Increase in Intensity with Incorporation Time.
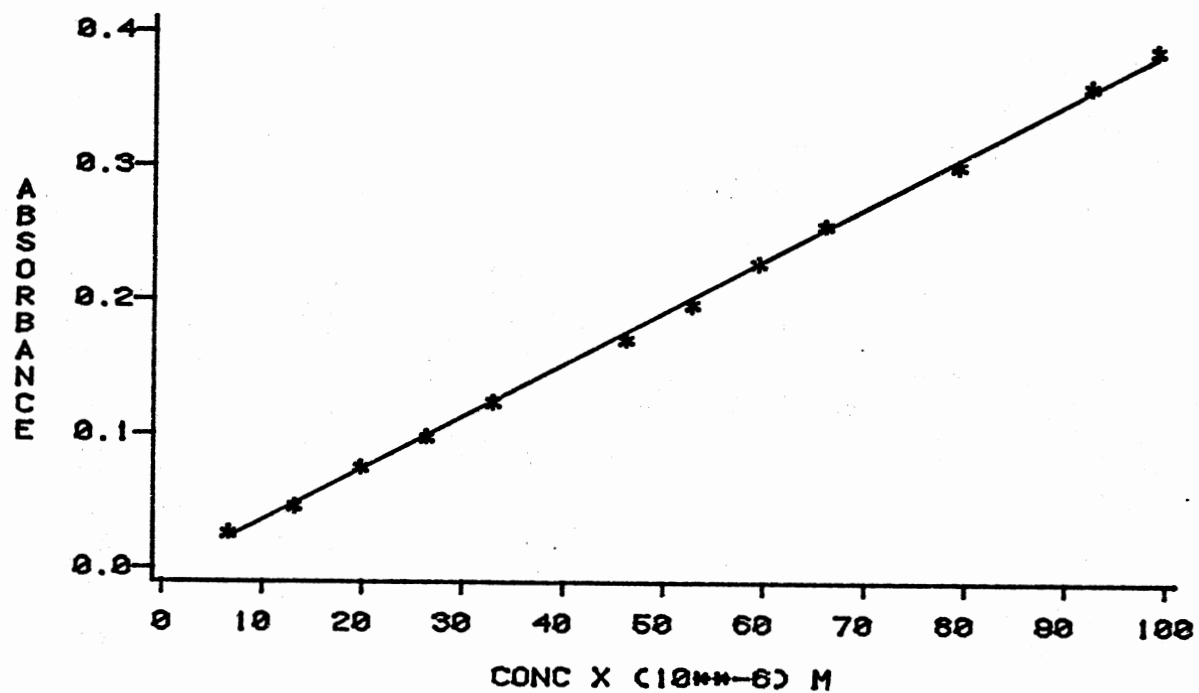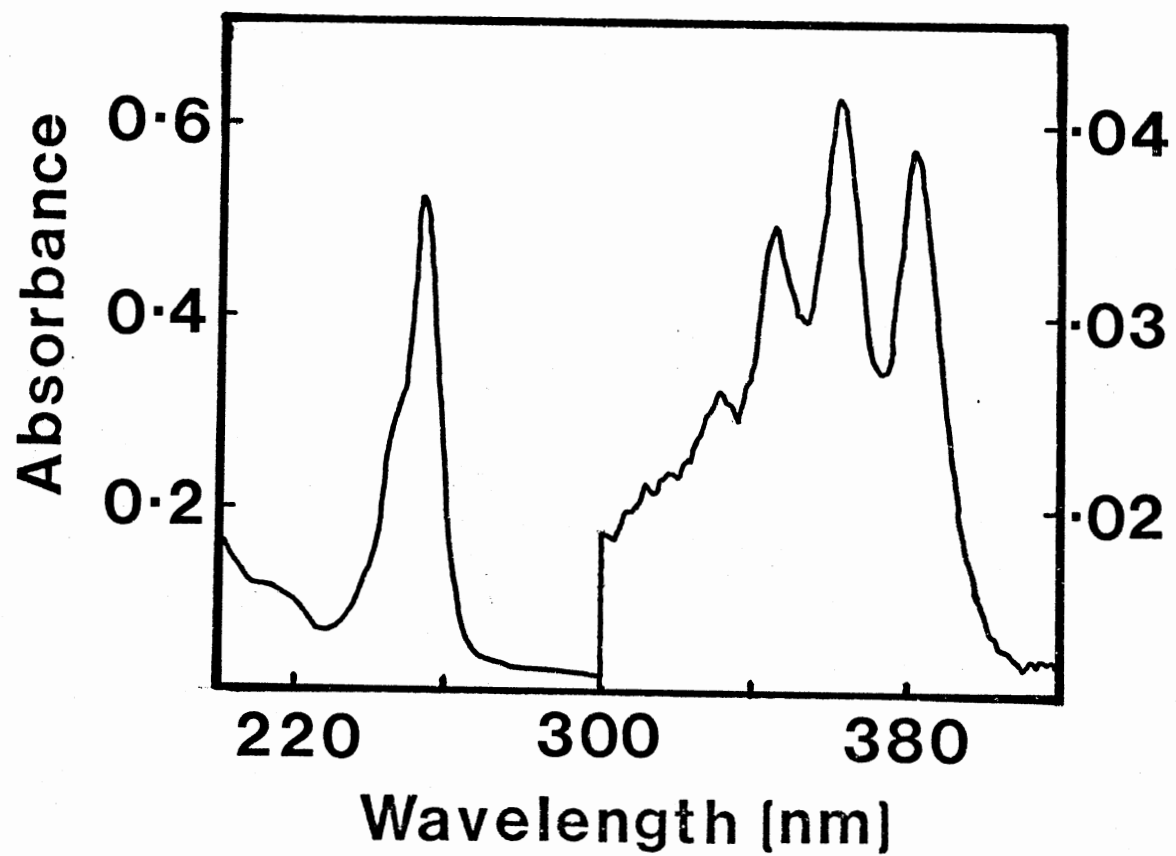
Figure 35.   Absorption Spectrum of 12-(9-Anthroyloxy)
Stearic Acid in Lipid Vesicles.
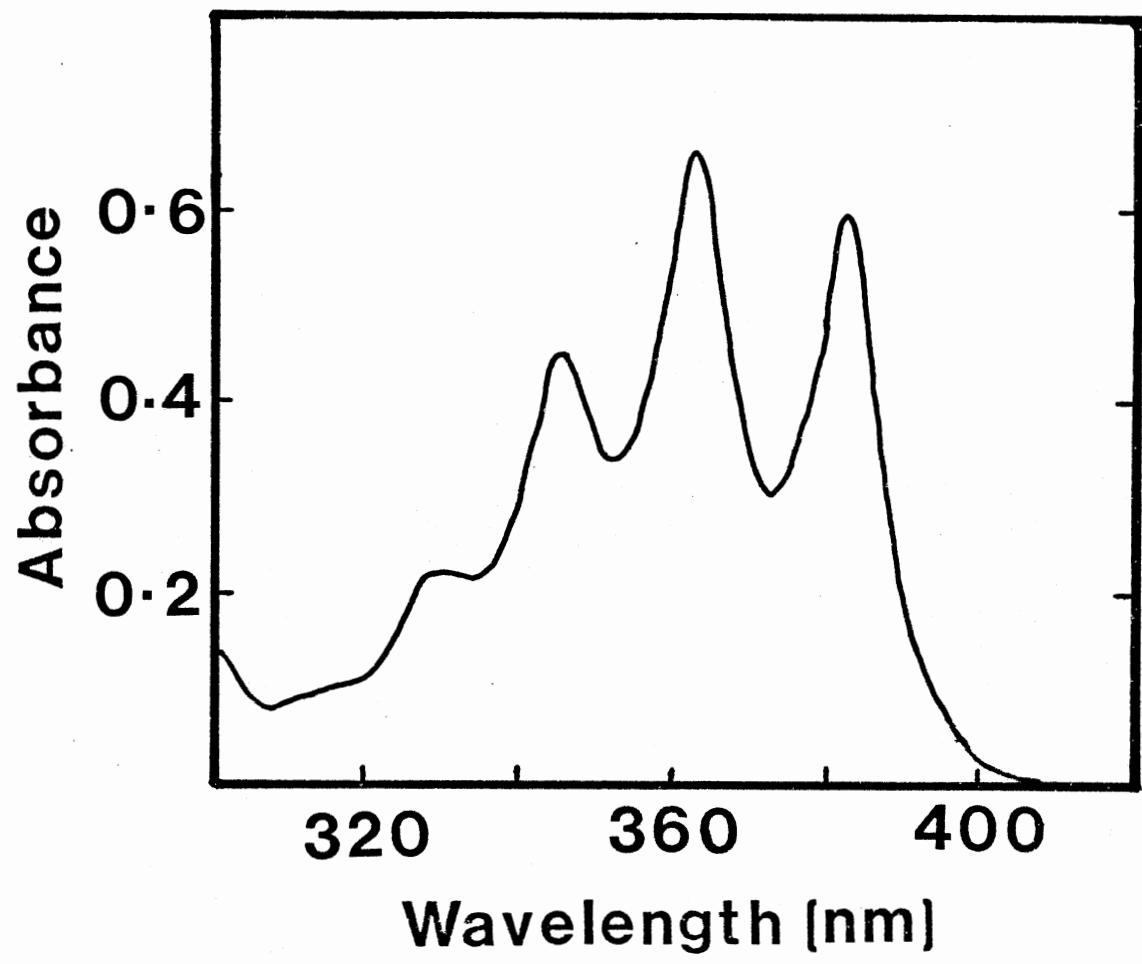
Figure 36.   Absorption Spectrum of 12-(9-Anthroyloxy)
Stearic Acid in Tetrahydrofuran.

12AS INCORPORATION
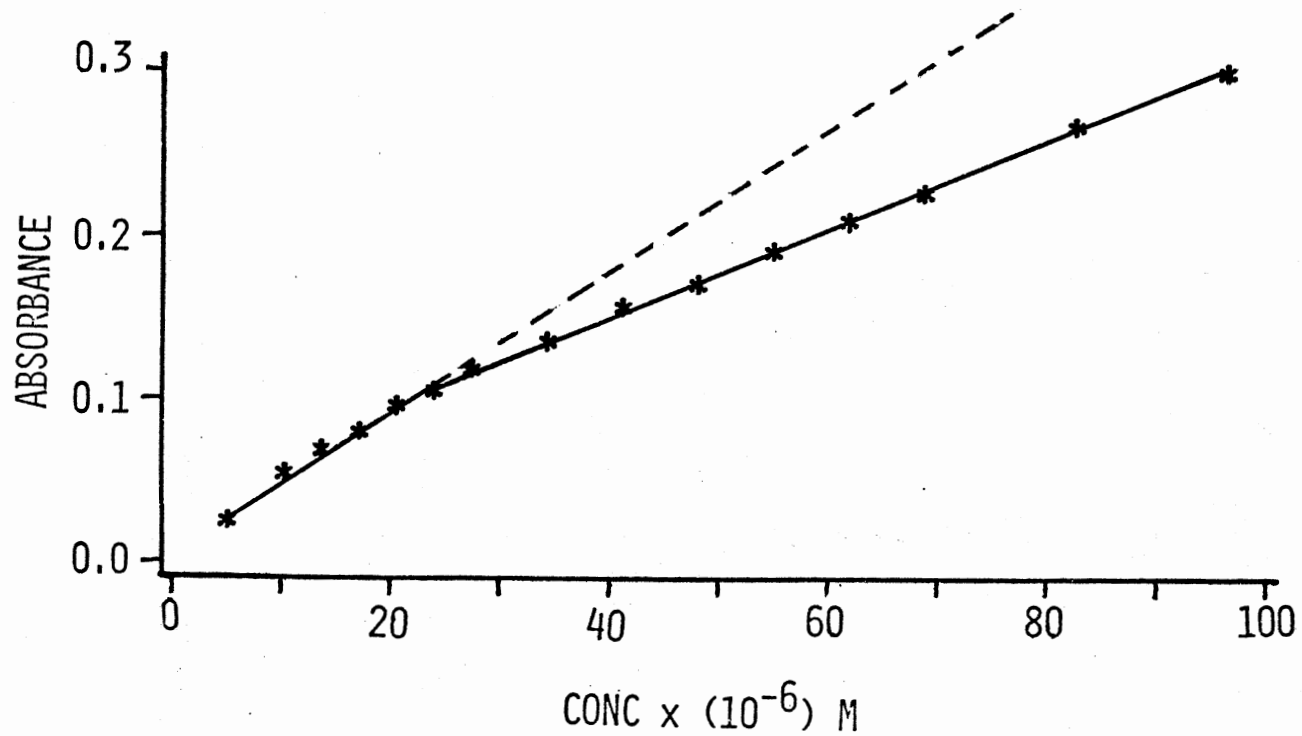
Figure 37. Absorption of the Incorporated 12-(9-Anthroyl-oxy)Stearic Acid at 340 nm as a Function of Probe Concentration in the 2.5 ml Suspension of Vesicles in Buffer.

12AS INCORPORATION
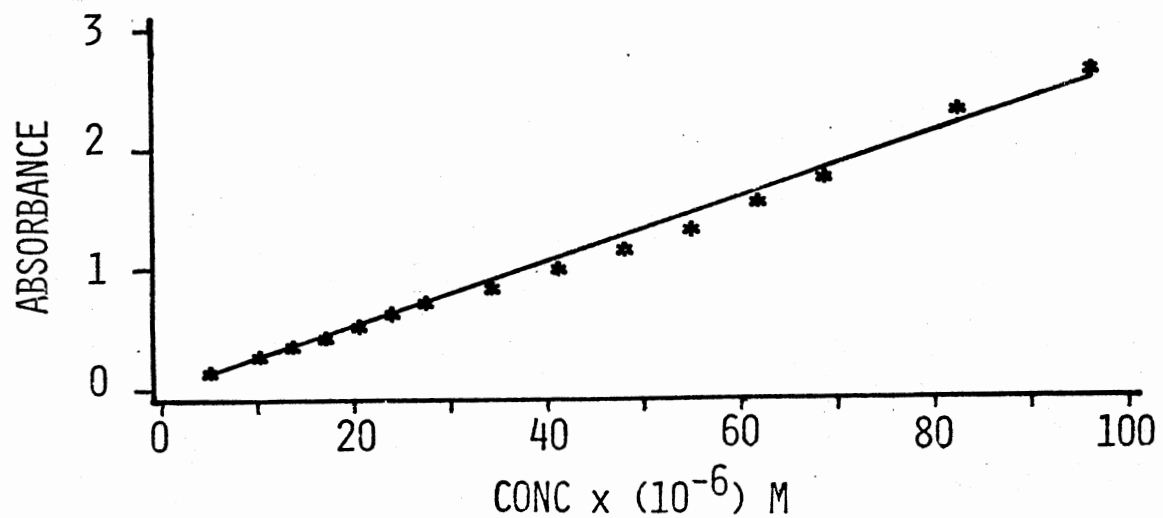
Figure 38. Absorption of the Incorporated 12-(9-Anth-
royloxy)Stearic Acid at 240 nm as a
Function of Probe Concentration in the
2.5 ml Suspension of Vesicles in Buffer.
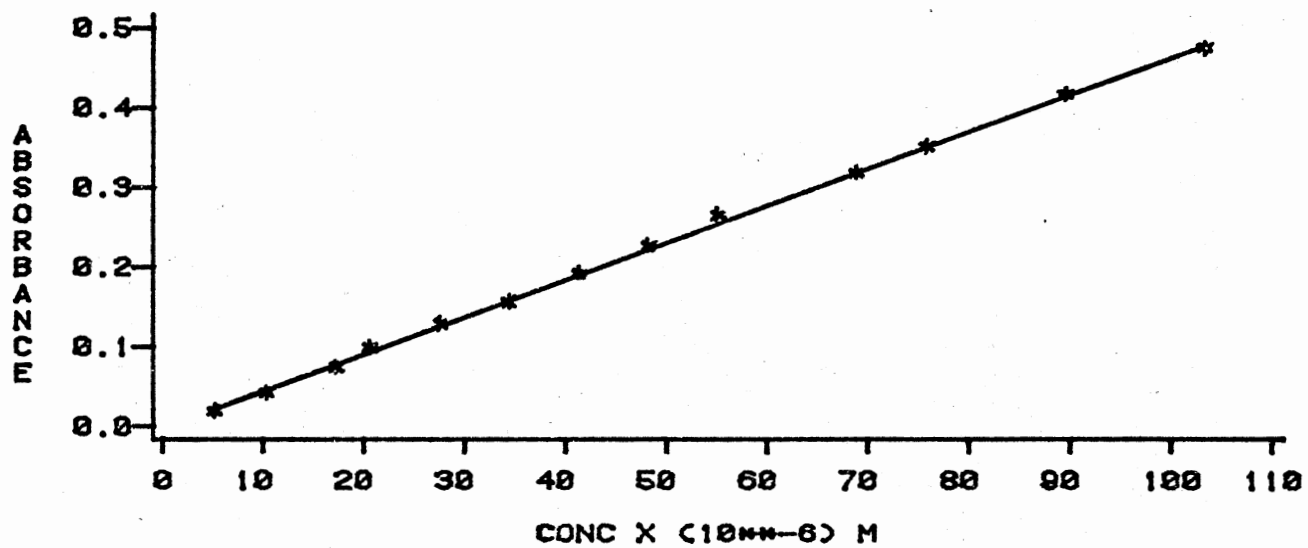
Figure 39. Beer's Law Plot of 12-(9-Anthroyloxy)Stearic
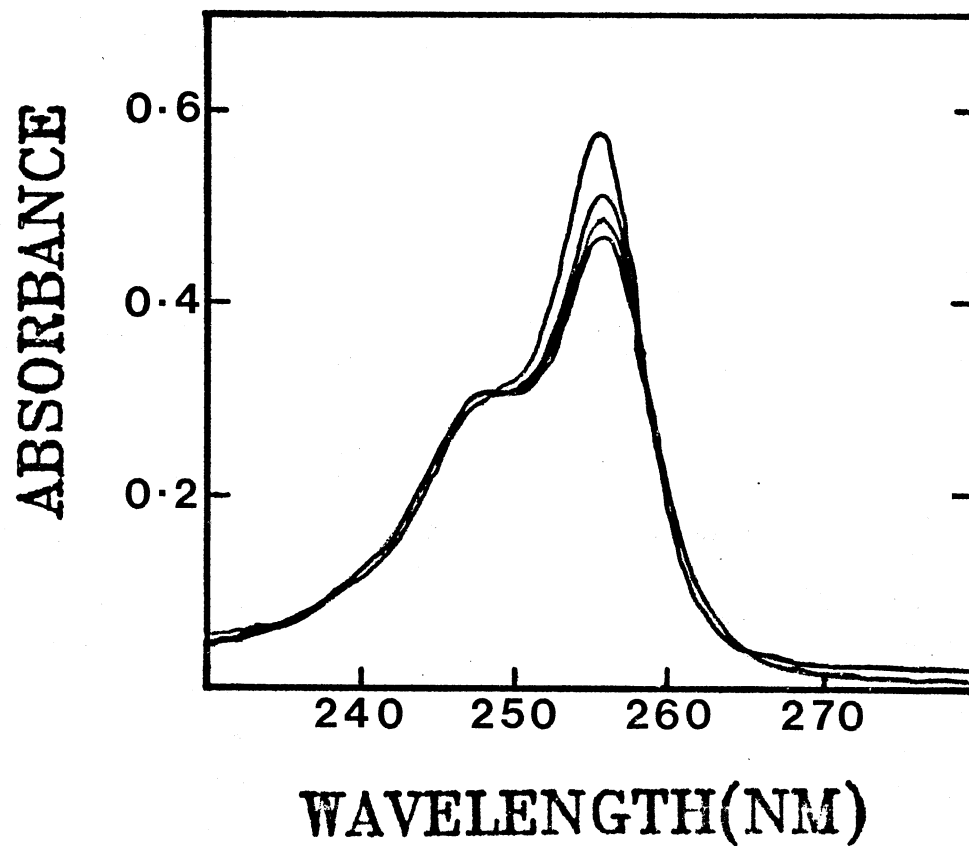Acid in Tetrahydrofuran at 340 nm.
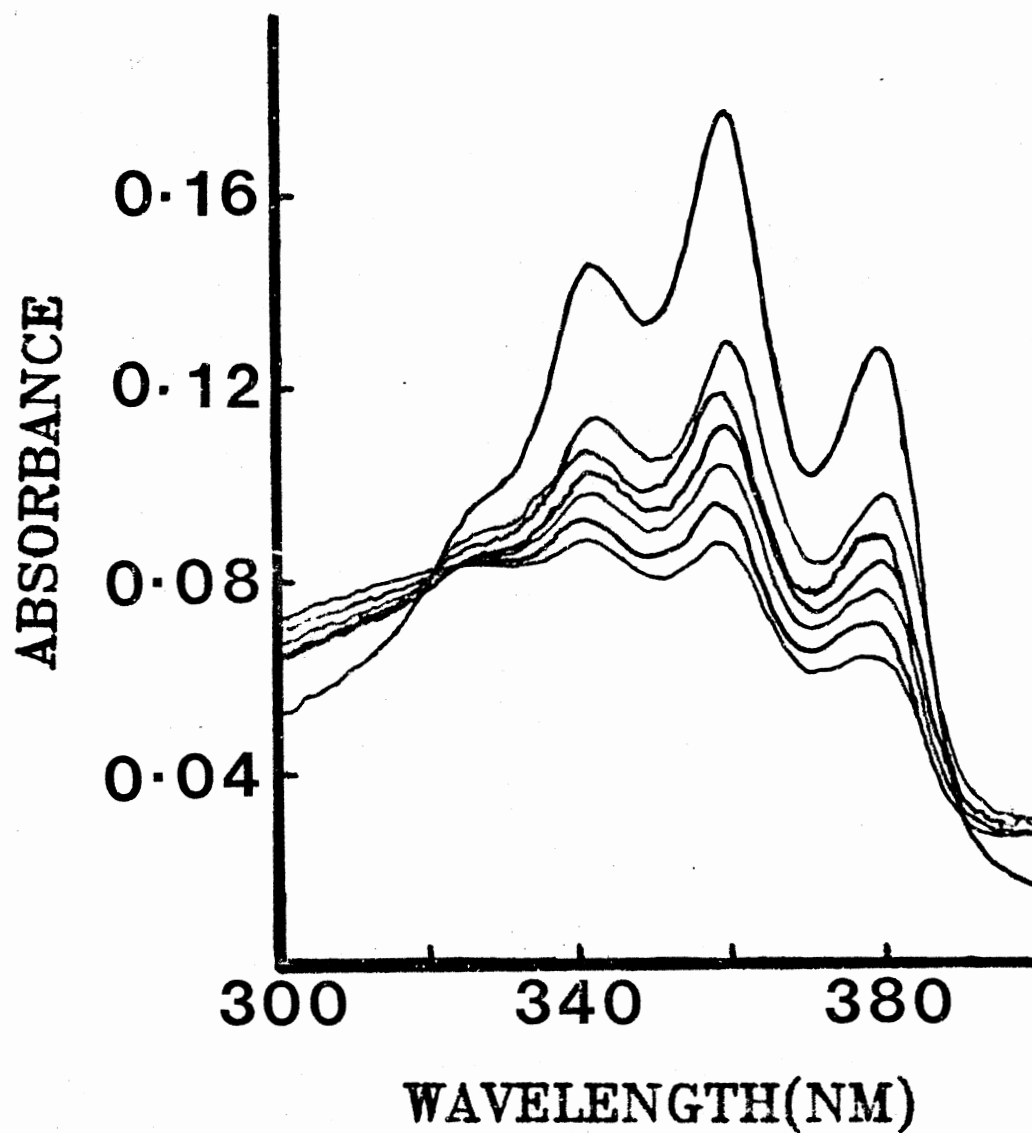
Figure 40.   Absorption Spectra Vs. Time of Incor-
             poration for 1,6-diphenylhexatriene.
             The Different Spectra Indicate an
             Increase in Intensity with Incorpora-
             tion Time.   The Top Curve is the
             Absorption Spectrum of 1,6-diphenyl-
             hexatriene After the Incorporation was
             Over.
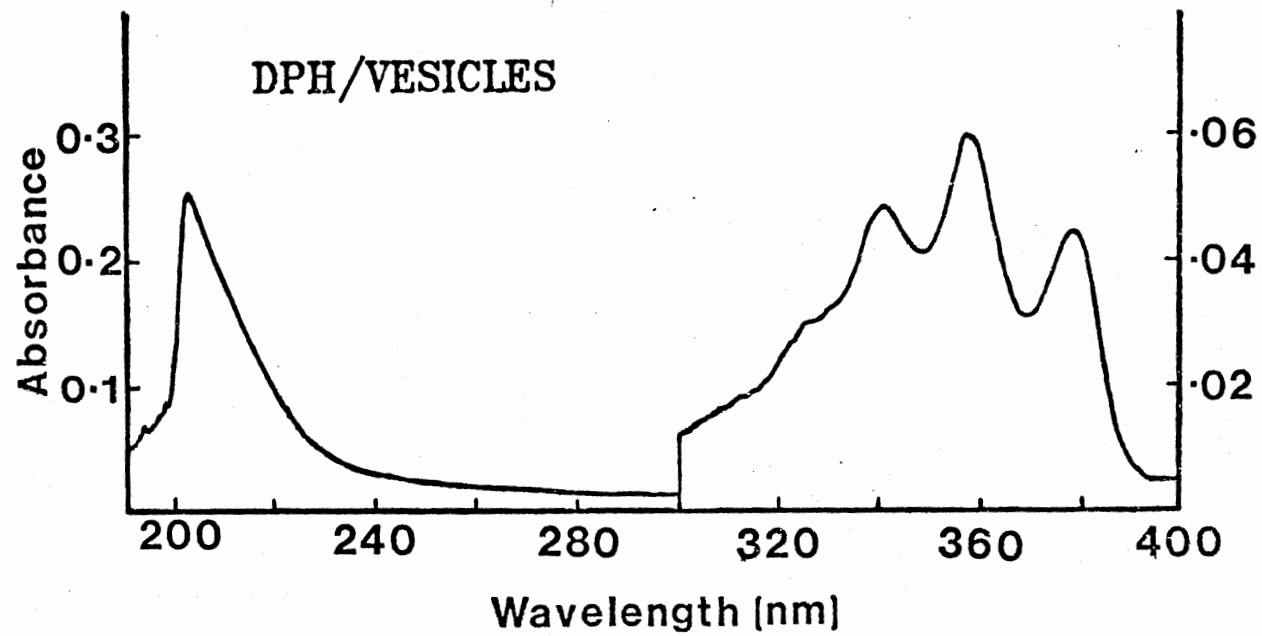
Figure 41.   Absorption Spectrum of 1,6-diphenylhexatriene in
              Lipid Vesicles.
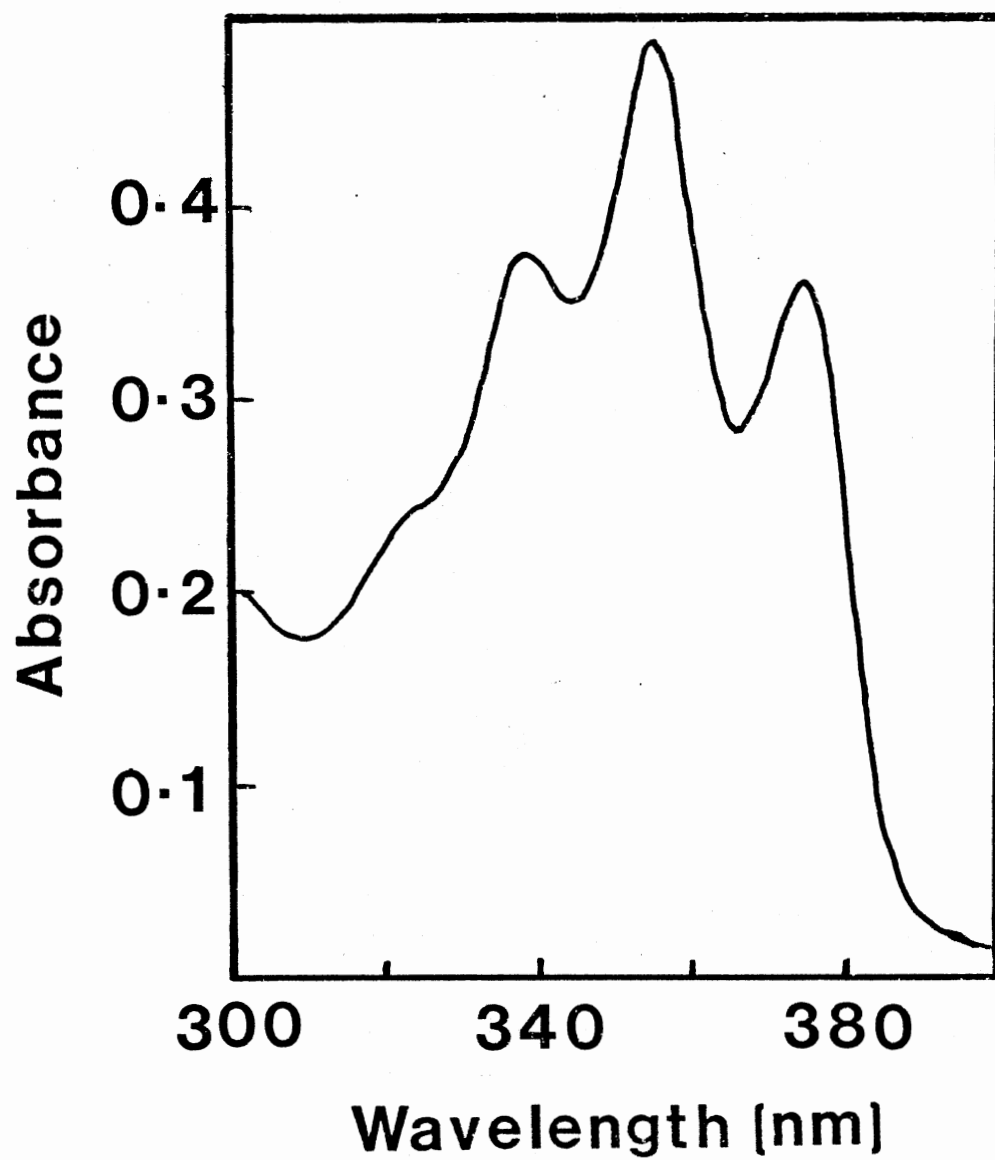
Figure 42.   Absorption Spectrum of 1,6-diphenyl-
             hexatriene in Tetrahydrofuran Solvent.

Tetrahydrofuran was found to be a good solvent for all the probes employed.

Since the saturation experiment was based on the differences in the absorption spectra, sharp break points were most evident at wavelengths where the differences were greatest. A comparison of the curves at 360 and 388 nm shows these sharp break points (Figures 43 and 44). On the other hand, when measurements were made at an isabsorptive point no break points in the linearity of the curves were observed, Figure 45. The same linearity was observed when performing the control experiments; and Beer's law plots of the control experiments, in which DPH was present in only one solvent system (tetrahydrofuran), showed a linearity over the concentration range used as shown in Figure 46, at 360 nm.

Conclusions

The above studies have shown that the deeper the penetration of the probe into the bilayer the lower is the saturating probe/lipid ratio. This critical ratio can be obtained with relative ease and accuracy for any fluorescent probe. Such a ratio seems to be quite high for probes located next to the surface and tend to reach a limiting value for those located in the middle of the bilayer (e.g. 1,6-diphenylhexatriene). These measurements have proved to be of great importance in assessing the validity of an excessive use of fluorescent probes in membrane studies.

DPH INCORPORATION
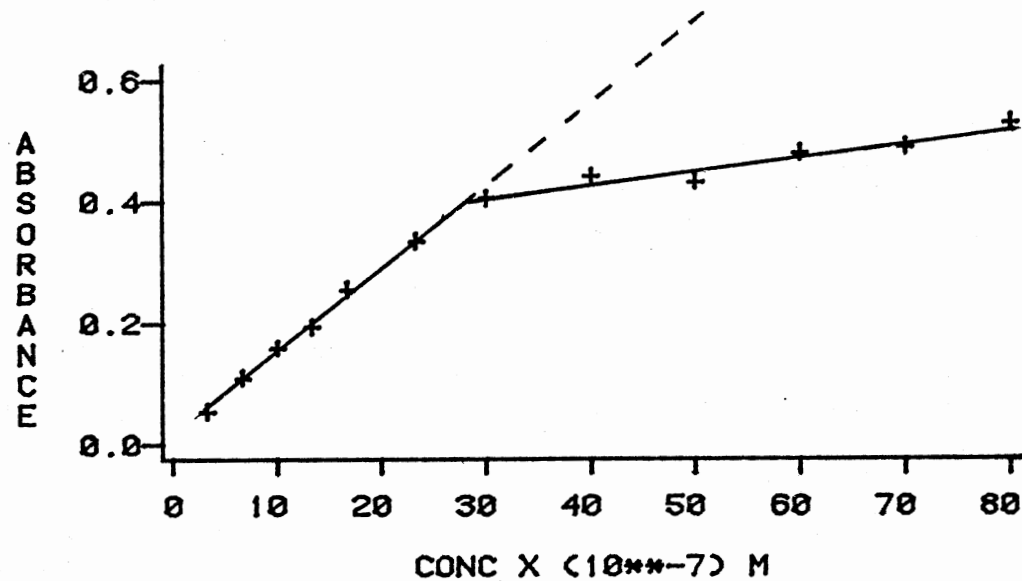
360 NM

Figure 43.   Absorption of the Incorporated 1,6-di-
phenylhexatriene at 360 nm as a
Function of Probe Concentration in the
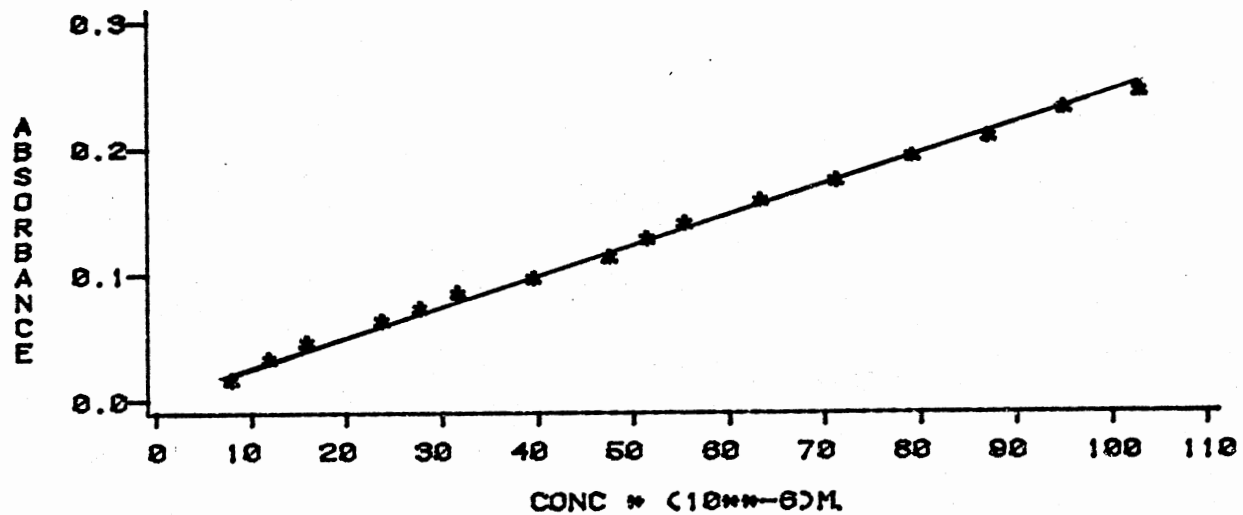2.5 ml Suspension of Vesicles in Buffer.

DPH INCORPORATION

CONC X (10**-7) M
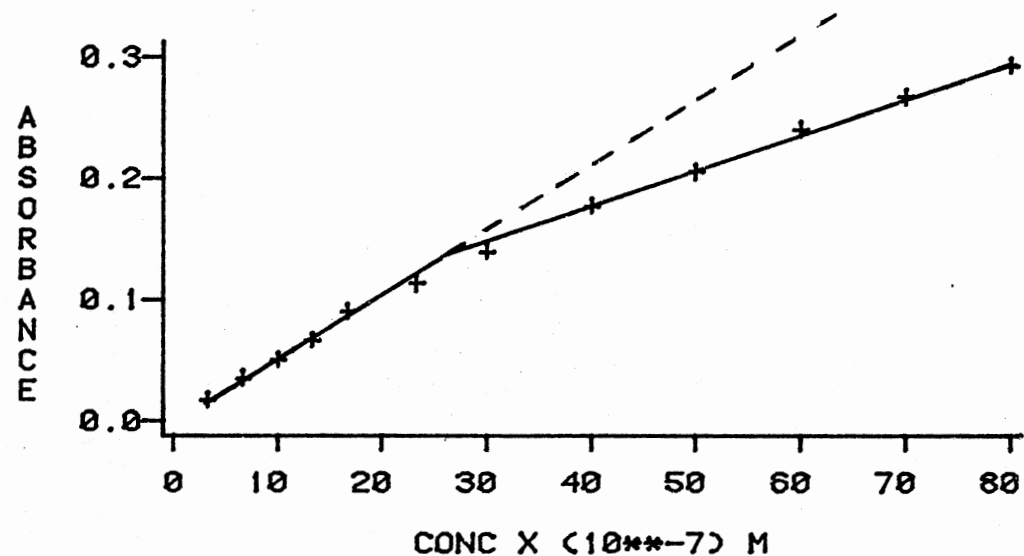
388 NM

Figure 44.   Absorption of the Incorporated 1,6-di-
phenylhexatriene at 388 nm as a
Function of Probe Concentration in the
2.5 ml Suspension of Vesicles in Buffer.
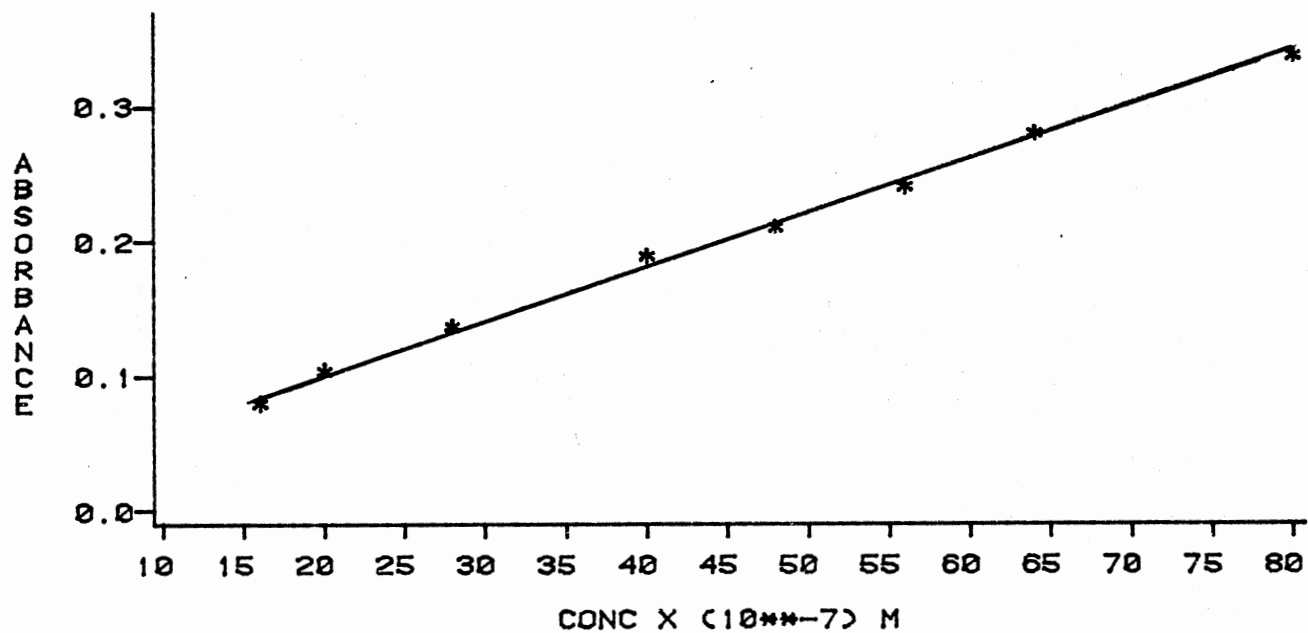
DPH INCORPORATION

320 NM

Figure 45.   Absorption of the Incorporated 1,6-diphenylhexa-
triene at 320 nm as a Function of Probe
Concentration in the 2.5 ml Suspension of
Vesicles in Buffer.
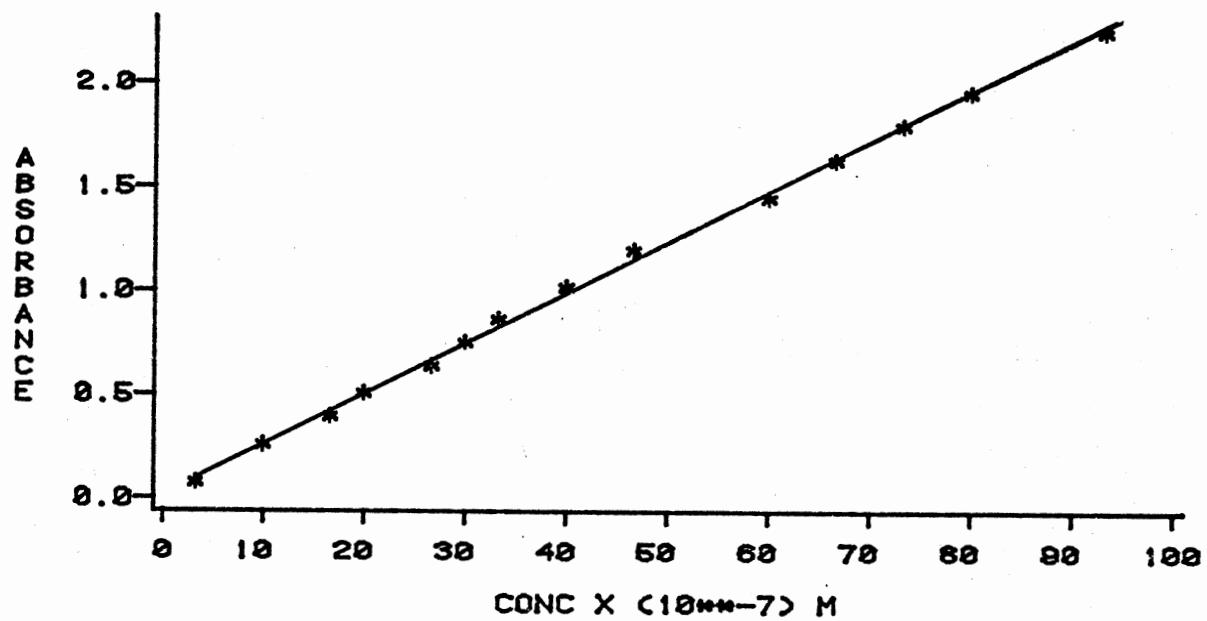
360 NM

Figure 46. Beer's Law Plot of 1,6-diphenylhexatriene in
Tetrahydrofuran Solvent at 360 nm.

There is a limit to probe concentrations which can be utilized in membrane systems. Saturation studies should be made for every new probe in each membrane system employed before any absorption or fluorescent measurements are taken.

While it is now appreciated that probes can saturate a bilayer system, a final question arises as to the extent of perturbation of the membrane system by such probes. An attempt to answer this question, employing polarization studies, is discussed in the next chapter.

CHAPTER V

MEMBRANE PERTURBATION AS MEASURED BY
FLUORESCENCE POLARIZATION

Introduction

One of the limitations of fluorescence probe analysis
of membranes is the actual introduction of foreign molecules
into the membrane system, hence causing a perturbation of
the membrane. Another concern arises as to the exact
location of the incorporated probes. This concern can be
easily overcome by proper design of the fluorescent probes.
These probes can be attached to macromolecules either by
covalent or non-covalent bonding (45). Covalent probes have
the advantage that their exact location in a membrane is
established by the location of the macromolecule.
Non-covalent probes, while not attached to a macromolecule
and so less easily located, introduce less perturbation to
the system. Hence, the need arises for examining the extent
of perturbation that these probes introduce into the system
in order to justify their extensive use in membrane studies.

The problem of membrane perturbation has been of recent
concern to several workers. In a detailed recent review
(45), Azzi commented on the application of fluorescent
probes to membrane studies and the perturbations they

introduce into the system. Other studies, like X-ray diffraction (139), have shown that some fluorescent probes do perturb the architecture of the membrane at high concentrations. However, such perturbations were not evident at low concentrations by these studies. In another study (134), a number of probes having different sizes were employed to compare the information obtained about the bilayer by the different probes. It was found that there was a range of packing imperfections caused by the different molecular probe structures. Hence, probes were suggested to be of a use in the detection of dynamic aspects of the membrane only rather than in absolute values of membrane parameters. In a study of a complex system of cytochrome-c-cardiolipin-water (140), fluorescence measurements were correlated with the lipid-protein interactions while on the other hand, the X-ray data gave no such evidence. This was an indication of the validity of fluorescent probe use in complex systems as opposed to other methods.

The perturbation problem was thought to be partially overcome by using lipid-mimic fluorescent probes. However, in a study of some incorporated anthroyl probes in DPPC vesicles (69), fluorescence depolarization and differential scanning calorimetry measurements showed a similar decrease in the lipid phase transition. These results showed that even the lipid-mimic fluorescent probes perturbed the bilayer packing, although the extent of perturbation

decreased as the anthroyl moiety was moved towards the center of the bilayer. In a more recent study (141), discrepencies instead of similarities between fluorimetric and calorimetric studies were reported. Differences detected in the pretransition as well as the main transition of multilamellar vesicles appeared to result from perturbations introduced by the fluorescent probes. These perturbations caused a lowering of both transition temperatures, although the lowering was more dramatic for the pretransition.

More recently (142), the fluorescent probe Merocyanine 540 was used to yield quantitative information about bilayer perturbation. Differential scanning calorimetric studies showed that at low dye:lipid ratios, the dye perturbs its own microenvironment; whereas any further increase in the dye concentration would result in perturbation of the whole lipid bilayer.

In an attempt to clarify the perturbation problem, a series of fluorescence polarization curves versus temperature for different probe/lipid ratios were measured.

Results and Discussion

Experimental Procedure

Fluorescence polarizations measurements were made on a home-built fluorometer. A description of the spectrofluorometer is included in chapter II. The automation of the entire fluorometer by the microcomputer

made the polarization measurements very precise and accurate. Since the whole process of the polarization measurements was controlled by the microcomputer, polarization values were found to be extremely reproducible to within 1% over a period of one year. A program was written to run the fluorescence emission and excitation spectra. Such a program enabled us to check occasionally for the Raman bands of the phospholipid molecules and the water solvent. Due to the interference of these intense bands with the polarization measurements, dilute solutions of vesicle suspensions were used. The best wavelength settings of both monochromators were chosen such that a minimal interference of Raman bands occured. Another computer program was used to calculate the grating correction factor of the emission monochromator. This correction factor was included in all polarization measurements.

Each polarization measurement reported was the result of an average of at least 100 readings of the photon counter. These readings were ratioed to the intensity of the solar cell to account for any short-term variation in the lamp intensity. The emission polarizers were moved manually during the process of the polarization measurements.

Stirring of the sample was found to be an important factor in measuring reproducible data. The stirrer was occasionally checked for any jittering in its movement since

such irregularities introduced some noise in the measurements. Stirring was also helpful in eliminating any temperature gradients created in the sample. Each polarization measurement was taken after the sample temperature had equilibrated for about 5 minutes. Several polarization measurements were taken for each temperature setting before the temperature was increased. These measured values were reproducible to within 1%. Temperature was increased by $1^{o}C$ for measurements taken below and above the phase transition. However, increments of $0.2 - 0.5^{o}C$ were employed for values near the phase transition. Polarization measurements were taken along both the heating and cooling directions of the sample for one experiment. Results were identical and showed the cooperativity of the phase transition as mentioned elsewhere (143).

It was noticed that evaporation of the buffer from the sample occurred if the vesicles were used for more than one experiment. That was due to the high temperatures reached during the polarization measurements. Care was exercised as to the exact volume of the sample since any variations would introduce error in the calculation of the absorbance values. Fresh samples of lipid vesicles were used for each perturbation experiment. These experiments involved the incorporation of different probe concentrations into the lipid vesicles. Concentrations were chosen to vary below and above the critical probe/lipid concentration ratios reported in Chapter IV, for comparison purposes.

Perturbation of Phase Transitions

Fluorescence polarization is extremely sensitive to the microenvironment of the probe and may also report on the state of the membrane as a whole. The phase transitions of the dipalmitoyl phosphatidylcholine vesicles can be observed by a study of the polarization curves of a set of n-(9-anthroyloxy)fatty acids as well as the commonly studied probe 1,6-diphenylhexatriene.

A comparison of the steady-state polarization values of the different probes used may be attributed to the membrane fluidity at the specific location where the probe resides. According to Lussan et al. the depolarization of fluorescent probes incorporated in small vesicles results from two contributions (144):

1. Intrinsic rotational motion of the chromophore, and

2. Rotational diffusion of the whole vesicles.

A careful study showed that the rotational motion was of great importance, while the latter contribution was negligible.

The difference in the polarization values measured below and above the gel-liquid crystalline phase transition can be used as a measure of the change in fluidity as the bilayer undergoes the phase transition. Comparison of these differences for all the probes employed would indicate the exact location at which the phase transition occurs inside the lipid matrix. Such differences would also provide some details about the extent of perturbations induced by the

probes. Any sudden decrease in polarization values occuring around the phase transition may be attributed to changes in the viscosity of the medium as well as changes in the lifetime of the excited state of the chromophore. In order to decide as to which factor contributes more to the polarization values, a study of lifetime measurements versus temperature is necessary.

Local perturbations of biological membranes are inherent in fluorescent studies even with the use of a minimal concentration of fluorescent probes. However, in order to study the extent of these local perturbations on the whole membrane, higher probe/lipid concentrations need to be employed.

Analysis of 1,6-Diphenylhexatriene
Polarization Curves

Examination of the polarization curves for 1,6-diphenylhexatriene incorporated in dipalmitoyl phosphatidylcholine vesicles with 1 and 2 µl of stock, shows a great similarity. Polarizations of 0.43 were detected below the phase transition of the lipid, as shown in Figure 47. Such a high polarization value indicates the presence of the probe in a very rigid medium. A phase transition between the liquid crystalline and gel states was observed at $41^{o}C$. Polarizations values approached a constant value of 0.11 above the phase transition in the range of 45 - $60^{o}C$. The change in polarization values of 0.32 measured

DPH/VESICLES
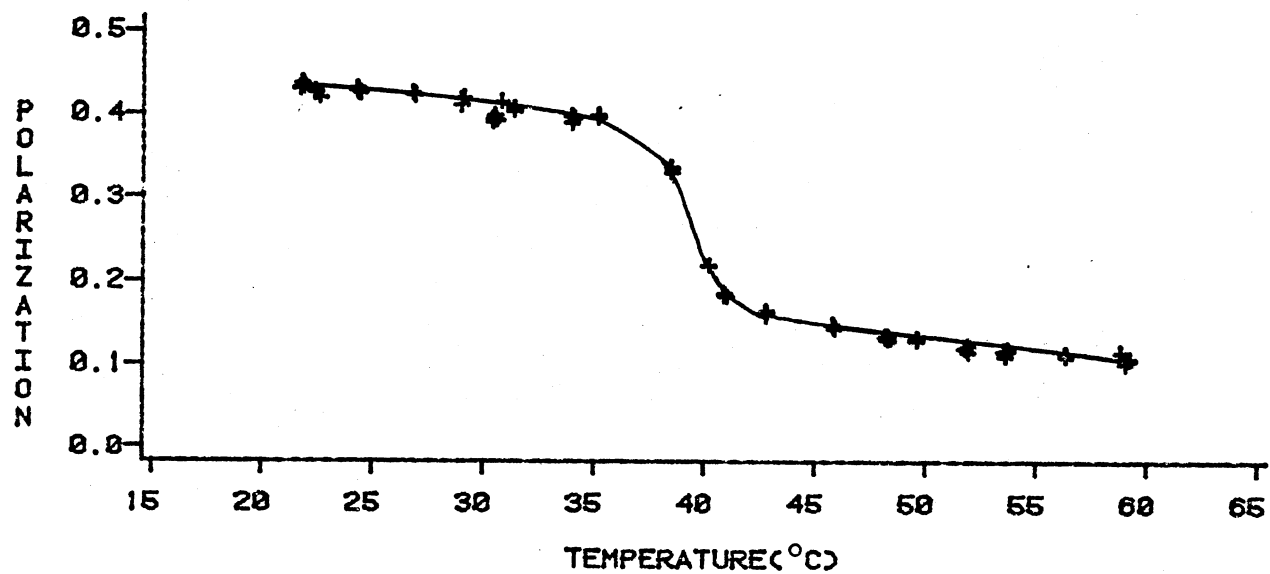
Figure 47.   Polarization as a Function of Temperature, For
             2 ul of 10^{-3} M Stock of 1,6-diphenyl
             hexatriene in Tetrahydrofuran Solvent Incor-
             porated into Dipalmitoyl Phosphatidylcholine
             Lipid Vesicles.

below and above the phase transition can be used as a measure of the fluidity change as the bilayer undergoes a phase transition. Comparing this change with other data would reveal some information as to the packing of the membrane. Significant changes in the polarization curves were observed for higher probe concentrations for the case of 10 μl of DPH stock, as evident in Figure 48. As the probe concentration was increased from 1 μl to 30 μl, a significant drop of 0.06 in polarization values was noticed below the phase transition as opposed to a drop of 0.01 above the phase transition. Great similarities in polarization curves were also observed for the 20 and 30 μl probe samples. A plot of the polarization values measured at 25°C versus the probe/lipid molar ratio shows a decrease in polarization values before reaching a plateau at a molar ratio of 0.02, Figure 49. Examination of figure 49 reveals the fact that even at small probe concentrations, the probe is perturbing its microenvironment and the whole lipid structure.

Further analysis of the polarization curves reveals important information about the transition temperatures. A plot of the first derivative of the polarization with respect to temperature versus temperature shows a sharp break in the curve as shown in Figure 50. The break point corresponds to an inflection point in the polarization curves indicating the phase transition of the lipids. Addition of excess dye caused major effects on the

DPH/VESICLES
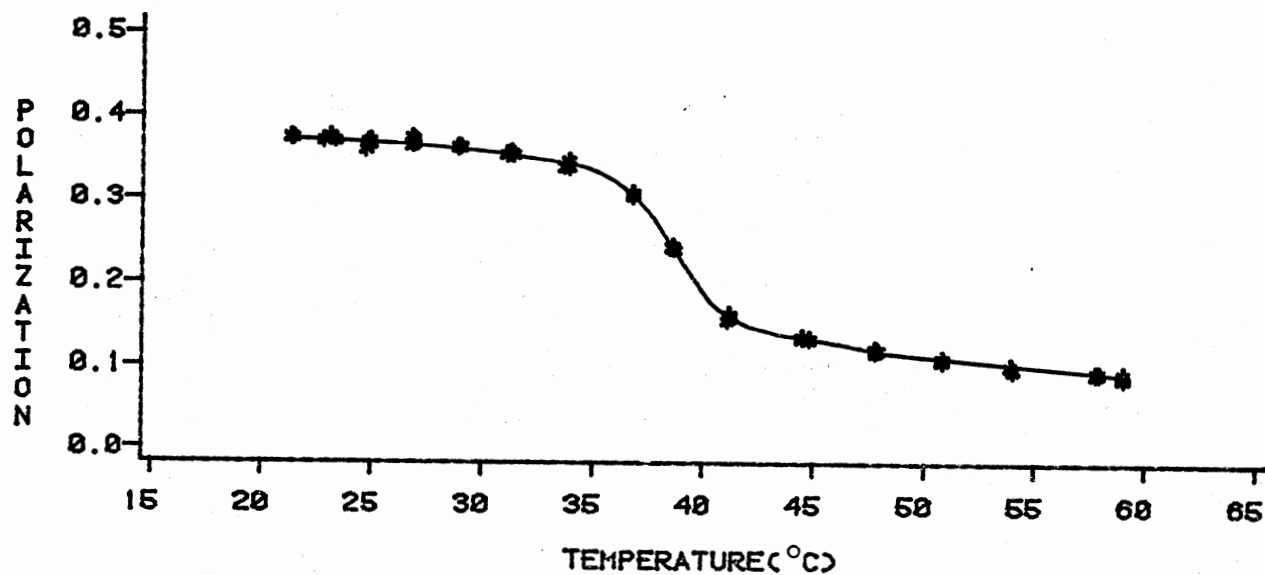
Figure 48. Polarization as a Function of Temperature, For
            10 ul of 10^{-3} M Stock of 1,6-diphenyl
            hexatriene in Tetrahydrofuran Solvent Incor-
            porated into Dipalmitoyl Phosphatidylcholine
            Lipid Vesicles.

DPH/VESICLES
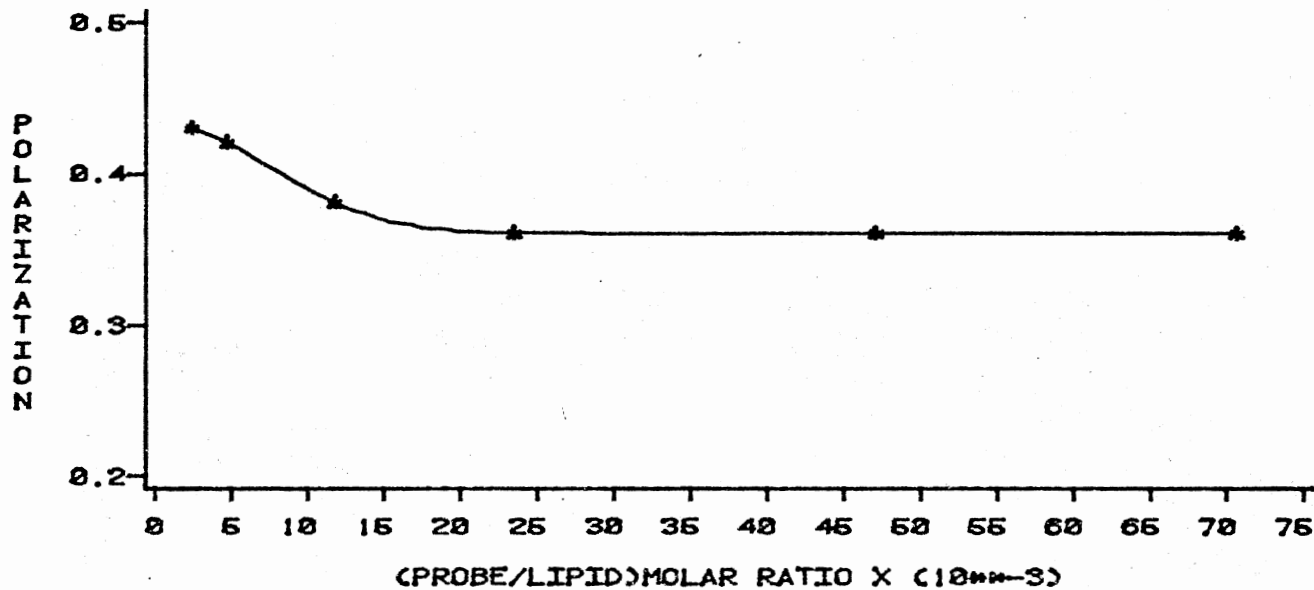
TEMP=25 °C

Figure 49.   Polarization as a Function of Probe/Lipid Molar
             Ratio in Case of 1,6-diphenylhexatriene Incor-
             porated into Dipalmitoyl Phosphatidylcholine
             Vesicles Measured at 25°C.

DPH(2UL)
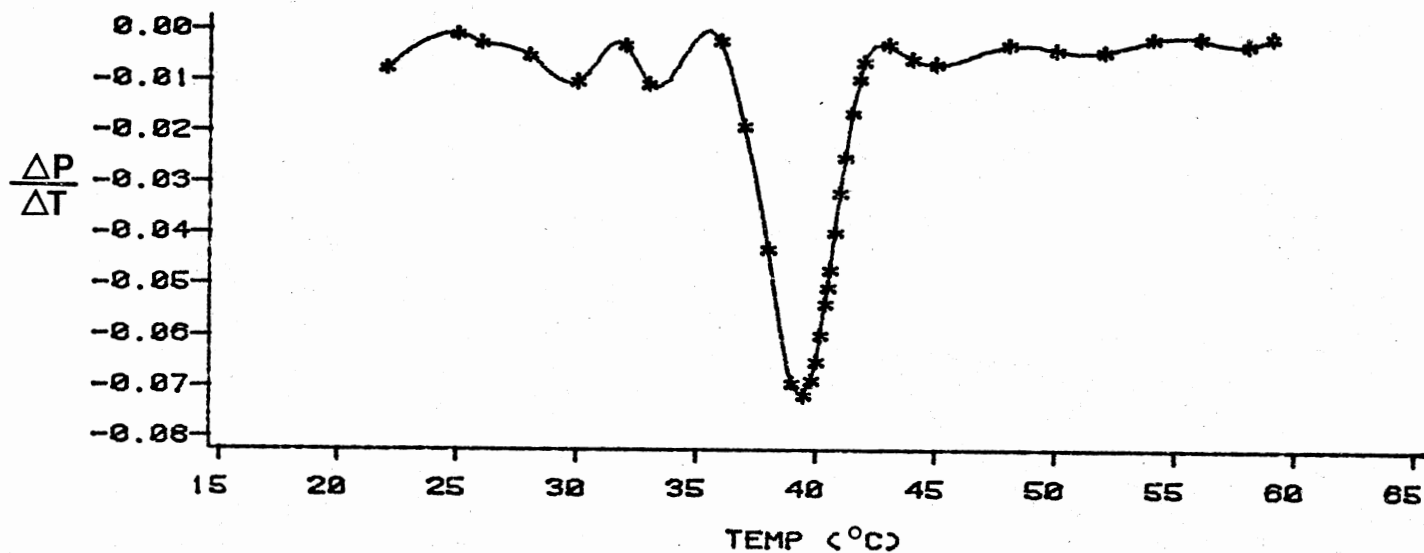
Figure 50. Change of Polarization With Respect to Temperature Vs. Temperature, in Case of 2 μl of 10^{-3} M Stock of 1,6-diphenylhexatriene in Tetrahydrofuran Solvent Incorporated into Dipalmitoyl Phosphatidylcholine Vesicles.

polarization values, depending on the amount of the added dye. Small concentrations, for example 2 and 5 μl of stock, showed a broadening of the phase transition with a break at 40°C. Higher concentrations, 10 - 30 μl of stock for example, showed great broadening in the phase transition, as evident in Figure 51. A pre-transition was noticed at 37°C while the main transition dropped to 39°C. Such information agrees with the data obtained in Figure 49 as to the perturbation of the whole lipid structure at probe/lipid molar ratios above 0.02.

In conclusion, the above study needs to be extended to involve the set of n-(9-anthroyloxy)fatty acid probes. Since each of these probes would reveal valuable information as to the fluidity of specific locations in the membrane. Furthermore, a similar study should be conducted for each probe concentration before any significant data about biological membranes is obtained.

DPH(10UL)
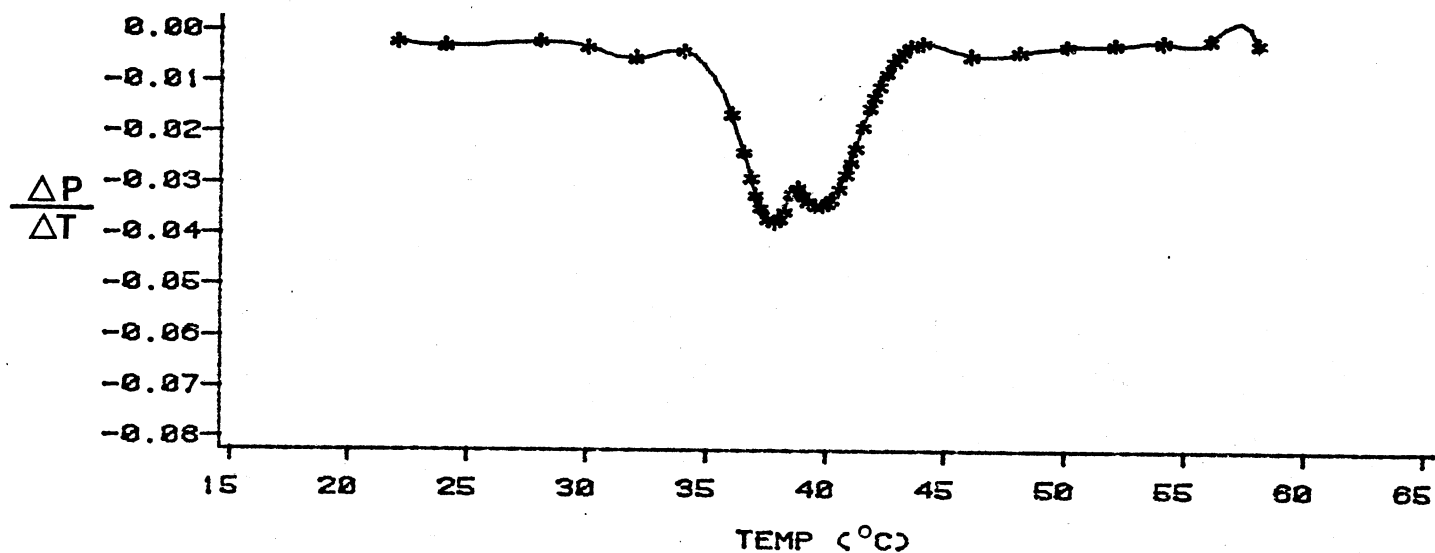
Figure 51. Change of Polarization With Respect to
Temperature Vs. Temperature, in Case of 10 μl
of 10^{-3} M Stock of 1,6-diphenylhexatriene
in Tetrahydrofuran Solvent Incorporated into
Dipalmitoyl Phosphatidylcholine Vesicles.

CHAPTER VI

CONCLUSIONS AND RECOMMENDATIONS

Edge Excitation Red Shift

Edge Excitation Red Shift is a photodynamic characteristic of dyes, which depends on the solute concentration, solvent polarity and viscosity among many other factors (Chapter I). The important feature observed in EERS is the shift in the emission band upon excitation at different wavelengths. Such a process could be an important tool if applied to biological systems.

EERS reflects small polarity changes in the probe's solvent cage. Hence, it can be used to obtain valuable information about the polarity and viscosity of the medium surrounding the chromophore and indicate the exact location of the probe inside the biological membrane. This technique is also very sensitive to the solute-solvent interaction and the relaxation of the solvent cage about the excited state dipole of the probe. The EERS feature is observed if excitation of the solute is accompanied by a large change in its dipole moment and the solvent reorientation relaxation time t_R is large compared with the fluorescence lifetime of the dye t_F.

Due to the sensitivity of this technique to the

solute's environment, EERS may be used in determining the mechanism by which fluorescent probes infer the information from their local environments and from the bulk lipid. Extensive studies were carried on in our laboratory to observe such a process in different cases of fluorescent probes incorporated into biological membranes. Several probes, including a set of n-(9-anthroyloxy)fatty acids and 1,6-diphenylhexatriene, were studied in model and real biological membranes as well as in different solvents. However, no success was achieved in observing this process. As an example, an EERS plot is shown in Figure 52 for the case of 16-(9-anthroyloxy)palmitic acid incorporated into dipalmitoyl phosphatidylcholine vesicles. Examination of this figure shows no shift in the emission band as the excitation wavelength is changed.

Most of the EERS results reported in the literature, were obtained at low temperatures (77 K), using highly viscous solvents such as glycerol. The fact that all our measurements were performed at room temperature and under normal membrane conditions might account for the absence of the EERS process.

In conclusion, further modification of the system needs to be done if the EERS effect is to be observed. Organic solvents, like quinine, acridine and their related compounds, for which the process was observed before need to be used. Probes with larger dipole moment changes between the ground and the first electronic excited states need to

EERS/16AP
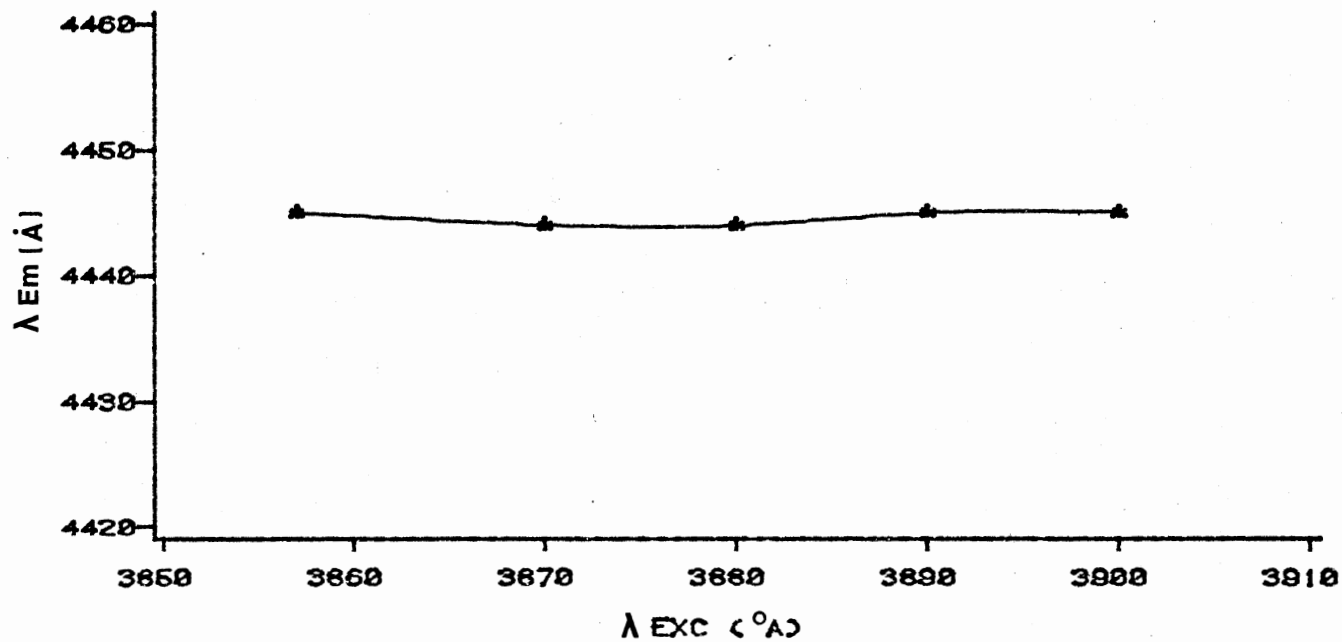
Figure 52. Fluorescence EERS of 16-(9-Anthroyloxy)Palmitic Acid Incorporated into Dipalmitoyl Phosphatidylcholine Vesicles.

be employed. Furthermore, the application of fluorescent probes to multilipid systems as well as multilamellar membranes might be needed to observe such a promising photodynamic process.

Activation Energy of Incorporation as
Measured by Absorption Spectroscopy

The incorporation process of the fluorescent probes into biological membranes was previously studied using fluorescence spectroscopy techniques (Chapter III). The permeation rate of these probes, on a time scale larger than 1 min, was shown to follow a first order kinetics. Results also showed that the activation energy for incorporation was a function of the distance of the chromophore from the polar end of the probe and the length of the acyl portion. These studies revealed valuable information as to the location of these fluorescent probes inside the membrane.

In order to gain more insight into the process of probe incorporation into biological membranes, absorption spectroscopy was used to follow the permeation rate. The same set of lipid-mimic fluorescent probes was employed. Probe incorporation was monitored by following the change (increase/decrease) in absorbance measurements. The change was exponential in form but seemed to increase linearily over long periods of time. All the incorporation curves for the different probes were similar in their exponential and long-term increase in intensity. These results were also

similar to the fluorescence measurements with the difference of the long-term increase. Analysis of the data was complicated, indicating the need for more studies to determine the reason for such an increase.

The observed linear increase may be attributed to the process of flip-flop of either the phospholipids or the fluorescent probes from one side of the biological membrane to the other. The process of flip-flop has been observed to take place over a long period of time (145). Hence, this guess might be valid due to the resemblence of these lipid-mimic fatty acid probes to the phospholipids. This study needs to be further extended for a better understanding of the incorporation process and the lipid flip-flop process.

Recommendations

The following recommendations for future research in this area are made based on the results of this study:

1. A similar study of probe incorporation rate and activation energy needs to be performed with positively and negatively charged lipids. This will indicate the effect of the lipid charge on the incorporation process.

2. A similar investigation of the membrane saturation and perturbation caused by the same fluorescent probes while employing lipids of different polarities.

3. Extension of the perturbation study to the set of n-(9-anthroyloxy)fatty acid probes, in order to correlate

the extent of membrane perturbation with the location of the chromophore inside the biological membrane.

4.   A similar type of study needs to be undertaken with a combination of different proteins and lipids as well as multilamellar systems.   This will provide a better understanding of the real biological system.

5.   The synthesis of anthroyl-derivative probes with the chromophore located at the 2-position and having phosphate head groups seems to be very promising.   These probes will mimic the real system and will align their chromophore parallel to the lipid chains introducing a minimal perturbation.

BIBLIOGRAPHY

1. Danielli, J. F. and Davson, H., _J. Cell. Comp. Physiol._, 5, 495 (1935).

2. Singer, S. J. and Nicolson, G. L., _Science_, 175, 720 (1972).

3. Chapman, D., "Physical Studies of Phospholipids and Biological Membranes" in _Biological Membranes_, K. Colbow (ed.) Simon Fraser university, Canada, 1975, Chapter 1.

4. Jain, M. K. and Wagner, R. C., _Introduction to Biological Membranes_, Wiley-Interscience, New York, 1980.

5. Weissmann, G. and Clairborne, R. (Ed.) _Cell Membranes_, HP Publishing Co, Inc., New York, New York, 1975.

6. Colbow, K. (ed.) _Biological Membranes_, Simon Fraser University, Canada, 1975.

7. Harrison, R. and Lunt, G. G., _Biological Membranes_, Halsted Press. John Wiley and sons, Inc., New York, 1975.

8. Korn, E. D., _Science_, 153, 1491 (1966).

9. Lippert, J. L. and Peticolas, W. L., _Proc. Nat. Acad. Sci._, (USA) 68, 1572 (1971).

10. Gaber, B. P., _American Laboratory._, 15, March (1977).

11. Keough, K. M., Oldfield, E., Chapman, D. and Benyon, P., _Chem. Phys. Lipids_, 10, 37 (1973).

12. Schmidt, C. F., Barenholz, Y. and Thompson, T. E., _Biochemistry_, 16, 2649 (1977).

13. Peterson, N. O. and Chan, S. I., _Biochemistry_, 16, 2657 (1977).

14. Godici, P. E. and Landsberger, F. R., _Biochemistry_, 13, 362 (1974).

15. Devaux, P. and McConnell, H. M., J. Amer. Chem. Soc., 94, 4475 (1972).

16. McNamee, M. G. and McConnell, H. M., Biochemistry, 12, 2951 (1973).

17. Renooji, W., Van Golde, L. M., Zwaal, R. F. A. and Van Deenan, L. L. M., Eur. J. Biochem., 61, 53 (1976).

18. Shinitzky, M. and Barenholz, Y., Biochim. Biophys. Acta., 515, 367 (1978).

19. Shinitzky, M. and Inbar, M., Biochim. Biophys. Acta., 433, 133 (1976).

20. Shinitzky, M., Dianonx, A. C., Gitler, C. and Weber, G., Biochemistry, 10, 2106 (1971).

21. Cogan, U., Shinitzky, M., Weber, G. and Nishida, T., Biochemistry, 12, 521 (1973).

22. Elson, E. L., Schlessinger, J., Koppel, D. E., Axelrod, D. and Webb. W. W., "Measurements of Lateral Transport on Cell Surfaces", in Membranes and Neoplasis: New Approaches and Strategies, Alan, R. Liss Inc., New York, 1976, (137-147).

23. Fahey, P. F., Koppel, D. E., Barak, L. S., Wolf, D. E., Elson, E. L. and Webb, W., Science, 195, 305 (1976).

24. Chapman, D., Ann. N. Y. Acad. Sci., 137, 745 (1966).

25. Esser, A. F. and Lanyi, J. K., Biochemistry, 12, 1933 (1973).

26. Ladbrooke, B. D., Williams, R. M. and Chapman, D., Biochim. Biophys. Acta., 150, 333 (1968).

27. Chapman, D., Q. Rev. Biophysics., 8, 185 (1975).

28. Luzzati, V. and Tardieu, A., Ann. Rev. Phys. Chem., 25, 79 (1974).

29. Gershfeld, N., Ann. Rev. Phys. Chem., 27, 349 (1976).

30. Lee, A. G., Biochim. Biophys. Acta., 472, 285 (1977).

31. Fifield, R., New Scientist, 16, 150 (1980).

32. De Kruijff, B., Cullis, P. R. and Radda, G. K., _Biochim. Biophys. Acta._, 426, 433 (1975).

33. Cater, B. A., Chapman, D., Hawes, S. and Saville, J., _Biochim. Biohys. Acta._, 363, 54 (1974).

34. Rand, R. P., Chapman, D. and Larsson, K., _Biophys. J._, 15, 1117 (1975).

35. Bashford, C. L., Morgan, C. G. and Radda, G. K., _Biochim. Biophys. Acta._, 426, 157 (1976).

36. Trauble, H., _J. Membrane. Biol._, 4, 193 (1971).

37. Brown, M. F. and Seelig, J., _Biochemistry_, 17, 381 (1978).

38. Papahadjopoulas, D., Jacobson, K., Nir, S. and Isac, T., _Biochim. Biophys. Acta._, 311, 330 (1973).

39. Ladbrooke, B. D. and Chapman, D., _Chem. Phys. Lipids._, 3, 304 (1969).

40. Lippert, J. L. and Peticolas, W. L., _Proc. Natl. Acad. Sci._, (USA) 68, 1572 (1971).

41. Oldfield, E. and Chapman, D., _FEBS. Letts._, 21, 303 (1972).

42. Oldfield, E. and Chapman, D., _FEBS. Letts._, 23, 285 (1972).

43. Pang, K. Y. and Miller, K., _Biochim. Biophys. Acta._, 511, 1 (1978).

44. Sakaniski, A., Mitaku, S. and Ikegani, A., _Biochemistry_, 18, 2636 (1979).

45. Azzi, A., _Q. Rev. Biophys._, 8, 237 (1975).

46. Stryer, L., _J. Mol. Biol._, 13, 482 (1965).

47. Patrick, J., Valeur, B., Monnerie, L. and Changeau, J., _J. Memb. Biol._, 5, 102 (1971).

48. Azzi, A., Chance, B., Radda, G. K. and Lee, C. P., _Proc. Natl. Acad. Sci._, (USA) 62, 612 (1969).

49. Dale, R. E., Chen, L. A. and Brand, L., _J. Biol. Chem._, 252, 7500 (1977).

50. Sene', C., Genest, D., Obrenovitch, A., Wahl, P. and Monsigny, M., _FEBS. Lett._, 88, 181 (1978).

51. Lakowicz, J. R. and Prendergast, F. G., Science, 200, 1399 (1978).

52. Obrenovitch, A., Sene', C., Negre, M-T. and Monsigny, M., FEBS. Lett., 88, 187 (1978).

53. Chen, L. A., Dale, R. E., Roth, S. and Brand, L., J. Biol. Chem., 252, 2163 (1977).

54. Lentz, B. R., Moore, B. M. and Barrow, D. A., Biophy. J., 25, 489 (1979).

55. McClure, W. O. and Edelman, G. M., Biochemistry, 6, 567 (1967).

56. Tasaki, I., Watanabe, A. and Halett, M., Proc. Natl. Acad. Sci., (USA) 68, 938 (1971).

57. Latt, S. A., Auld, D. S. and Vallee, B. L., Proc. Natl. Acad. Sci., (USA) 67, 1383 (1970).

58. Chen, R. F. and Kernohan, J. C., J. Biol. Chem., 242, 5813 (1967).

59. Yguerbide, J., Epstein, H. F. and Stryer, L., J. Mol. Biol., 51, 573 (1970).

60. Parker, C. W., Yoo, T., Johnson, M. C. and Godt, S. M., Biochemistry, 6, 3408 (1967).

61. Lee, C. P., Biochemistry, 10, 4375 (1971).

62. Eilermann, L. J. M., Biochim. Biophys. Acta., 211, 231 (1970).

63. Vaughen, W. M. and Weber, G., Biochemistry, 9, 464 (1970).

64. Maddy, A. H., Biochim. Biophys. Acta., 88, 390 (1964).

65. Marinetti, G. V. and Gray, G. M., Biochim. Biophys. Acta., 135, 580 (1967).

66. Yguerabide, J. and Stryer, L., Proc. Natl. Acad. Sci., (USA) 68, 1217 (1971).

67. Waggoner, A. S. and Stryer, L., Proc. Natl. Acad. Sci., (USA) 67, 579 (1970).

68. Vanderkooi, J., Fischkoff, S., Chance, B. and Cooper, R. A., Biochemistry, 13, 1589 (1974).

69. Cadenhead, D. A., Kellner, B. M. J., Jacobson, K. and
        Papahadjopoulas, D., Biochemistry, 16, 5386
        (1977).

70. Thulborn, K. R., Treloar, F. F. and Sawyer, W. H.,
        Biochem. Biophys. Res. Comm., 81, 42 (1978).

71. Tilley, L., Thulborn, K. R. and Sawyer, W. H., J.
        Biol. Chem., 254, 2592 (1979).

72. Stanley, R. J., Willing, R. I., Thulborn, K. R. and
        Sawyer, W. H., Chem. Phys. Lipids., 24, 11
        (1979).

73. Bowen, E. J. and Sahu, J., J. Phys. Chem., 63,
        4 (1959).

74. Oster, G. and Nishijima, Y., J. Amer. Chem. Soc.,
        78, 1581 (1956).

75. Layton, D., Azzi, A. and Graziotti, P., FEBS. Lett.,
        36, 87 (1973).

76. Stryer, L., J. Amer. Chem. Soc., 88, 5708 (1966).

77. Radda, G. K., Biochem. J., 132, 385 (1971).

78. McClure, W. O. and Edelman, G. M., Biochemistry,
        5, 1908 (1966).

79. Lakowicz, J. R. and Weber, C., Biochemistry, 12,
        4161 (1973).

80. Novosad, Z., Knapp, R. D., Gotto, A. M., Pownall, H. J.
        and Morrisett, J. D., Biochemistry, 15, 3176
        (1976).

81. Stryer, L. and Haughland, R. P., Proc. Natl. Acad.
        Sci., (USA) 58, 719 (1967).

82. Perrin, F., Ann. Phys.(Paris) 12, 169 (1929).

83. Borochov, H. and Shinitzky, M., Proc. Natl. Acad.
        Sci., (USA) 73, 4526 (1976).

84. Shinitzky, M. and Inbar, M., Biochim. Biophys. Acta.,
        433, 133 (1976).

85. Rosenthal, K. S., Swanson, P. E. and Storm, D. R.,
        Biochemistry, 15, 5783 (1976).

86. Engelhard, V. H., Esko, J. D., Storm, D. R. and
        Glaser, M., Proc. Natl. Acad. Sci., (USA)
        73, 4432 (1976).

87. Shattil, S. J. and Cooper, R. H., _Biochemistry,_ 15, 4832 (1976).

88. Lentz, B. R., Barenholz, Y. and Thompson, T. E., _Biochemistry,_ 15, 4521 (1976).

89. Lentz, B. R., Barenholz, Y. and Thompson, T. E., _Biochemistry,_ 15, 4529 (1976).

90. Kinosita, K. Jr., Mitaku, S. and Ikegani, A., _Biochim. Biophys. Acta.,_ 393, 10 (1975).

91. Kinosita, K. Jr., Kawato, S. and Ikegani, A., _Biophys. J.,_ 20, 289 (1977).

92. Chen, R. F., _Anal. Biochem.,_ 19, 374 (1967).

93. Fletcher, A. N., _J. Phys. Chem.,_ 72, 2742 (1968).

94. Rubinov, N. and Tomin, V. I., _Opt. Spectrosc.,_ 29, 578 (1970).

95. Khalil, O. S., Seliskar, C. J. and McGlynn, S. P., _J. Chem. Phys.,_ 58, 1607 (1973).

96. Itoh, K. and Azumi, T., _Chem. Phys. Lett.,_ 22, 395 (1973).

97. Klopffer, W., _Chem. Phys. Lett.,_ 11, 482 (1971).

98. Birks, J. B., _Photophysics of Aromatic Molecules._ Wiley-Interscience, London (1970), Chapter 5.

99. Galley, W. C. and Purkey, R. M., _Proc. Natl. Acad. Sci.,_ 67, 1116 (1970).

100. Itoh, K. I. and Azumi, T., _J. Chem. Phys.,_ 62, 3431 (1975).

101. Gangola, P., Joshi, N. B. and Pant, D. D., _Chem. Phys. Lett.,_ 51, 144 (1977).

102. Gangola, P., Joshi, N. B. and Pant, D. D., _Chem. Phys. Lett.,_ 60, 329 (1979).

103. Parker, C. A. _Photoluminescence of Solutions,_ Elsevier Publishing Company, Amesterdam, 1968.

104. Freedman, R. B. and Radda, G. K., _FEBS. Lett.,_ 3, 150 (1969).

105. Radda, G. K. and Smith, D. S., _Biochim. Biophys. Acta.,_ 318, 197 (1973).

106. Fortes, G. P. A. and Hoffman, J. F., J. Memb. Biol., 16, 79 (1974).

107. Barker, R. W., Barrett-Bee, K. J., Berden, J. A., McCall, C. E. and Radda, G. K., Dynamic of Energy Transducing Membranes, Elseveir, Amsterdam, 1974, p 321.

108. Haynes, D. H. and Simkowitz, P., J. Memb. Biol., 33, 63 (1977).

109. Parsegian, A., Nature (London), 221, 844 (1969).

110. Kosower, N. S., Kosower, E. M., Sholmo, L. and Pluznik, D. H., Biochim. Biophys. Acta., 507, 128 (1978).

111. Lang, M., Koivursaari, U. and Hietanen, E., Biochim. Biophys. Acta., 539, 195 (1978).

112. Esko, J. D., Gilmore, J. R. and Glaser, M., Biochemistry, 16, 1881 (1977).

113. Gratzel, M. and Thomas, J. K., J. Amer. Chem. Soc., 95, 6885 (1973).

114. Infelta, P. P., Gratzel, M. and Thomas, J. K., J. Phys. Chem., 78, 190 (1974).

115. Chen, M., Gratzel, M. and Thomas, J. K., Chem. Phys. Letts., 24, 65 (1974).

116. Pownall, H. and Smith, L., Biochemistry, 13, 2594 (1975).

117. Tsong, T. Y., Biochemistry, 14, 5409 (1975).

118. Rockley, M. G. and Najjar, D. S., Biochim. Biophys. Acta., 644 (1981) in press.

119. Saunders, L., Perrin, J. and Gammack, D., J. Pharm. Pharmacol., 14, 567 (1962).

120. Huang, Ching-Hsein., Biochemistry, 8, 344 (1969).

121. Hauser, H., Biochim. Biophys. Res. Commun., 45, 1049 (1971).

122. Brunner, J., Skrabal, P., and Hauser, H., Biochim. Biophys. Acta., 455, 322 (1976).

123. Kremer, J.M.H., Esker, M.W.J.v.d., Pathmamanoharan, C. and Wiersema, P. H., Biochemistry, 16, 3932

(1977).

124. Green, D. E. and Fleischer, S. "Metabolism and significance of lipids", R. M. C. Dawson and D. N. Rodes (Eds.), Wiley-Interscience, New York, New York 1964, p. 584.

125. Batzri, S. and Korn, E. D., Biochim. Biophys. Acta., 298, 1015 (1973).

126. Azumi, T. and McGlynn, S. P., J. Chem. Phys., 37, 2413 (1962).

127. Carraway, K. L., Huggins, J. W., Sherblom, A. P., Chestnut, R. W., Buck, R. L., Howard, S. P., Ownby, C. L. and Carraway, C. A. C. (1978) in Glycoprotein and Glycolipids in Disease (F. F. Walborg, Jr., ed.) American Chemical Society Symposium # 80, 432-445.

128. Arjunan, P., Shymasundar, N., Berlin, K. D., Najjar, D. S. and Rockley, M. G., J. Org. Chem., 46, 626 (1981).

129. Lelkes, P. I., Kapitkovsky, A., Eibl, H. and Miller, I. R., FEBS Letts 103, 181 (1979).

130. Haigh, E., Thulborn, K. R., Nichol, L. W. and sawyer, W. H., Aust. J. Biol. Sci., 31, 447 (1978).

131. Thulborn, K. R. and Sawyer, W. H., Biochim. Biophys. Acta., 511, 125 (1978).

132. Radda, G. K., Current Topics in Bioenergetics (Sanadi, R., ed.) Academic Press, New York, New York, 1972, p. 81.

133. Radda, G. K. and Vanderkooi, J. M., Biochim. Biophys. Acta., 265, 509 (1972).

134. Badley, R. A., Martin, W. G. and Schneider, H., Biochemistry, 12, 268 (1973).

135. Krishnan, K. S. and Balaram, P., FEBS Letts, 60, 419 (1975).

136. Haigh, E. A., Thulborn, K. R., Nichol, L. W. and Sawyer, W. H., Aust. J. Biol. Sci., 31, 1 (1978).

137. Trauble, H. and Overath, P., Biochim. Biophys. Acta., 307, 491 (1973).

138. Willard, H. H., Merritt, L. L. (Jr.) and Dean,

J. A., Instrumental Methods of Analysis
D. Van Nostrand Company, New York, N. Y.
1974, chp. 7.

139. Wilkins, M. H. F., Ann. N.Y. Acad. Sci., 195, 291 (1972).

140. Letellier, L. and Schechter, E., Eur. J. Biochim., 40, 507 (1973).

141. Lentz, B. R., Freire, E. and Biltonen, R. L., Biochemistry, 17, 4475 (1978).

142. Lelkes, P. I., Bach, D. and Miller, I. R., J. Memb. Biol., 54, 141 (1980).

143. Thulborn, K. R., Ph.D. Thesis: University of Melbourne, Australia (1979).

144. Lussan, C. and Fuacon, J. F., FEBS. Letts., 19, 186 (1971).

145. Roseman, M., Litman, B. J. and Thompson, T. E., Biochemistry., 14, 4826 (1975).

APPENDIX A

LISTING OF COMPUTER PROGRAMS

```
]LD MENU
]LIST
5 D$ = ""
10   CALL  - 936
20   PRINT "    **** MENU ****"
30   PRINT
40   PRINT "INPUT: "
50   HTAB 7: PRINT "1 IF YOU WANT TO RUN DADA2"
60   HTAB 7: PRINT "2 IF YOU WANT CORRECTION FACTOR"
70   HTAB 7: PRINT "3 IF YOU WANT TO TAKE POLARIZATION VALUES"
75   HTAB 7: PRINT "4 IF YOU WANT TO RUN SCANNER
76   HTAB 7: PRINT "5 IF YOU WANT TO RUN DADA3"
80   INPUT "WHAT ONE DO YOU WANT?....";A
85   CALL  - 936
90   ON A GOTO 100,110,120,130,140
93   IF A < 1 OR A > 4 THEN 80
100   PRINT D$;"RUN DADA2"
110   PRINT D$;"RUN CORRECTION FACTOR"
120   PRINT D$;"RUN POLARIZATION"
130   PRINT D$;"RUN SCANNER"
140   PRINT D$;"RUN DADA3"
```

```
]LD CORR FACT
]LIST
0   REM   THIS IS CORRECTION FACTOR
5 D$ = ""
6   CALL  - 936
10   DIM HH(50),HV(50),H1(50),H2(50)
20 PO$(1) = "H/H":PO$(2) = "H/V"
30   INPUT "#OF SUCCESSIVE READINGS FOR EACH VALUE";NR
35   INPUT "TIME TO CHANGE POLARIZERS?(X 5 SEC)";DE
40 F(2) = NR:F(3) = NR
50   INPUT "#OF TRIALS = ";NT
60 N = 2:A =  - 16384 + (256 * N)
70   CALL  - 936
75   HTAB 12: PRINT "CORRECTION FACTOR"
89 XK = 1
90   FOR L = 1 TO NT
91   POKE 37,10: PRINT " "
92   PRINT "CHANGE POLARIZERS"
94   PRINT : PRINT "TO": PRINT PO$(XK)
95   PRINT "TRIAL #";L: GOSUB 1600
96   POKE 37,10: PRINT " "
97   PRINT "NOW TAKING VALUES"
99 SP = 0:SS = 0
100   FOR JK = 1 TO 5
110   GOSUB 1400: GOSUB 1200
120 SP = SP + AB(3)
130 SS = SS + AB(2)
140   NEXT JK
150   IF XK = 1 THEN 170
160 HV(L) = SP / SS
162 XK = 1
```

```
165   GOTO 180
170 HH(L) = SP / SS
172 XK = 2: GOTO 91
180   NEXT L
199 SC = 0
200   FOR JG = 1 TO NT
210 SC = SC + (HV(JG) / HH(JG))
220   NEXT JG
230 SC = SC / NT
290   CALL   - 936
300   PRINT : PRINT "CORRECTION FACTOR = ";SC
310   PRINT : PRINT "DO RECORD THE WAVELENGTH"
320   GOSUB 1600
330   GOTO 2200
800   GOTO 2200
1000   REM   TEMPERATURE
1010 T = 5
1020 AB(1) = 0
1030   FOR I = 1 TO F(1)
1040   POKE A + 1, T
1050 X =   PEEK (A)
1060 AB(1) = AB(1) + X
1070   NEXT I
1075 AB(1) = AB(1) / F(1)
1080 AB(1) = AB(1) * 100 / 144
1090 AX% =   INT (AB(1) * 10)
1100 AB(1) = AX% / 10
1110   RETURN
1200 S = 4
1210 AB(2) = 0
1220   FOR I = 1 TO F(2)
```

```
1230  POKE A + 1.5
1240  X =   PEEK (A)
1250  AB(2) = AB(2) + X
1260  NEXT I
1270  AB(2) = AB(2) / F(2)
1280  AB(2) = AB(2) * 5 / 261
1290  AX% =   INT (AB(2) * 1000)
1300  AB(2) = AX% / 1000
1310  RETURN
1400  PC = 3
1410  AB(3) = 0
1420  FOR I = 1 TO F(3)
1430  POKE A + 1.PC
1440  X =   PEEK (A)
1450  AB(3) = AB(3) + X
1460  NEXT I
1470  AB(3) = AB(3) / F(3)
1480  AB(3) = AB(3) * 5 / 255
1490  AX% =   INT (AB(3) * 1000)
1500  AB(3) = AX% / 1000
1510  RETURN
1600  REM   THIS IS THE DELAY ROUTINE
1610  FOR JK = 1 TO DE
1620  FOR I = 1 TO 3963: NEXT I
1630  NEXT JK
1640  RETURN
2200  PRINT "TAKE NOTE"
2201  INPUT "RETURN FOR MENU"; A$
2202  PRINT D$; "RUN MENU"
```

```
]LD POLARIZATION
]LIST
0    DIM HH(50),HV(50)
2    DIM VH(50),VV(50),V1(50),V2(50)
3    CALL  - 936
5 D$ = ""
10 N = 2:A =  - 16384 + (256 * N):PO$(1) = "V/H":PO$(2) = "V/V"
20    INPUT "#OF READINGS TO TAKE AT EACH T";NT
30    INPUT "# OF READINGS OF P/C AND S/C";NR:F(2) = NR:F(3) = NR
35    INPUT "CORRECTION FACTOR = ";CF
36    INPUT "DELAY FOR CHANGES (X5 SEC.)";DE
40    CALL  - 936
50    HTAB 15: PRINT "POLARIZATION DATA"
90 XK = 1
100   FOR L = 1 TO NT
105   POKE 37,10: PRINT " "
106   PRINT "TRIAL #";L
110   PRINT PO$(XK)
119   PRINT ""
120   POKE 37,5: PRINT " ": PRINT "CHANGE POLARIZERS TO"
122   GOSUB 1600: PRINT "": POKE 37,5: PRINT " ": PRINT "NOW TAKING VALUES
      OF"
130 PZ = 0:SZ = 0
140   FOR L1 = 1 TO 5
150   GOSUB 1200
160   GOSUB 1400
170 PZ = PZ + AB(3)
180 SZ = SZ + AB(2)
190   NEXT L1
200 RZ = PZ / SZ
205   IF XK = 1 THEN 210
```

```
206 VV(L) = RZ:V1(L) = PZ
207  GOTO 220
210 VH(L) = RZ:V2(L) = PZ
220  IF XK = 1 THEN 230
225 XK = 1: GOTO 250
230 XK = 2
240  GOTO 105
250  NEXT L
300  POKE 37,13
310  PRINT " "
320  FOR I = 1 TO NT
330  PRINT "  #"; I;" ";
340  NEXT I
345  PRINT
350  PRINT " V/H "
360  FOR I = 1 TO NT
365  PRINT VH(I);"   ";
370  NEXT I
371  PRINT : PRINT "P. C. FOR V/H"
372  FOR I = 1 TO NT: PRINT V2(I);"   "; : NEXT I
375  PRINT
376  PRINT : PRINT
380  PRINT " V/V "
390  FOR I = 1 TO NT
400  PRINT VV(I);"   ";
410  NEXT I
415  PRINT
420  PRINT "P. C. FOR V/V"
430  FOR I = 1 TO NT
440  PRINT V1(I);"   ";
450  NEXT I
490 X1 = 0:X2 = 0
```

```
500   FOR JK = 1 TO NT
510 X1 = X1 + VV(JK)
520 X2 = X2 + VH(JK)
530   NEXT JK
540 X1 = X1 / NT
550 X2 = X2 / NT
560 P = (X1 - CF * X2) / (X1 + CF * X2)
570   PRINT : PRINT "POLARIZATION = ";P
572 F(1) = 30: GOSUB 1000
573   PRINT "TEMPERATURE = ";AB(1);" C. "
580 DE = 3
585   PRINT : PRINT
590   PRINT "GO TO NEW TEMPERATURE"
595   PRINT "ENTER 'MENU' IF YOU WANT THAT"
600   INPUT "OTHERWISE JUST PRESS RETURN";QX$
605   IF QX$ = "MENU" THEN 607
606   GOTO 610
607   PRINT D$;"RUN MENU"
610   CALL  - 936: GOTO 100
650   GOTO 2200
1000   REM   TEMPERATURE
1010 T = 5
1020 AB(1) = 0
1030   FOR I = 1 TO F(1)
1040   POKE A + 1,T
1050 X =  PEEK (A)
1060 AB(1) = AB(1) + X
1070   NEXT I
1075 AB(1) = AB(1) / F(1)
1080 AB(1) = AB(1) * 100 / 144
1090 AX% =  INT (AB(1) * 10)
1100 AB(1) = AX% / 10
1110   RETURN
```

```
1200 S = 4
1210 AB(2) = 0
1220  FOR I = 1 TO F(2)
1230  POKE A + 1, S
1240 X =   PEEK (A)
1250 AB(2) = AB(2) + X
1260  NEXT I
1270 AB(2) = AB(2) / F(2)
1280 AB(2) = AB(2) * 5 / 261
1290 AX% =   INT (AB(2) * 1000)
1300 AB(2) = AX% / 1000
1310  RETURN
1399  REM  THIS IS THE PHOTON COUNTER ROUTINE
1400 PC = 3
1410 AB(3) = 0
1420  FOR I = 1 TO F(3)
1430  POKE A + 1, PC
1440 X =   PEEK (A)
1450 AB(3) = AB(3) + X
1460  NEXT I
1470 AB(3) = AB(3) / F(3)
1480 AB(3) = AB(3) * 5 / 255
1490 AX% =   INT (AB(3) * 1000)
1500 AB(3) = AX% / 1000
1510  RETURN
1600  REM  THIS IS THE DELAY ROUTINE
1610  FOR JK = 1 TO DE
1620  FOR I = 1 TO 3963: NEXT I
1630  NEXT JK
1640  RETURN
2200  END
```

```
]LIST
10   TEXT : HOME :D$ =  CHR$ (4):S$ = ",S6":V$ = ",V0"
20   INPUT "DO YOU WANT TO SET LAMBDAS?(Y/N)";Q$
30   IF Q$ = "N" THEN 110
40   INPUT "LAMBDA EX. = ";BX
50   INPUT "LAMBDA EM. = ";BM
60   PRINT D$;"OPEN LAMBDAS";V$;S$
70   PRINT D$;"WRITE LAMBDAS"
80   PRINT BX
85   PRINT BM
90   PRINT D$;"CLOSE"
100   GOTO 150
110   PRINT D$;"OPEN LAMBDAS";V$;S$
120   PRINT D$;"READ LAMBDAS"
130   INPUT BX
135   INPUT BM
140   PRINT D$;"CLOSE"
150   PRINT D$;"BL SCAN3"
160   PRINT : PRINT "LAMBDA EX: ";BX;"   LAMBDA EM: ";BM
170   INPUT "HOW MANY INSTRX SETS? (10 MAX.)  ";SET
180   FOR I = 1 TO SET
190   PRINT "SET # ";I
200   PRINT "***************"
210   INPUT "CHART...UNITS OF 41.67A/IN TIMES ";CS(I)
220   INPUT "SCAN SPD(1-220)SLOW-FAST ";SS(I)
230   INPUT "WHICH TO SCAN(M/X)";Q$(I)
240   INPUT "EX. START WAVELENGTH";XS(I)
250  ES(I) = 2 * XS(I)
260   IF XS(I) < 5000 THEN 300
270   PRINT "EX. MONO CAN'T GO BEYOND 5000....SORRY"
280   PRINT "DON'T MAKE THE SAME ERROR FOR END OF SCAN....ITS NOT PROTECTED
      !"
```

```
290   GOTO 240
300   INPUT "EM. START WAVELENGTH";MS(I)
310   INPUT "END WAVELENGTH OF SCAN";EL(I)
320   IF Q$(I) = "M" THEN 340
330 CS(I) = 2 * CS(I):EL(I) = EL(I) * 2
340   NEXT I
350   REM  SET UP SCAN WINDOW
360   HOME : POKE 35,21: VTAB 23:X$ = "000" +  STR$ ( INT (BM)): PRINT " LA
      MBDA EM. "; RIGHT$ (X$,4);
370   X$ = "000" +  STR$ ( INT (BX)): PRINT "       2*LAMBDA EX. "; RIGHT$ (X
      $,4)
380   FOR I = 1 TO SET
390   GOSUB 990: REM  RESET MONS.
400   Y = EL(I):Z = MS(I): IF Q$(I) = "X" THEN Z = ES(I)
410   GOSUB 950: GOSUB 810
420   HOME : PRINT "NOW RUNNING SCAN #"; I;". ": PRINT
430   IF Q$(I) = "M" THEN 450
440   PRINT "SCANNING EXCITATION FROM ": PRINT XS(I);" TO ";EL(I) / 2;" (AC
      TUAL VALUES). ": GOSUB 760: GOTO 460
450   PRINT "SCANNING EMISSION FROM": PRINT MS(I);" TO ";EL(I);". ": GOSUB 7
      50
460   VTAB 15: PRINT "PRESS 'ESC' TO STOP"
470   IF Y > Z THEN  GOSUB 790
480   IF Y < Z THEN  GOSUB 800
490   GOSUB 770: POKE 30,CS(I): POKE 31,CS(I): POKE 25,255 - SS(I)
500   CALL 24576: IF  PEEK ( - 16384) > 127 THEN 670
510   IF Q$(I) = "X" THEN 530
520 BM = Y:BX = ES(I): GOTO 540
```

```
530 BM = MS(I):BX = Y
540  GOSUB 990:BX = ES(I):BM = MS(I): NEXT I
550  GOSUB 870


PLEASE CALL DAD
     A"
570  TEXT : VTAB 15: FLASH : FOR X = 15 TO 23: PRINT "
                           "; : NEXT X
580  NORMAL : VTAB 16: HTAB 10: PRINT "  "; : HTAB 16: PRINT "    "; : HTAB
     21: PRINT "  "; : HTAB 27: PRINT "      "
590  HTAB 10: PRINT " "; : HTAB 12: PRINT " "; : HTAB 16: PRINT " "; : HTAB 1
     9: PRINT " "; : HTAB 21: PRINT " "; : HTAB 23: PRINT " "; : HTAB 27: PRINT
     " "; : HTAB 30: PRINT " "
600  HTAB 10: PRINT " "; : HTAB 13: PRINT " "; : HTAB 16: PRINT " "; : HTAB 1
     9: PRINT " "; : HTAB 21: PRINT " "; : HTAB 24: PRINT " "; : HTAB 27: PRINT
     " "; : HTAB 30: PRINT " "
610  HTAB 10: PRINT " "; : HTAB 14: PRINT " "; : HTAB 16: PRINT "    "; : HTAB
     21: PRINT " "; : HTAB 25: PRINT " "; : HTAB 27: PRINT "     "
620  HTAB 10: PRINT " "; : HTAB 13: PRINT " "; : HTAB 16: PRINT " "; : HTAB 1
     9: PRINT " "; : HTAB 21: PRINT " "; : HTAB 24: PRINT " "; : HTAB 27: PRINT
     " "; : HTAB 30: PRINT " "
630  HTAB 10: PRINT " "; : HTAB 12: PRINT " "; : HTAB 16: PRINT " "; : HTAB 1
     9: PRINT " "; : HTAB 21: PRINT " "; : HTAB 23: PRINT " "; : HTAB 27: PRINT
     " "; : HTAB 30: PRINT " "
640  HTAB 10: PRINT "  "; : HTAB 16: PRINT " "; : HTAB 19: PRINT " "; : HTAB
     21: PRINT "  "; : HTAB 27: PRINT " "; : HTAB 30: PRINT " "
650  FOR I = 1 TO 100: PRINT ""; : FOR X = 1 TO 1000: NEXT X, I
660  END
670  POKE  - 16368,0: GOSUB 910: GOSUB 840: REM   ESCAPE
680  INPUT "WOULD YOU LIKE TO CONTINUE WITH ANOTHER INSTRUCTION SET? ";Q$
690  IF Q$ = "N" THEN  END
700  IF Q$ <  > "Y" THEN 680
```

```
710    INPUT "WHICH ONE ? ";I
720    I = I - 1: NEXT I
730    POP : POKE   - 16368,0: GOSUB 910::BX = Z: GOSUB 870: GOTO 680
740    POP : POKE   - 16368,0: GOSUB 910:BM = Z:BX = ES(I): GOSUB 870: GOTO 6
       80
750    POKE 24587,91: POKE 24590,90: POKE 24686,92: POKE 24696,92: RETURN : REM
          EMISSION POKES
760    POKE 24587,89: POKE 24590,88: POKE 24686,115: POKE 24696,115: RETURN
       : REM  EXCITATION POKES
770    POKE 24602,93: POKE 24605,92: RETURN : REM   CHART ON
780    POKE 24602,95: POKE 24605,94: RETURN : REM   CHART OFF
790    POKE 24612,24: POKE 24615,105: POKE 24621,105: POKE 24627,105: POKE 2
       4633,105: POKE 24638,176: POKE 49988,200: RETURN : REM    FORWARD POKE
       S
800    POKE 24612,56: POKE 24615,233: POKE 24621,233: POKE 24627,233: POKE 2
       4633,233: POKE 24638,144: POKE 49988,128: RETURN : REM   REVERSE POKES

810 A =   INT (Y / 100):C =   INT (A / 10) * 6 + A: POKE 26,C
820 B = Y - A * 100:D =   INT (B / 10) * 6 + B: POKE 27,D
830    RETURN
840 BM = MS(I):BX = Z: IF Q$(I) = "M" THEN 860
850    GOTO 870
860 BX = ES(I):BM = Z
870    PRINT D$;"OPEN LAMBDAS";V$;S$
880    PRINT D$;"WRITE LAMBDAS"
882    PRINT BX
884    PRINT BM
890    PRINT D$;"CLOSE"
900    PRINT : RETURN
910 A =   PEEK (6):B =   PEEK (7):C =   PEEK (8):D =   PEEK (9)
920 Z = (A -   INT (A / 16) * 6) * 100 + (B -   INT (B / 16) * 6) + (C -   INT
       (C / 16) * 6) / 100 + (D -   INT (D / 16) * 6) / 10000
```

```
930    RETURN
940    REM   THIS ROUTINE POKES IN THE CURRENT VALUE OF THE MONO SCANNED IN B
       CD.
950 P = Z * 10000:A =   INT (P / 1000000): POKE 6,  INT (A / 10) * 6 + A
960 B =   INT ((P - A * 1000000) / 10000): POKE 7,  INT (B / 10) * 6 + B
970 C =   INT ((P - A * 1000000 - B * 10000) / 100): POKE 8,  INT (C / 10) *
       6 + C
980 D =   INT (P - A * 1000000 - B * 10000 - C * 100): POKE 9,  INT (D / 10)
       * 6 + D: RETURN
990    HOME : PRINT "RESETTING EM. TO ";MS(I);: PRINT " AND EX. TO ";XS(I): PRINT
       : PRINT "PRESS 'ESC' TO STOP. ": GOSUB 780
1000   POKE 25,45: IF BX = ES(I) THEN 1050
1010 Z = BX:Y = ES(I): GOSUB 760: GOSUB 940: GOSUB 810: IF Y < Z THEN 1040

1020   GOSUB 790: CALL 24576: IF  PEEK ( - 16384) < 128 THEN 1050
1030   GOTO 730
1040   GOSUB 800: CALL 24576: IF  PEEK ( - 16384) > 127 THEN 740
1050   IF BM = MS(I) THEN   RETURN
1060 Z = BM:Y = MS(I): GOSUB 810: GOSUB 750: GOSUB 940: IF Y < Z THEN 1090

1070   GOSUB 790: CALL 24576: IF  PEEK ( - 16384) < 128 THEN   RETURN
1080   GOTO 670
1090   GOSUB 800: CALL 24576: IF  PEEK ( - 16384) > 127 THEN 670
1100   RETURN
```

```
6000-    AD 00 C0     LDA    $C000
6003-    C9 9B        CMP    #$9B
6005-    F0 78        BEQ    $607F
6007-    AD 10 C0     LDA    $C010
600A-    AD 59 C0     LDA    $C059
600D-    AD 58 C0     LDA    $C058
6010-    A5 19        LDA    $19
6012-    20 A8 FC     JSR    $FCA8
6015-    C6 1E        DEC    $1E
6017-    D0 0A        BNE    $6023
6019-    AD 5F C0     LDA    $C05F
601C-    AD 5E C0     LDA    $C05E
601F-    A5 1F        LDA    $1F
6021-    85 1E        STA    $1E
6023-    F8           SED
6024-    18           CLC
6025-    A5 09        LDA    $09
6027-    69 94        ADC    #$94
6029-    85 09        STA    $09
602B-    A5 08        LDA    $08
602D-    69 06        ADC    #$06
602F-    85 08        STA    $08
6031-    A5 07        LDA    $07
6033-    69 00        ADC    #$00
6035-    85 07        STA    $07
6037-    A5 06        LDA    $06
6039-    69 00        ADC    #$00
603B-    85 06        STA    $06
603D-    D8           CLD
603E-    B0 3F        BCS    $607F
6040-    A0 03        LDY    #$03
6042-    A5 07        LDA    $07
6044-    20 69 60     JSR    $6069
6047-    A5 07        LDA    $07
6049-    20 65 60     JSR    $6065
```

```
604C-    A5 06         LDA    $06
604E-    20 69 60      JSR    $6069
6051-    A5 06         LDA    $06
6053-    20 65 60      JSR    $6065
6056-    A5 06         LDA    $06
6058-    C5 1A         CMP    $1A
605A-    D0 A4         BNE    $6000
605C-    A5 07         LDA    $07
605F-    C5 1B         CMP    $1B
6060-    F0 1D         BEQ    $607F
6062-    4C 00 60      JMP    $6000
6065-    4A            LSR
6066-    4A            LSR
6067-    4A            LSR
6068-    4A            LSR
6069-    29 0F         AND    #$0F
606B-    09 B0         ORA    #$B0
606D-    99 73 07      STA    $0773,Y
6070-    88            DEY
6071-    60            RTS
6072-    A9 B0         LDA    #$B0
6074-    A0 04         LDY    #$04
6076-    88            DEY
6077-    99 73 07      STA    $0773,Y
607A-    D0 FA         BNE    $6076
607C-    AD 10 C0      LDA    $C010
607F-    60            RTS
6080-    C0 60         CPY    #$60
6082-    00            BRK
6083-    00            BRK
6084-    FF            ???
6085-    FF            ???
6086-    FF            ???
6087-    FF            ???
6088-    FF            ???
6089-    FF            ???
```

```
LD SCANNER
]LIST
10   REM ********SCANNER*********
15   HOME :D$ =  CHR$ (4): POKE 35,21: POKE 25,210: POKE 26,120: POKE 27,50
     : POKE 28,35
20   PRINT "DO YOU WANT INSTRUCTIONS? "; : GET Q$: PRINT : PRINT : IF Q$ = "
     N" THEN 55
25   IF Q$ <  > "Y" THEN 20
30   PRINT "PREVIOUS LAMBDAS ARE STORED ON THE DISK AND SHOULD NOT NEED TO
     BE SET UNLESS A  MONOCHRONOMETER HAS BEEN MOVED. "
35   PRINT "YOU MAY CHOOSE FOR CHART TO RECORD OR   NOT, CHOOSE WHICH MONOC
     H. TO SCAN AND   CHOOSE TO SCAN FORWARDS OR BACKWARDS.    AFTER THE LA
     ST CHOICE THE SCAN BEGINS. "
40   PRINT "THE KEYS 1-4 ARE SPEED SETTINGS. THE    SCAN ALWAYS STARTS OUT
     ON SETTING #1    (VERY SLOW). THE SPEED CAN BE CHANGED BYHITTING ONE
     OF THESE KEYS ANYTIME DURINGTHE SCAN. ANY OTHER KEY STOPS THE SCAN. "
45   PRINT "   KEY #1 -- 38 NM/MIN": PRINT "          2 -- 110": PRINT "
        3 -- 610": PRINT "          4 -- 1100"
50   PRINT "HIT ANY KEY TO CONTINUE  "; : GET Q$: HOME
55   PRINT "DO YOU WANT TO SET LAMBDAS (Y/N)?"; : GET Q$: PRINT : PRINT
60   IF Q$ = "N" THEN 95
65   IF Q$ <  > "Y" THEN 55
70   INPUT "LAMBDA EX. (AS READ FROM MACHINE)";BX: INPUT "LAMBDA EM. ";BM: PRINT

75   PRINT D$;"OPEN LAMBDAS,V0,S6"
80   PRINT D$;"WRITE LAMBDAS"
85   PRINT BX: PRINT BM
90   PRINT D$;"CLOSE"
95   PRINT D$;"BL SCAN": IF Q$ = "Y" THEN 110
100   PRINT D$;"OPEN LAMBDAS,V0,S6"
105   PRINT D$;"READ LAMBDAS": INPUT BX: INPUT BM: PRINT D$;"CLOSE"
110   VTAB 23:X$ = "000" +  STR$ ( INT (BM)): PRINT " LAMBDA EM. "; RIGHT$
     (X$,4);
115  X$ = "000" +  STR$ ( INT (BX)): PRINT "        2*LAMBDA EX "; RIGHT$ (X
     $,4): HOME
```

```
120   PRINT "RECORD SCAN ON CHART? ";: GET Q$: PRINT : PRINT : POKE 24599,9
      .5: POKE 24602,94: REM CHART OFF
125   IF Q$ = "N" THEN 145
130   IF Q$ <  > "Y" THEN 120
135   PRINT "CHART UNITS OF 41.67 A/IN TIMES WHAT    INTEGRAL FACTOR? ";: GET
      CH: PRINT : PRINT
140   PRINT "CHART AT ";CH * 41.67;" A/IN": PRINT : POKE 30,CH: POKE 31,CH:
       POKE 24599,93: POKE 24602,92: REM CHART ON
145 Z = RM: POKE 24584,91: POKE 24587,90: POKE 24688,92: POKE 24698,92: REM
      SCAN EM
150   PRINT "SCAN EMISSION OR EXCITATION (M/X)? ";: GET S$: PRINT : PRINT :
       IF S$ = "M" THEN 165
155   IF S$ <  > "X" THEN 150
160   POKE 30,CH * 2: POKE 31,CH * 2:Z = EX: POKE 24584,89: POKE 24587,88: POKE
      24688,115: POKE 24698,115: REM SCAN EX
165 P = Z * 10000: REM POKE IN LAMBDA SCANNED,250-258
170 A =   INT (P / 1000000): POKE 6, INT (A / 10) * 6 + A
175 B =   INT ((P - A * 1000000) / 10000): POKE 7, INT (B / 10) * 6 + B
180 C =   INT ((P - A * 1000000 - B * 10000) / 100): POKE 8, INT (C / 10) *
      6 + C
185 D =   INT (P - A * 1000000 - B * 10000 - C * 100): POKE 9, INT (D / 10)
      * 6 + D
190   POKE 24609,24: POKE 24612,105: POKE 24618,105: POKE 24624,105: POKE 2
      4630,105: POKE 24635,176: POKE 49988,200: REM SCAN FORWARD
195   PRINT "SCAN FORWARD OR REVERSE (F/R) ?";: GET Q$: PRINT : PRINT : IF
      Q$ = "F" THEN 210
200   IF Q$ <  > "R" THEN 195
205   POKE 24609,56: POKE 24612,233: POKE 24618,233: POKE 24624,233: POKE 2
      4630,233: POKE 24635,144: POKE 49988,128: REM SCAN BACKWARD
```

```
210 CALL 24576: REM -SCAN-
215 P1 = PEEK (6):P2 = PEEK (7):P3 = PEEK (8):P3 = PEEK (9)
220 Z = (P1 - INT (P1 / 16) * 6) * 100 + (P2 - INT (P2 / 16) * 6) + (P3 -
    INT (P3 / 16) * 6) / 100 + (P4 - INT (P4 / 16) * 6) / 10000
225 IF F$ = "F" AND Z = 0 THEN Z = 10000
230 IF S$ = "M" THEN BM = Z
235 IF S$ = "X" THEN BX = Z
240 PRINT D$;"OPEN LAMBDAS.V0,S6"
245 PRINT D$;"WRITE LAMBDAS"
250 PRINT BX: PRINT BM
255 PRINT D$;"CLOSE"
260 PRINT "ANOTHER SCAN?";: GET Q$: PRINT : PRINT : IF Q$ = "Y" THEN 120
265 IF Q$ < > "N" THEN 260
270 PRINT "THE LAMBDAS HAVE BEEN STORED ON THE DISK ... IT'S BEEN REAL F
    UN ... GOODBYE";: GET Q$: TEXT : HOME
275 END
```

```
*6000LLLL
6000-    A2 01           LDX    #$01
6002-    AD 00 C0        LDA    $C000
6005-    30 4F           BMI    $6056
6007-    AD 5B C0        LDA    $C05B
600A-    AD 5A C0        LDA    $C05A
600D-    B5 18           LDA    $18,X
600F-    20 A8 FC        JSR    $FCA8
6012-    C6 1E           DEC    $1E
6014-    D0 0A           BNE    $6020
6016-    AD 5D C0        LDA    $C05D
6019-    AD 5C C0        LDA    $C05C
601C-    A5 1F           LDA    $1F
601E-    85 1E           STA    $1E
6020-    F8              SED
6021-    18              CLC
6022-    A5 09           LDA    $09
6024-    69 94           ADC    #$94
6026-    85 09           STA    $09
6028-    A5 08           LDA    $08
602A-    69 06           ADC    #$06
602C-    85 08           STA    $08
602E-    A5 07           LDA    $07
6030-    69 00           ADC    #$00
6032-    85 07           STA    $07
6034-    A5 06           LDA    $06
6036-    69 00           ADC    #$00
6038-    85 06           STA    $06
603A-    D8              CLD
603B-    B0 37           BCS    $6074
603D-    A0 03           LDY    #$03
603F-    A5 07           LDA    $07
6041-    20 6B 60        JSR    $606B
```

```
6044-   A5 07       LDA   $07
6046-   20 67 60    JSR   $6067
6049-   A5 06       LDA   $06
604B-   20 68 60    JSR   $6068
604E-   A5 06       LDA   $06
6050-   20 67 60    JSR   $6067
6053-   4C 02 60    JMP   $6002
6056-   C9 B1       CMP   #$B1
6058-   30 24       BMI   $607E
605A-   C9 B5       CMP   #$B5
605C-   10 20       BPL   $607E
605E-   29 0F       AND   #$0F
6060-   AA          TAX
6061-   AD 10 C0    LDA   $C010
6064-   4C 07 60    JMP   $6007
6067-   4A          LSR
6068-   4A          LSR
6069-   4A          LSR
606A-   4A          LSR
606B-   29 0F       AND   #$0F
606D-   09 B0       ORA   #$B0
606F-   99 5A 07    STA   $075A,Y
6072-   88          DEY
6073-   60          RTS
6074-   A9 B0       LDA   #$B0
6076-   A0 04       LDY   #$04
6078-   88          DEY
6079-   99 5A 07    STA   $075A,Y
607C-   D0 FA       BNE   $6078
607E-   AD 10 C0    LDA   $C010
6081-   60          RTS
6082-   00          BRK
6083-   00          BRK
```

APPENDIX B

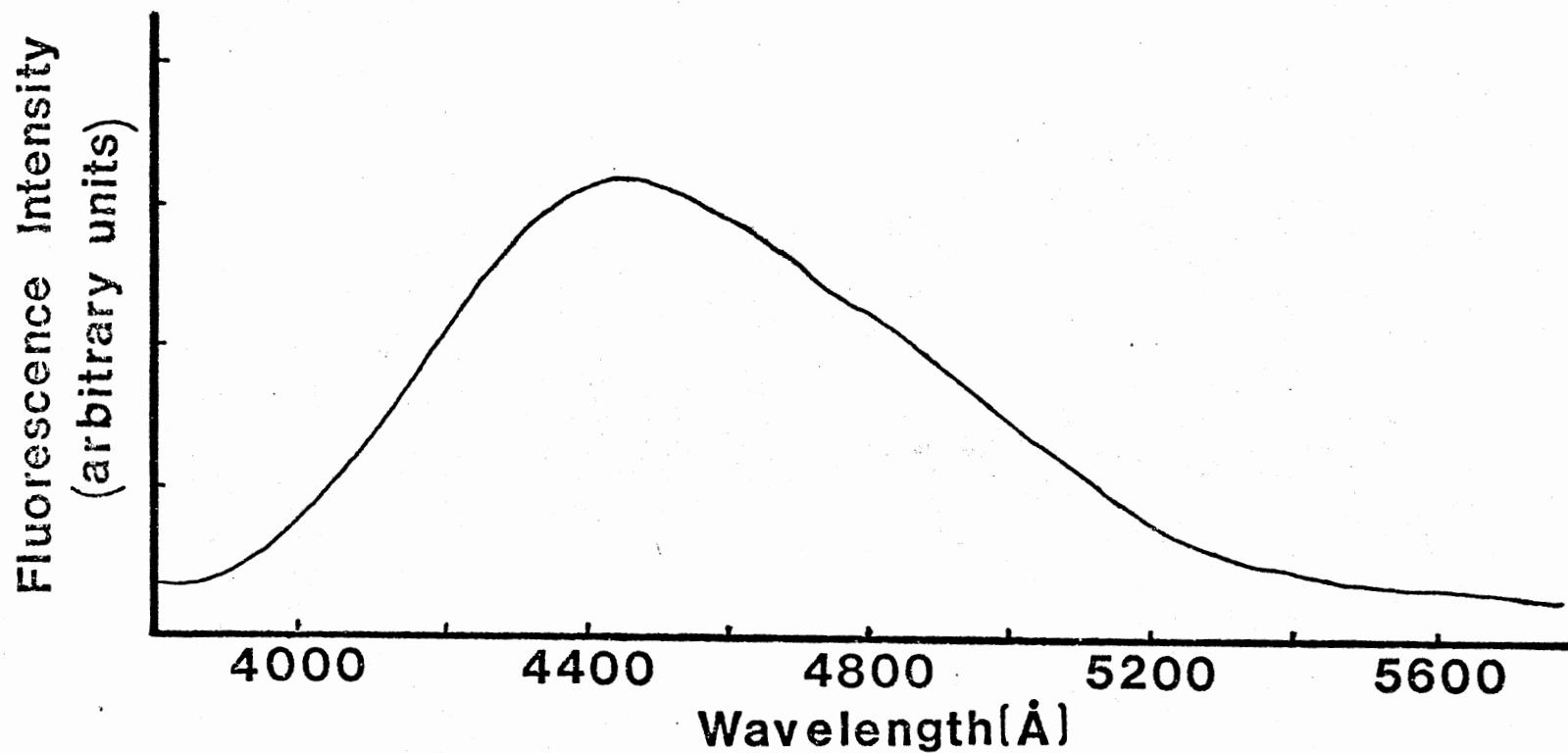EMISSION AND EXCITATION SPECTRA

OF INCORPORATED PROBES

Figure 53. Fluorescence Emission Spectrum of 16-(9-anthroyloxy)
Palmitic Acid Incorporated into Dipalmitoyl Phosphatidyl-
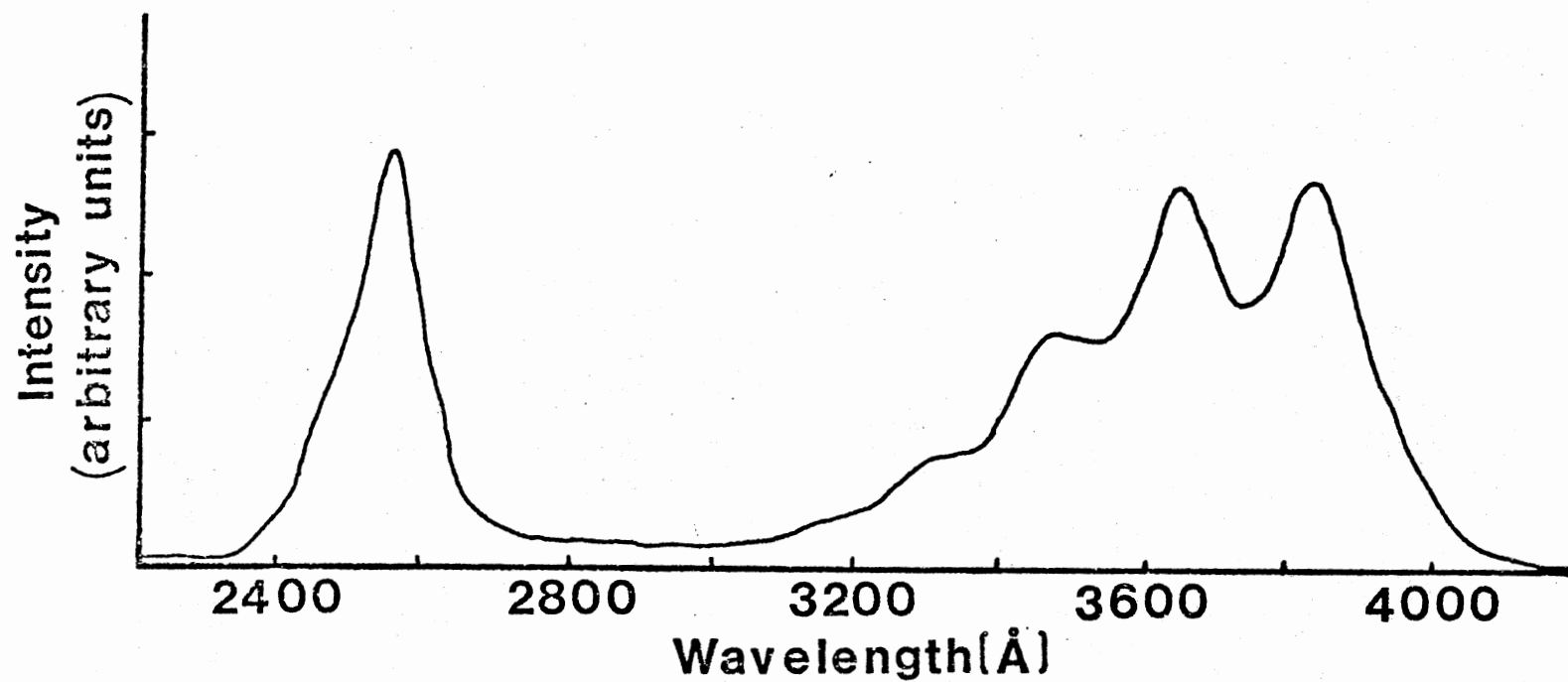choline Vesicles. Excitation Wavelength = 3660 Å.

Figure 54. Excitation Spectrum of 16-(9-anthroyloxy)Palmitic
Acid Incorporated into Dipalmitoyl Phosphatidylcholine
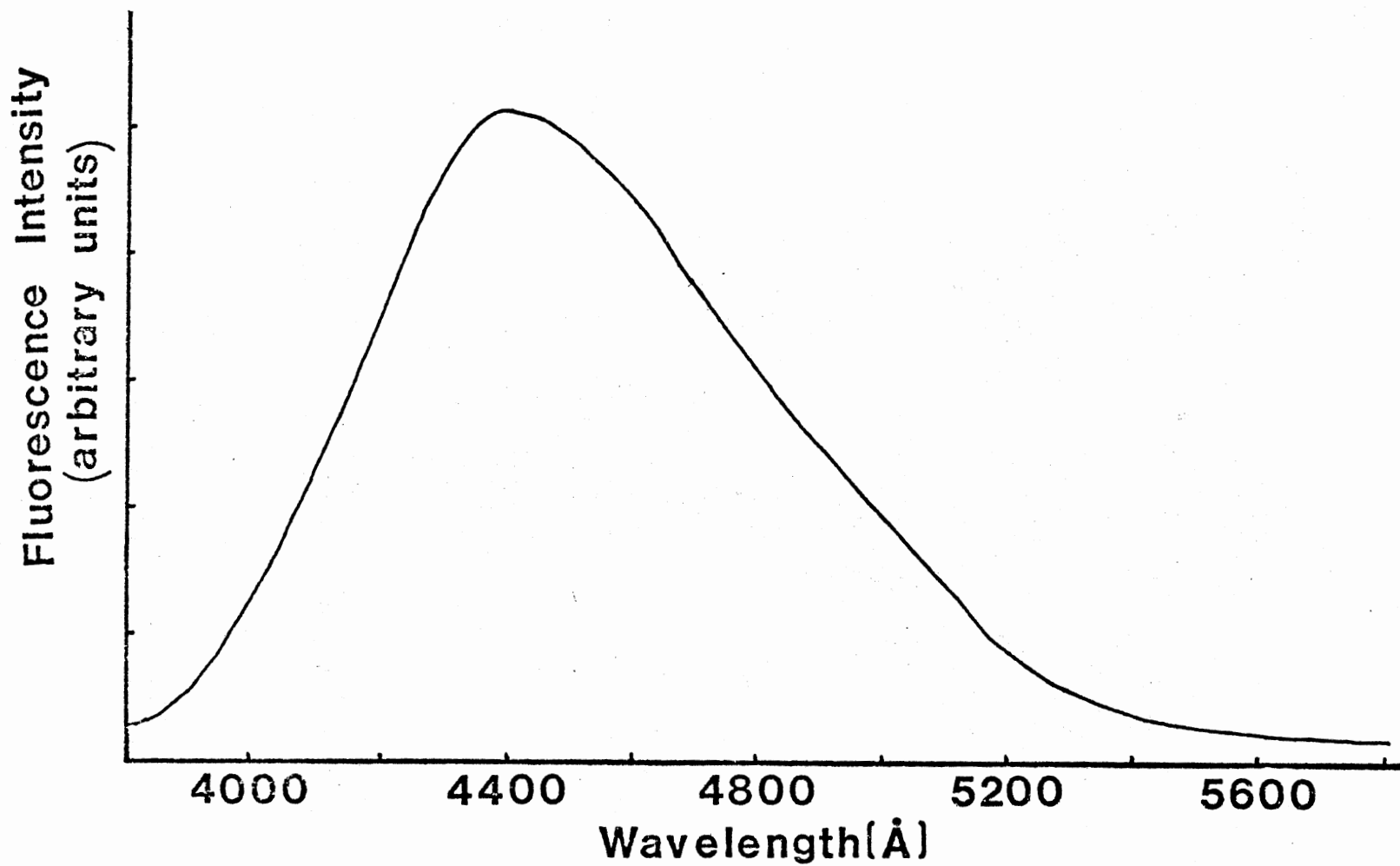Vesicles. Emission Wavelength = 4500 Å.

Figure 55. Fluorescence Emission Spectrum of 16-(9-anthroyloxy) Palmitic Acid In Tetrahydrofuran. Excitation Wavelength = 3660 Å.
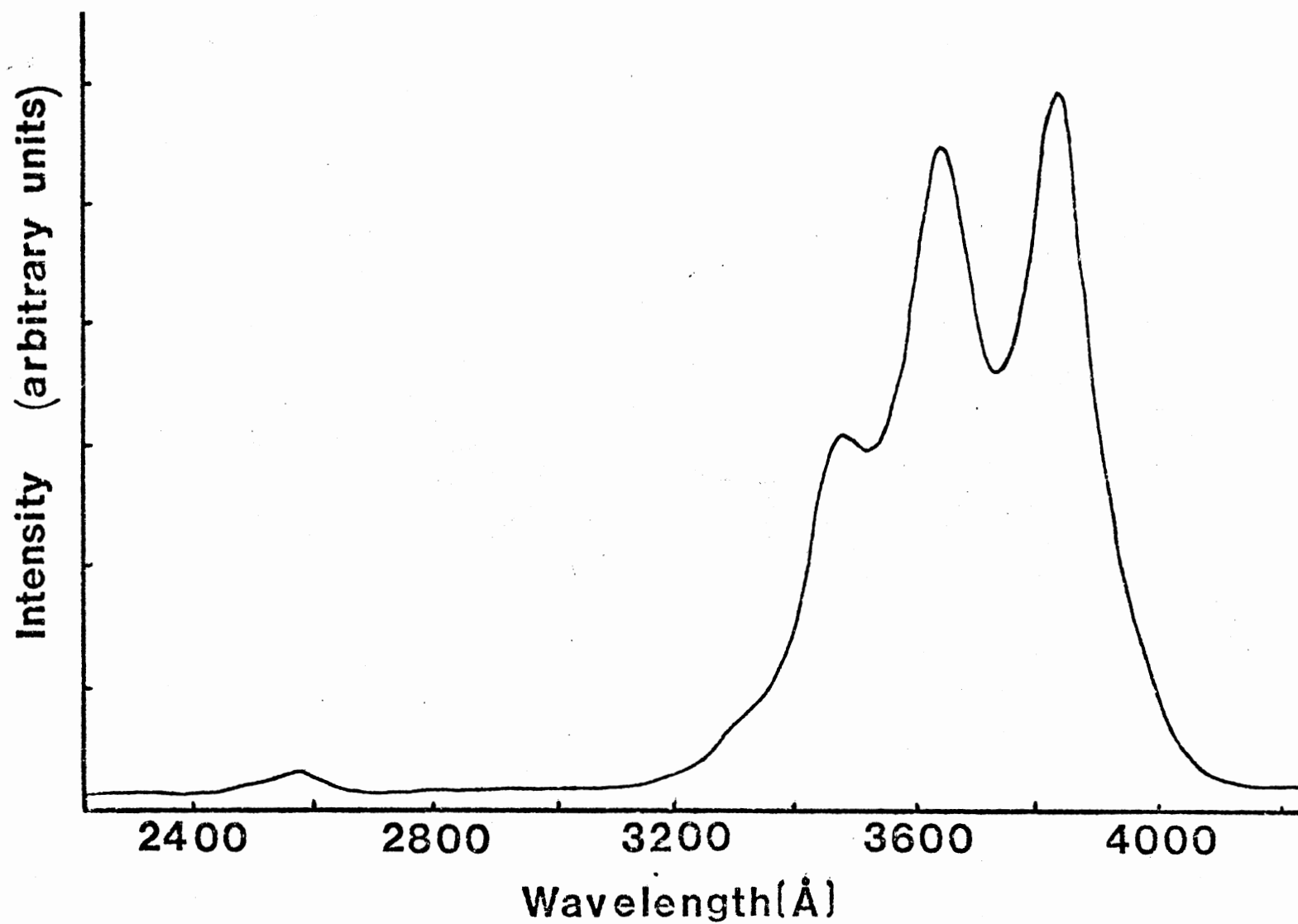
Figure 56.   Excitation Spectrum of 16-(9-anthroyloxy)Palmitic Acid
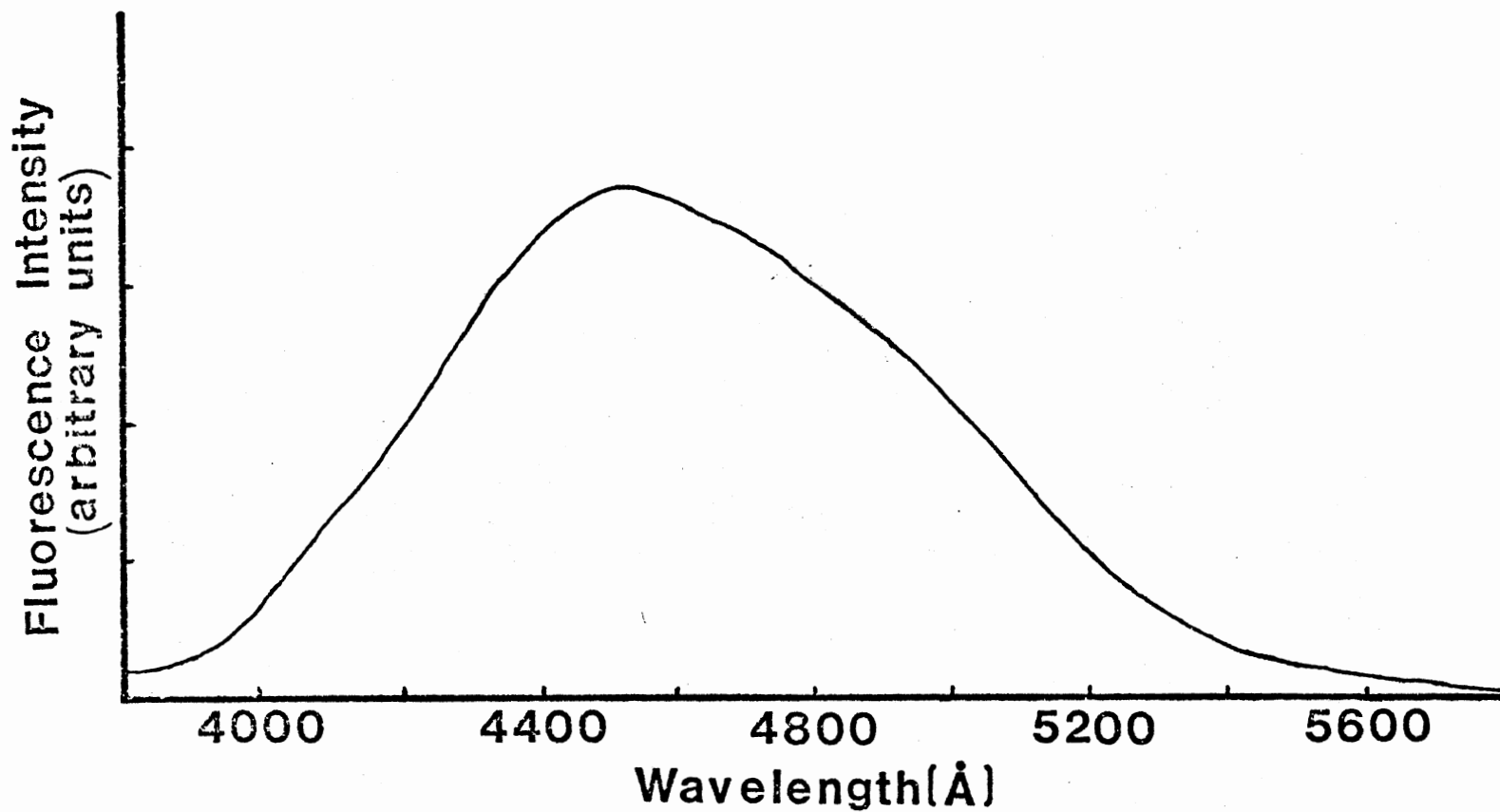in Tetrahydrofuran.   Emission Wavelength = 4500 Å.

Figure 57. Fluorescence Emission Spectrum of 16-(9-anthroyloxy) Palmitic Acid In Ethanol. Excitation Wavelength = 3660 Å.
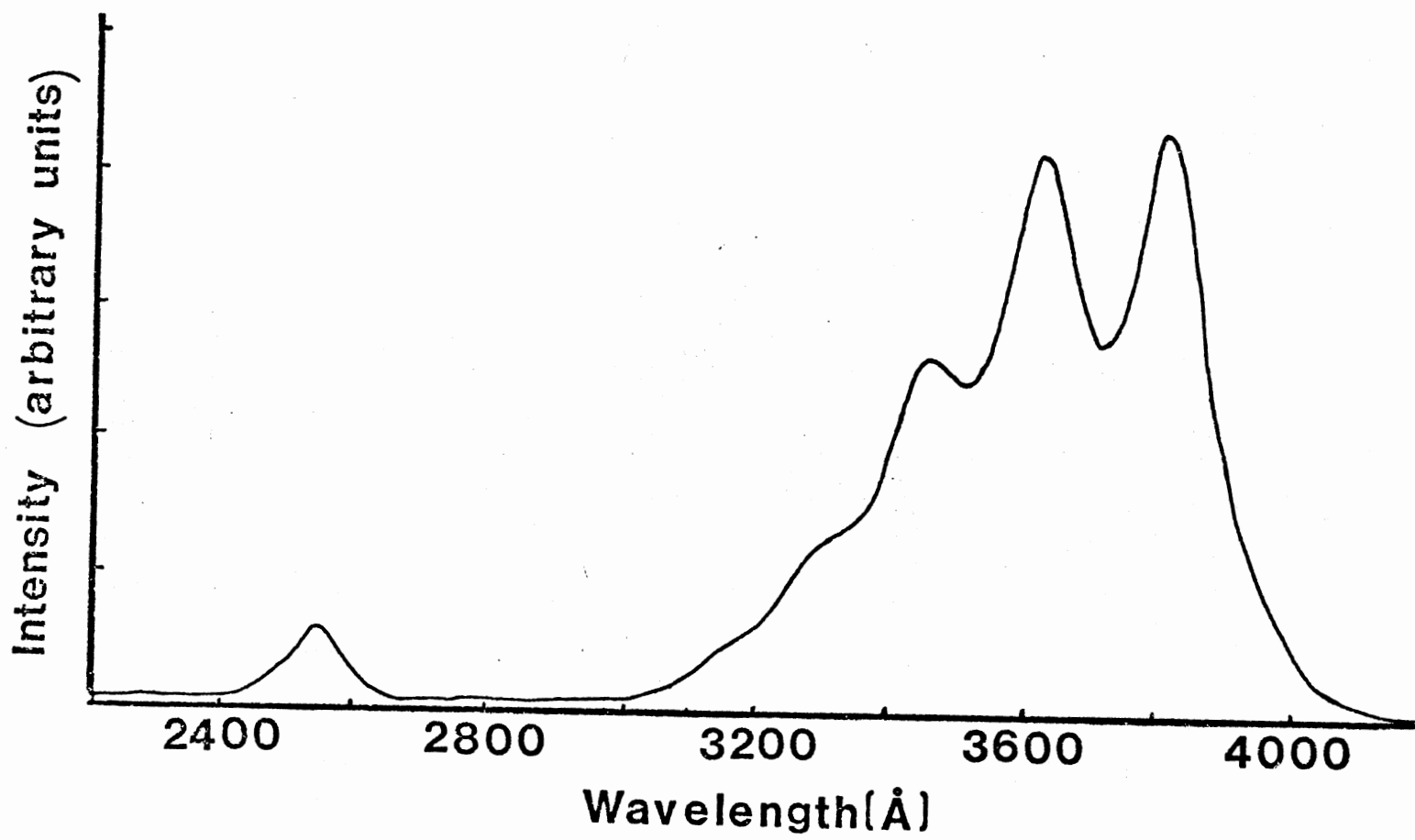
Figure 58.   Excitation Spectrum of 16-(9-anthroyloxy)Palmitic
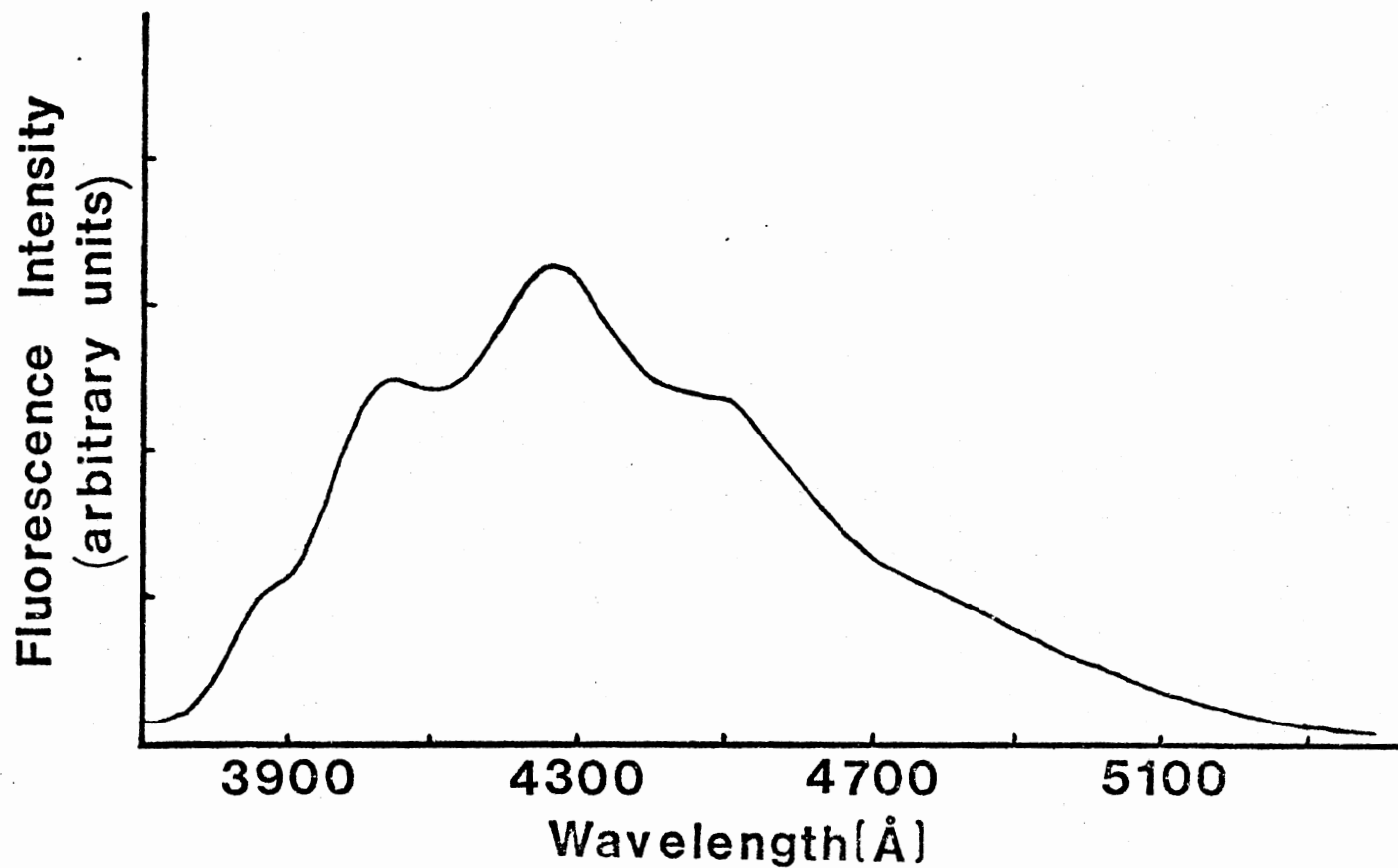in Ethanol.   Emission Wavelength = 4500 Å.

Figure 59.   Fluorescence Emission Spectrum of 1,6-diphenylhexatriene
Incorporated into Dipalmitoyl Phosphatidylcholine
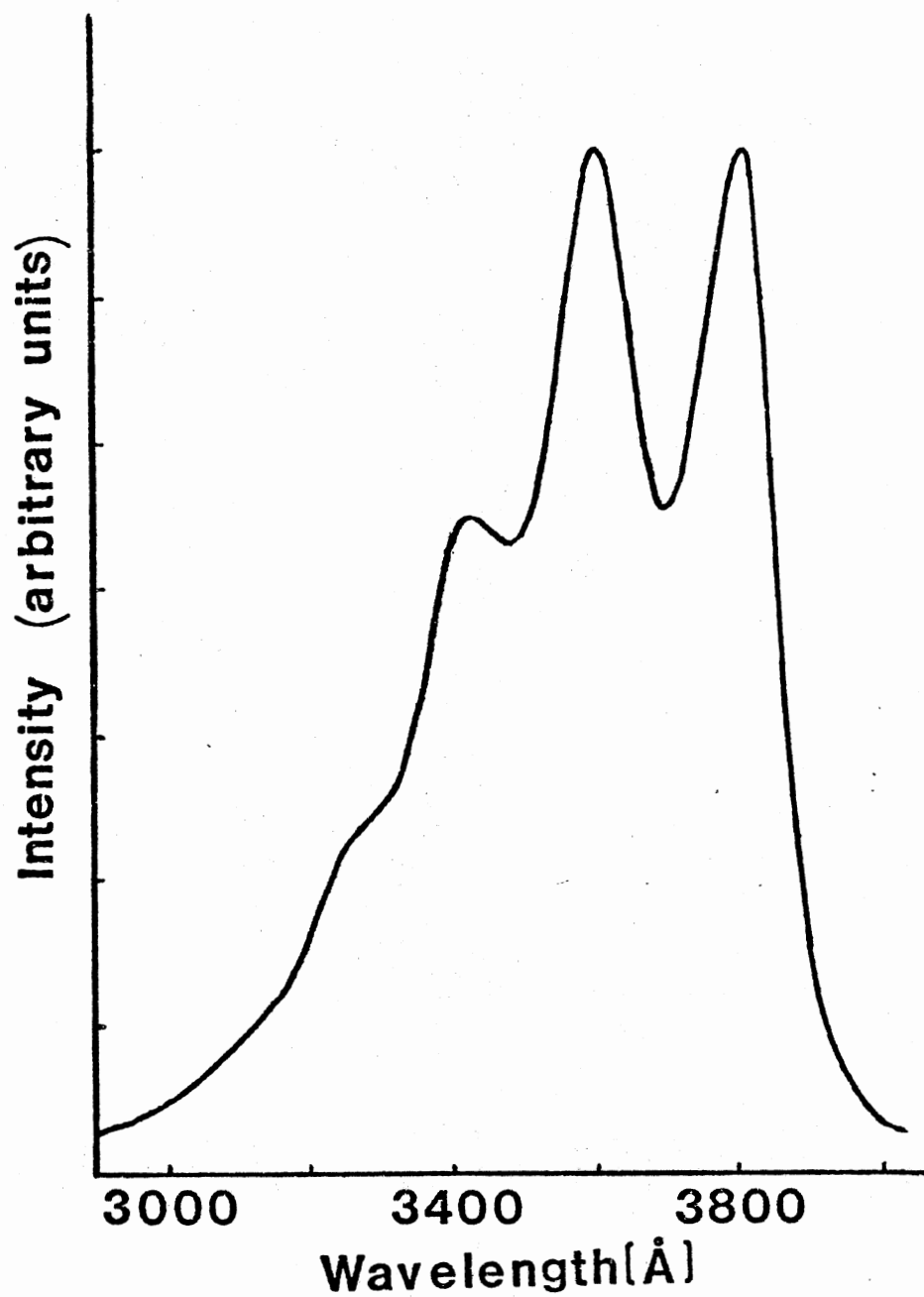Vesicles.   Excitation Wavelength = 3300 Å.

Figure 60.   Excitation Spectrum of 1,6-diphenyl-
             hexatriene Incorporated into
             Dipalmitoyl Phosphatidylcholine
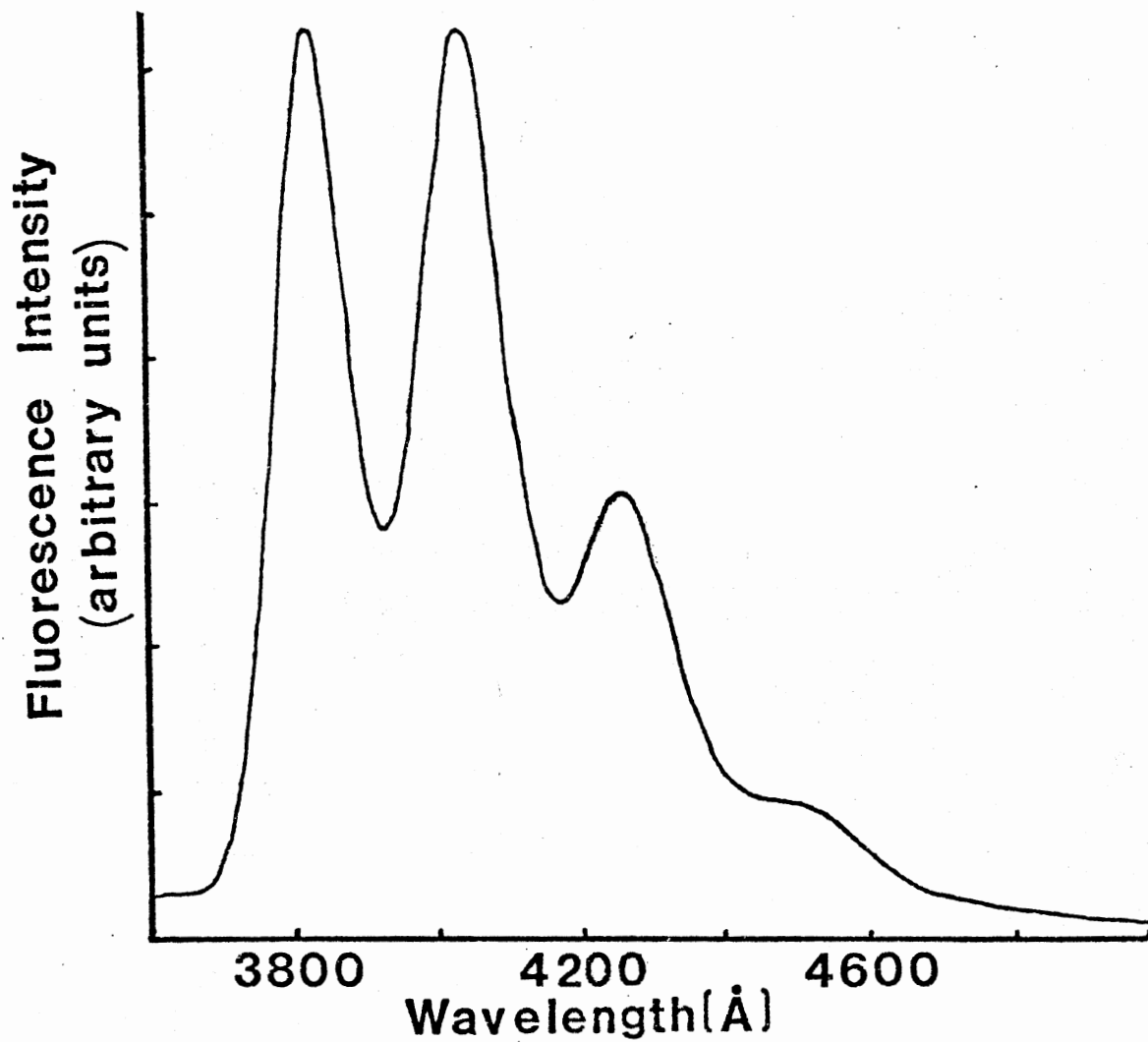   Vesicles.   Emission Wavelength = 4500 Å.

Figure 61. Fluorescence Emission Spectrum of Anthracene
Incorporated into Dipalmitoyl Phosphatidyl-
choline Vesicles. Excitation Wavelength =
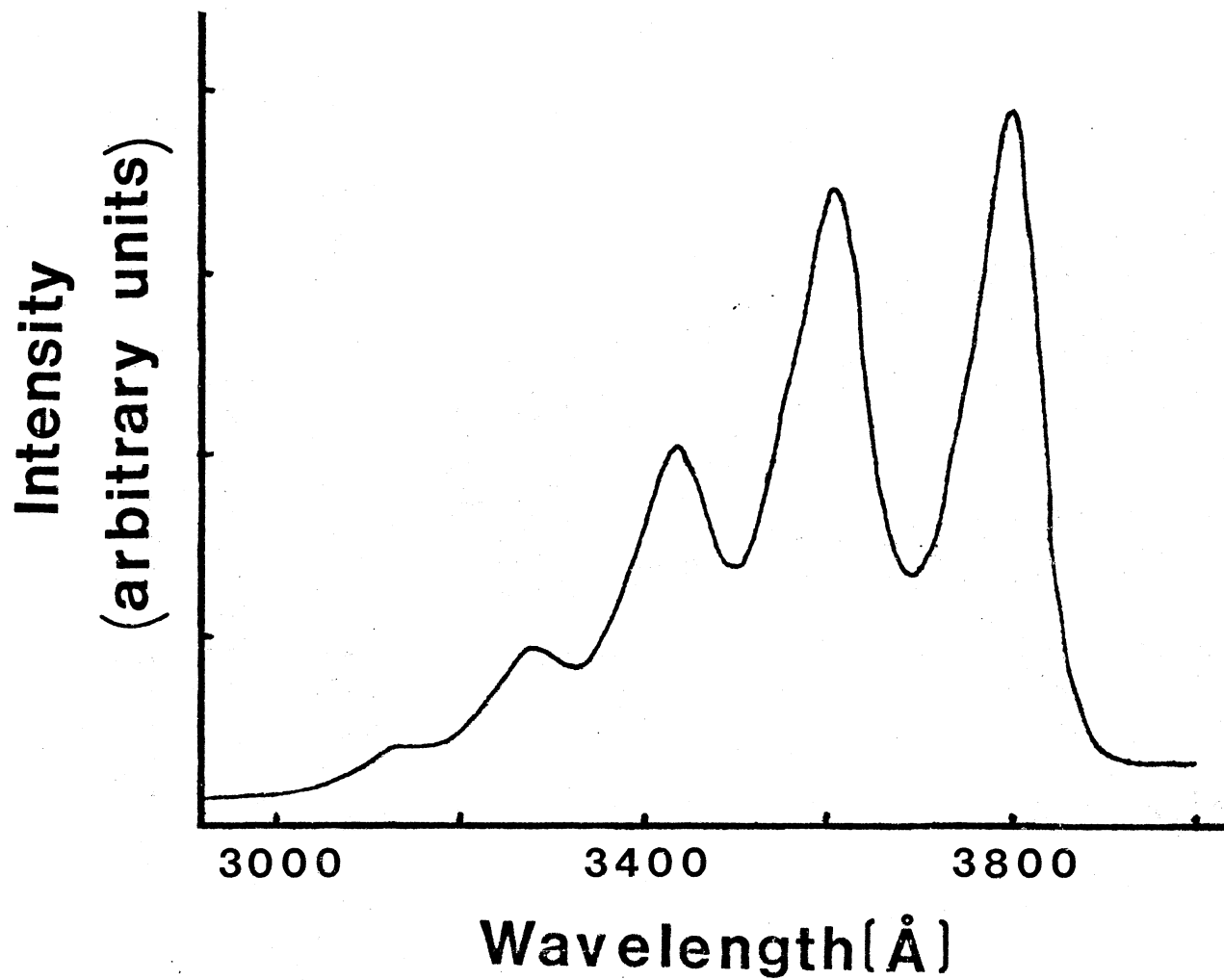3400 Å.

Figure 62. Excitation Spectrum of Anthracene Incorporated into
Dipalmitoyl Phosphatidylcholine Vesicles.
Emission Wavelength = 4010 Å.
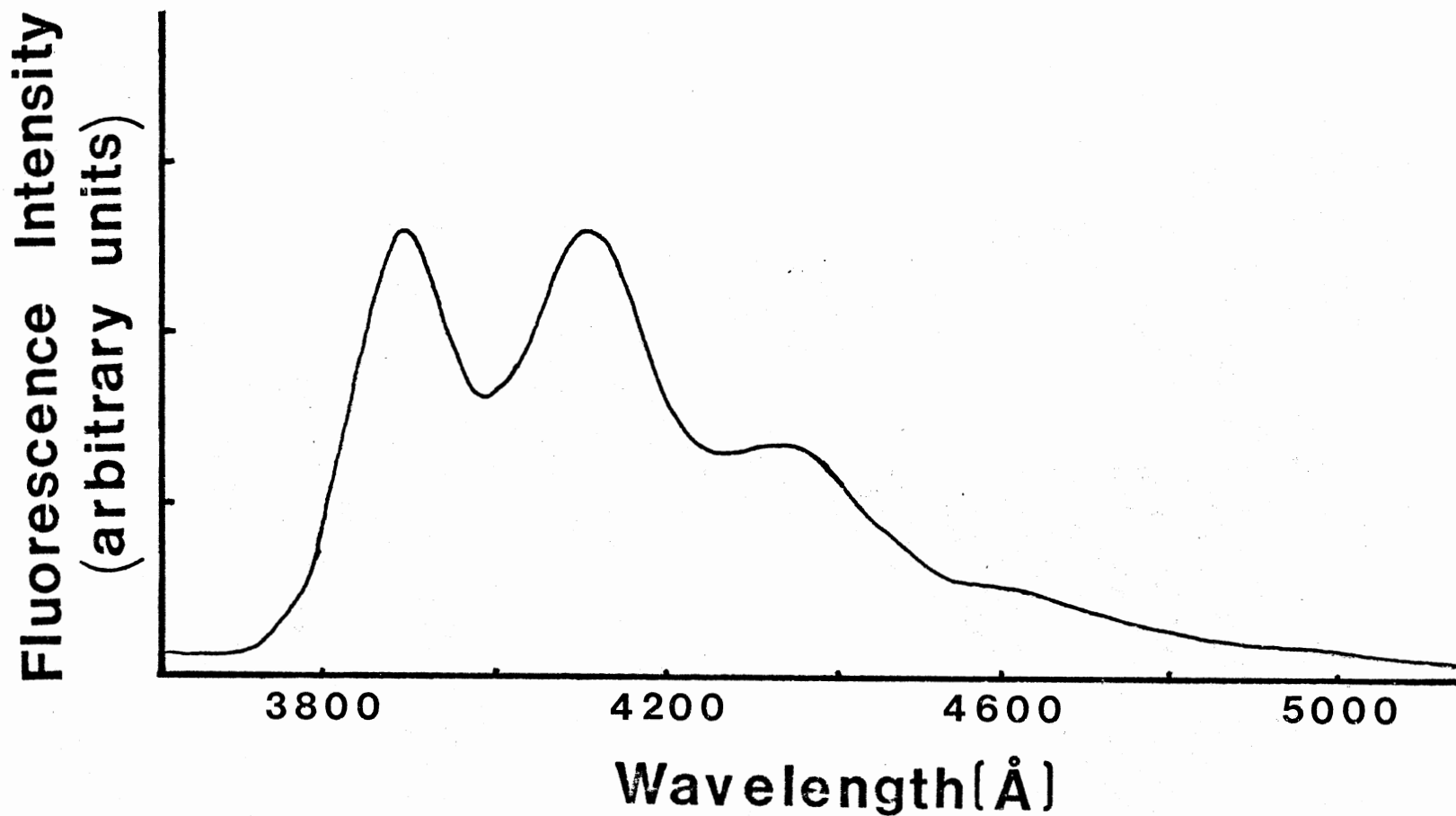
Figure 63.   Fluorescence Emission Spectrum of Methyl 5-(2-Anthryl)
             Pentanoate Incorporated into Dipalmitoyl Phosphatidyl-
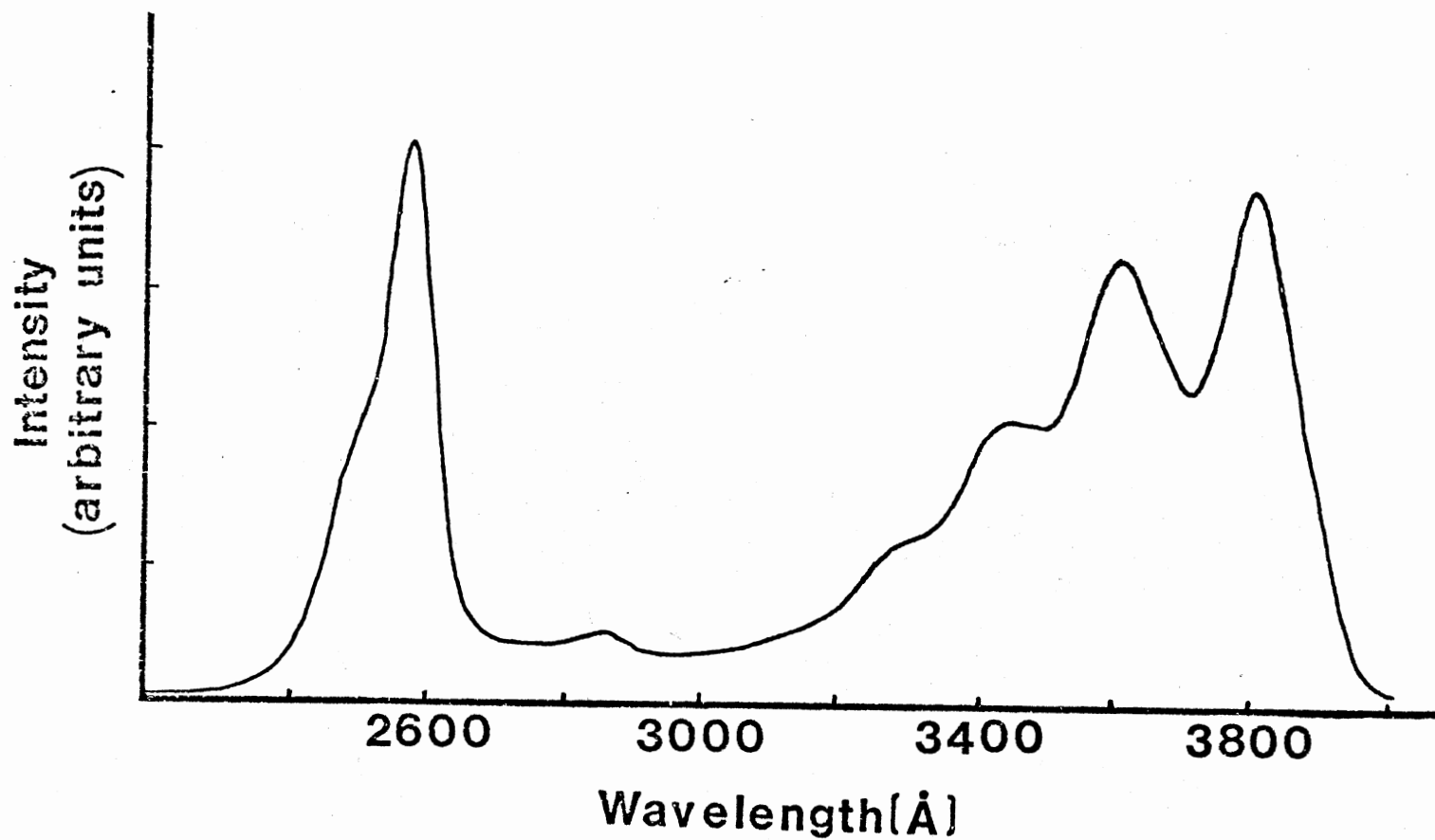   choline Vesicles.   Excitation Wavelength = 3400   Å.

Figure 64. Excitation Spectrum of Methyl 5-(2-Anthryl)Pentanoate
Incorporated into Dipalmitoyl Phosphatidylcholine
Vesicles. Emission Wavelength = 4050 Å.

APPENDIX C

PUBLICATIONS

Syntheses of Selected ε-(2- or 9-Anthryl)alkanoic Acids and Certain Esters—Carbon-13 Spin-Lattice Relaxation Time Measurements of Methyl 5-(2-Anthryl)pentanoate and Methyl 7-(2-Anthryl)heptanoate

Palanisamy Arjunan, Nagaraj Shymasundar, K. Darrell Berlin,* Dada Najjar, and Mark G. Rockley*

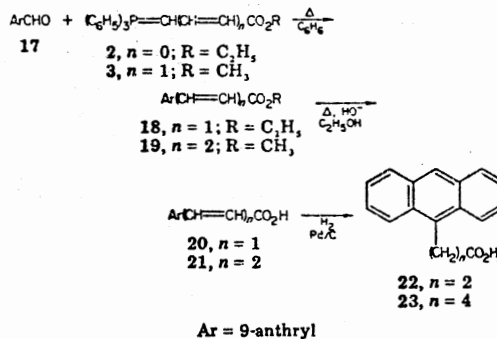*Department of Chemistry, Oklahoma State University, Stillwater, Oklahoma 74078*

Fluorescent probes have been widely applied in the study of microenvironments of large biological structures such as proteins and membranes.[1] Such probes with hydrophilic and hydrophobic properties have made it

Scheme I

Ar = 2-anthryl

Scheme II

Ar = 9-anthryl
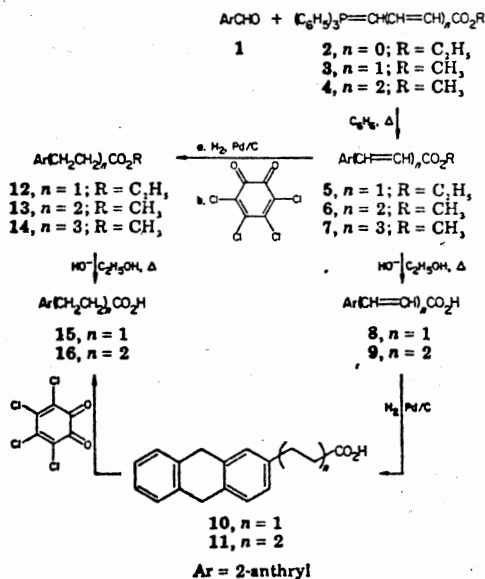
possible to study certain regions of membranes. Waggoner and Stryer[2] synthesized some fluorescent probes to study the hydrophilic regions of membranes. Since the above probes provided only a hydrolyzable fluorescent marker, Stoffel and Michaelis[3] developed a class of anthracene-labeled fatty acids and phospholipids. However, the bulky anthracene residue of the above probes was not transported through the membrane or used by fatty acid kinase or acyltransferase for the biosynthesis of membrane phospholipids of the *E. coli* mutant.[3] In connection with other studies concerned with biological mimics, we had occasion to prepare several ε-(2- and 9-anthryl)alkanoic acids and esters which have a general structural formula shown below.

$$Ar(CH_2)_nCO_2R$$

Ar = 2-anthryl, 9-anthryl

n = 2, 4, 6

R = H, CH_3, C_2H_5
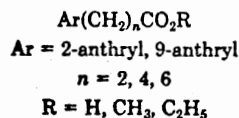
(1) (a) W. W. Mantulin and H. J. Pownall, *Photochem. Photobiol.* **26**, 69 (1977); (b) A. Waggoner, *Enzymes Biol. Membr.* 1, 119 (1976); (c) L. Stryer, *Science*, 162, 526 (1968).

(2) A. S. Waggoner and L. Stryer, *Proc. Natl. Acad. Sci. U.S.A.*, **67**, 579 (1970).

(3) W. Stoffel and G. Michaelis, *Z. Physiol. Chem.*, 357, 7, 21 (1976).

Only a very few examples of such compounds could be found in the literature. We report herein the syntheses for seven compounds of the general type above as well as spin-lattice relaxation times (T_1 values) for ^{13}C for two of the esters. The relaxation times are well-known to be good indicators of the motional characteristics of the atoms in long-chain mimics.[26] Schemes I and II outline our approach.
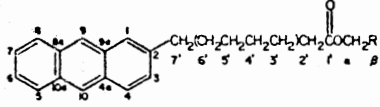
Results and Discussion

2-Anthraldehyde (1) was prepared in several steps from readily available 2-methylanthraquinone (Aldrich)[4-11] in a modest overall yield (37.4%). Phosphoranes 2, 3, and 4 were made from the corresponding phosphonium salts by the literature procedures.[12-16] A Wittig reaction[16-18] of 1 with phosphoranes 2, 3, and 4 gave the expected unsaturated esters 5, 6, and 7. Saponification of esters 5 and 6 yielded the unsaturated acids 8 and 9 in good yield. Hydrogenation (atmospheric pressure) of 8 and 9 over 10% Pd/C gave 9,10-dihydro derviatives 10 and 11, respectively. Formation of 9,10-dihydro derivatives during hydrogenation, although not expected, is not unreasonable as the 9 and 10 positions in the anthracene ring are very reactive.[19] The above 9,10-dihydro derivatives were aromatized with o-chloranil in benzene. Saturated esters 12, 13, and 14 were obtained via hydrogenation and aromatization without isolating the dihydro derivatives of the corresponding unsaturated esters 5, 6, and 7. Saponification of the esters 12 and 13 with 10% alcoholic KOH solution yielded the saturated acids 15 and 16.

Wittig reaction[18] of 9-anthraldehyde (17) with phosphoranes 2[15] and 3[13] gave the unsaturated esters 18[20] and 19,[18] respectively. Saponification of esters 18 and 19 using 10% alcoholic KOH yielded the corresponding unsaturated acids 20[21] and 21 which were then hydrogenated over 10% Pd/C to obtain the saturated acids 22 and 23, respectively.

Structures of compounds 5–16 and 18–23 were confirmed by spectral data and elemental analyses. IR, UV, and ^{1}H NMR spectral data, melting points, and elemental analysis for compounds 5–16 and 18–23 are provided in the experimental section. ^{13}C NMR chemical shifts for esters 12–14 and T_1 values for carbons in esters 13 and 14 are listed in Table I. Assignments of ^{13}C chemical shifts were made by using model compounds[22-24] and a good agreement among the data for 12, 13, and 14 was observed with respect to the chemical shifts of identical carbon

(4) M. A. Iljinsky, L. G. Gindin, and V. A. Kasakova, *C. R. Acad. Sci. SSSR*, **20**, 555 (1938).

(5) E. Bornstein, *Chem. Ber.*, **16**, 2609 (1883).

(6) E. L. Stogryn, *J. Med. Chem.*, **17**, 563 (1974).

(7) H. Limpricht, *Justus Liebigs Ann. Chem.*, **309**, 115 (1899).

(8) F. A. Carlack and E. Mosettig, *J. Am. Chem. Soc.*, **67**, 2255 (1945).

(9) F. H. C. Stewart, *Aust. J. Chem.*, **13**, 478 (1960).

(10) R. Ratcliffe and R. Rodehorst, *J. Org. Chem.*, **35**, 4000 (1970).

(11) P. H. Gore, *J. Chem. Soc.*, 1616 (1959).

(12) A. I. Vogel, "A Text-Book of Practical Organic Chemistry", Longman, London, 1973.

(13) E. Buchta and F. Andree, *Chem. Ber.*, **92**, 3111 (1959).

(14) S. I. Heilbron, E. R. H. Jones and D. G. O'Sullivan, *J. Chem. Soc.*, 866 (1946).

(15) G. Aksnes, *Acta Chem. Scand.*, **15**, 438 (1961).

(16) Y. Badar, W. J. S. Lockley, T. P. Toube, B. C. L. Weedon, and L. R. G. Valadon, *J. Chem. Soc., Perkin Trans. 1*, 1416 (1973).

(17) A. J. Gradwell and J. T. Guthrie, *Polymer*, **17**, 643 (1976).

(18) G. Kresze, J. Firl, and H. Braun, *Tetrahedron*, **25**, 4481 (1969).

(19) E. Clar in "Polycyclic Hydrocarbons", Academic Press, New York, 1964, Vol. 1, Chapter 22, p 288.

(20) J. W. Cook, R. S. Ludwiczak, and R. Schoental, *J. Chem. Soc.*, **112**, (1950).

(21) C. H. Davis and M. Carmack, *J. Org. Chem.*, **12**, 76 (1947).

(22) P. E. Hansen, *Org. Magn. Reson.*, **12**, 109 (1979).

(23) D. Doddrell and A. Allerhand, *J. Am. Chem. Soc.*, **93**, 15558 (1971); C. Chachaty, Z. Wolkowski, F. Piriou, and G. Lukacs, *J. Chem. Soc., Chem. Commun.*, 951 (1973).

(24) J. B. Stothers, "Carbon-13 NMR Spectroscopy", Academic Press, New York, 1972, Chapter 5.

carbon	12	13	14
C-1	125.9	125.5 (1.5)	125.5 (1.6)
C-2	137.2	138.7 (15.2)	139.2 (14.6)
C-3	128.0	127.8 (1.5)	127.8 (1.5)
C-4	126.7	125.7 (15)	125.6 (1.4)
C-5	127.9	127.2 (1.3)	127.1 (1.1)
C-6^c	124.9	124.7 (0.9)	124.9 (1.0)
C-7^c	125.1	124.9 (0.9)	124.6 (1.0)
C-8	128.2	127.9 (1.5)	127.9 (1.5)
C-9	125.4	125.0 (1.1)	125.1 (1.2)
C-10	125.8	125.3 (1.1)	125.1 (1.2)
C-4a	130.4	130.3 (25.1)	130.3 (25.1)
C-8a	131.6	131.6 (22.7)	131.6 (23.0)
C-9a	131.7	131.7 (22.6)	131.7 (22.4)
C-10a	131.3	131.1 (23.3)	131.0 (22.6)
C-1' (C=O)	172.6	173.6 (37.2)	173.8 (38.5)
C-2'	35.5	35.8 (1.1)	36.0 (1.0)
C-3'	31.3	24.6 (1.4)	24.8 (1.4)
C-4'		33.8 (1.7)	28.8 (1.1)
C-5'		30.2 (1.1)	28.8 (1.1)
C-6'			33.9 (1.9)
C-7'			30.6 (1.0)
C-α	60.3	51.3 (6.1)	51.2 (6.2)
C-β	14.2		

^{a} Chemical shifts in parts per million downfield from internal tetramethylsilane in DCCl$_3$. ^{b} ^{13}C spin-lattice relaxation time in seconds. ^{c} May be interchanged.

nuclei in the anthracene ring as well as the related carbon nuclei in the alkyl side chain. The T_1 values dropped to a minimum in the middle of the side chain which is also rather normal.[23] Differences in T_1 values of individual carbon nuclei in the side chain of 13 and 14 are perhaps due to a motional gradient (segmental motion[25]) of the alkyl chains. Decreased T_1 values of carbon nuclei that are attached *directly* to an anthracene ring are not surprising since the anthracene ring can probably hinder the independent motion of the ε-carbon in the side chain of 15 and 16. This type of steric interaction is not unusual and a recent study of T_1 measurements on carbon in some 9-(anthroyloxy)alkyl carboxylates[26] supports our observations. In view of the recent observations[28] that 9-anthryl derivatives can cause a large perturbation in the packing of lipid bilayers, no T_1 measurements were performed on 22 or 23.

Experimental Section

Melting points (uncorrected) were determined with a Thomas-Hoover capillary apparatus. IR spectral data were collected on a Beckman IR-5A unit. NMR spectral signals were recorded in parts per million (ppm) downfield from Me$_4$Si on a Varian XL-100(15) NMR spectrometer equipped with a Nicolet TT-100 PFT accessory operating at 100.1 MHz for ^{1}H NMR and at 25.2 MHz for ^{13}C NMR. All T_1 measurements were made on the above

(25) G. C. Levy, *Acc. Chem. Res.*, **6**, 161 (1973).

(26) S. R. Johns, R. I. Willing, K. R. Thulborn, and W. H. Sawyer, *Chem. Phys. Lipids*, **24**, 11 (1979).

(27) The T_1 measurements were made by using the FIRFT method in the literature; see D. Canet, G. C. Levy, and I. R. Peat, *J. Mag. Reson.*, **18**, 199 (1975); see also K. Ramarajan, Ph.D. Dissertation, Oklahoma State University, 1980.

(28) D. A. Cadenhead, B. M. J. Kellner, K. Jacobson, and D. Papahajopoulos, *Biochemistry*, **16**, 5386 (1977); A. E. McGrath, C. G. Morgan, and G. K. Radda, *Biochim. Biophys. Acta*, **426**, 173 (1976).

(29) G. Izoret, F. Moritz, and J. J. Brun, *Bull. Soc. Chim. Fr.*, 1769 (1962).

NMR spectrometer operating at 25.2 MHz for ^{13}C observation.[27] UV spectral data were recorded on a Cary Model 14 recording spetrophotometer. Elemental analyses were performed by Galbraith Laboratories, Knoxville, TN. 2-Anthraldehyde (1) was prepared from 2-methylanthraquinone (Aldrich).[4,11] Phosphoranes 2, 3, and 4 were made by published procedures.[12-16] 9-Anthraldehyde (17, Aldrich) was purchased and used as such. Organic extracts were dried with MgSO₄ and a rotoevaporator was used to remove organic solvents during the usual workup. Hydrogenations were performed in a Parr hydrogenation apparatus over a 4-h period in all cases. Workup of the hydrogenation mixture consisted of filtration followed by evaporation of the filtrate to give a semisolid. This crude solid was treated with o-chloranil to effect the aromatization of the anthracene ring.

Preparation of Esters 5, 6, 7, 18, and 19. General Method.[17,18] A mixture of the corresponding anthraldehyde and Wittig reagent in benzene was boiled under N₂ for 24 h and the mixture was allowed to cool. Removal of benzene left a semisolid which, upon trituration (petroleum ether or anhydrous C₂H₅OH) and recrystallization, gave the expected unsaturated ester.

Ethyl 3-(2-Anthryl)prop-2-enoate (5).[29] Aldehyde 1 (0.500 g, 2.4 mmol) reacted with phosphorane 2 (0.870 g, 2.4 mmol) to give 0.46 g (68.7%) of 5: mp 203–204 °C (lit.[19] mp 188–89 °C); IR (KBr) ν_{max} 1695, 1626 cm⁻¹; ¹H NMR (DCCl₃) δ 1.34 (3 H, t, CH₃), 4.30 (2 H, q, CH₂), 6.50 (1 H, d, vinylic H), 7.40–8.14 (8 H, m, Ar H and vinylic H), 8.38 (2 H, d, Ar H).

Methyl 5-(2-Anthryl)penta-2,4-dienoate (6). Aldehyde 1 (1.0 g, 5 mmol) was condensed with phosphorane 3 (2.4 g, 7 mmol) to produce 0.5 g (36%) of 6: mp 233–234 °C dec (C₆H₆); IR (KBr) ν_{max} 1700, 1625 cm⁻¹; ¹H NMR (DCCl₃) δ 3.78 (3 H, s, CH₃), 5.96–6.01 (1 H, d, H₂CO₂CCH=C), 6.80–8.38 (12 H, m, Ar H and HC=CH); UV (anhydrous C₂H₅OH) λ_max 412 nm (ε 5856), 385 (5856), 385 (17117), 367 (19820), 354 (16667), 326 (76677), 314 (64865), 246 (40991), 228 (27928).

Anal. Calcd for C₂₀H₁₆O₂: C, 83.31; H, 5.59. Found: C, 83.50; H, 5.70.

Methyl 7-(2-Anthryl)hepta-2,4,6-trienoate (7). [6-(Methoxycarbonyl)hexa-2,4-dien-1-yl]triphenylphosphonium bromide[16] (4.53 g, 10 mmol) was dissolved in water (300 mL), made alkaline with aqueous NaOH (10%) solution, and then extracted with benzene (5 × 100 mL). The dried benzene extract was concentrated (ca. 50 mL), and this was treated with aldehyde 1 (1.0 g, 5 mmol) to yield 0.3 g (19.7%) of 7: mp 234.5–236 °C dec (C₆H₆); IR (KBr) ν_{max} 1710, 1625 cm⁻¹; ¹H NMR (DCCl₃) δ 3.8 (3 H, s, CH₃), 5.99–6.14 (1 H, d, CH), 7.00–7.12 (1 H, d, CH), 7.44–8.40 [13 H, m, Ar H and (CH=HC)₂]; UV (anhydrous C₂H₅OH) λ_max 415 nm (ε 30496), 410 (35816), 390 (35106), 354 (63830), 340 (32624), 225 (14184), 220 (12766).

Anal. Calcd for C₂₂H₁₈O₂: C, 84.05; H, 5.77. Found: C, 84.04; H, 5.84.

Ethyl 3-(9-Anthryl)prop-2-enoate (18).[20] Reaction of aldehyde 17 (1.03 g, 5 mmol) with phosphorane 2 (1.74 g, 5 mmol) gave 1.10 g (80%) of 18: mp 79–80 °C (petroleum ether, lit.[20] mp 79–80 °C); IR (KBr) ν_{max} 1694, 1626 cm⁻¹; ¹H NMR (DCCl₃) δ 1.38 (3 H, t, CH₃), 4.3 (2 H, q, CH₂), 6.34 (1 H, d, C=CH), 7.3–8.7 (10 H, m, Ar H).

Methyl 5-(9-Anthryl)penta-2,4-dienoate (19).[18] Aldehyde 17 (1.03 g, 5 mmol) condensed with phosphorane 3 (1.79 g, 5 mmol) to produce 1.20 g (83%) of 19: mp 147–148 °C (lit.[18] mp 150 °C); IR (KBr) ν_{max} 1694, 1626 cm⁻¹; ¹H NMR (DCCl₃) δ 3.8 (3 H, s, CH₃), 6.02 (1 H, dd, C=CH), 6.70 (1 H, dd, C=CH), 7.34–8.20 (10 H, m, C=CH and Ar H), 8.34 (1 H, s, Ar H).

Anal. Calcd for C₂₀H₁₆O₂: C, 83.33; H, 5.55. Found: C, 83.47; H, 5.95.

3-(2-Anthryl)prop-2-enoic Acid (8).[28] Hydrolysis of ester 5 (0.550 g, 2 mmol) with 10% alcoholic KOH solution (50 mL) over a 2-h period afforded 0.420 g (85%) of acid 8: mp >310 °C (lit.[28] mp >310 °C); IR (KBr) ν_{max} 1681, 1613 cm⁻¹.

5-(2-Anthryl)penta-2,4-dienoic Acid (9). Hydrolysis of ester 6 (30 mL) over a 2-h period afforded 0.280 g (82%) of acid 9: mp 294–296 °C; IR (KBr) ν_{max} 1667, 1600 cm⁻¹. This highly insoluble material was used in the next step without further purification to give the new acid 11.

3-(9-Anthryl)prop-2-enoic Acid (20).[21] Hydrolysis of ester 18 (0.550 g, 2.5 mmol) with 10% alcoholic KOH solution (20 mL) over a 2-h period gave 0.450 g (90%) of acid 20: mp 244–245 °C

(C₂H₅OH, lit.[21] mp 247 °C); IR (KBr) ν_{max} 1695, 1600 cm⁻¹.

5-(9-Anthryl)penta-2,4-dienoic Acid (21). Hydrolysis of ester 19 (0.720 g, 2.5 mmol) with alcoholic KOH solution (50 mL) yielded after 3 h 0.600 g (88%) of acid 21: mp 271–272 °C (C₂H₅OH); IR (KBr) ν_{max} 1667, 1600 cm⁻¹; ¹H NMR (DCCl₃–TFA) δ 6.00 (1 H, d, C=CH), 6.72 (1 H, dd, C=CH), 7.20–7.40 (4 H, m, C=CH and Ar H), 7.64–7.70 (1 H, m, Ar H), 7.84–7.88 (1 H, m, Ar H), 7.9–8.14 (2 H, m, Ar H), 8.20–8.35 (2 H, m, Ar H), 8.4 (1 H, s, Ar H).

Anal. Calcd for C₁₉H₁₄O₂: C, 83.21; H, 5.10. Found: C, 82.82; H, 5.37.

3-(9,10-Dihydro-2-anthryl)propanoic Acid (10). Hydrogenation (atmospheric pressure) of acid 8 (0.248 g, 1 mmol) in anhydrous C₂H₅OH (20 mL) over 10% Pd/C (30 mg) afforded 0.210 g (84%) of acid 10: mp 141–142 °C (ether–petroleum ether); IR (KBr) ν_{max} 1695, 1587 cm⁻¹; ¹H NMR DCCl₃) δ 2.6–2.7 (2 H, m, CH₂), 2.73–3.20 (3 H, m, H₂CCO₂H), 3.8 (4 H, s, CH₂), 7.1–7.4 (7 H, m, Ar H).

Anal. Calcd for C₁₇H₁₆O₂: C, 80.95; H, 6.35. Found: C, 80.79; H, 6.52.

5-(9,10-Dihydro-2-anthryl)penta-2,4-dienoic Acid (11). Hydrogenation (atmospheric pressure) of acid 9 (0.274 g, 1 mmol) over 10% Pd/C (30 mg) in anhydrous C₂H₅OH (30 mL) afforded 0.230 g (83%) of acid 11: mp 120–121 °C (ether–petroleum ether; IR (KBr) ν_{max} 1695, 1587 cm⁻¹; ¹H NMR (DCCl₃) δ 1.60–1.90 (4 H, m, CH₂), 2.30–3.00 (4 H, m, CH₂), 2.30–3.00 (4 H, m, CH₂), 3.88 (4 H, s, CH₂), 6.9–7.5 (7 H, m, Ar H).

Anal. Calcd for C₁₉H₂₀O₂: C, 81.43; H, 7.14. Found: C, 81.49; H, 7.15.

Ethyl 3-(2-Anthryl)propanoate (12). Ester 5 (0.3 g, 1.1 mmol) was hydrogenated (atmospheric pressure) over 10% Pd/C (40 mg) in anhydrous C₂H₅OH and the product obtained was boiled with o-chloranil (Aldrich, 0.270 g, 1.1 mmol) in benzene (ca. 10 mL) for 3 h under N₂. Workup of the reaction mixture afforded 0.225 g (75%) of ester 12: mp 121–123 °C (C₂H₅OH); IR (KBr) ν_{max} 1725 cm⁻¹; ¹H NMR (DCCl₃) δ 1.1–1.3 (3 H, t, CH₃), 4.02–4.22 (2 H, q, O–CH₂), 3.06–3.22 (2 H, t, C(O)CH₂), 2.68–2.82 (2 H, t, CH₂CH₂), 7.22–8.30 (9 H, m, Ar H); ¹³C NMR (see Table I); UV (anhydrous C₂H₅OH) λ_max 376 nm (ε 5568), 367 (2561) 357 (6570), 347 (3675), 340 (4844), 329 (2895), 324 (3007), 316 (2394), 307 (3452), 255 (248148), 247 (103704).

Anal. Calcd for C₁₉H₁₈O: C, 81.99; H, 6.52. Found: C, 81.80; H, 6.77.

Methyl 5-(2-Anthryl)pentanoate (13). Ester 6 (0.4 g, 1.4 mmol) was hydrogenated (atmospheric pressure) over 10% Pd/C (60 mg) in anhydrous C₂H₅OH (75 mL), and the product obtained was then boiled with o-chloranil (Aldrich, 0.35 g, 1.4 mmol) in benzene (50 mL) for 3 h under N₂. Workup of the reaction mixture afforded 0.182 g (45%) of ester 13: mp 105–106 °C (C₂H₅OH); IR (KBr) ν_{max} 1725 cm⁻¹; ¹H NMR (DCCl₃) δ 1.68–1.78 (4 H, m, CH₂CH₂), 2.3–2.46 (2 H, m, Ar CH₂), 2.72–2.88 (2 H, m, H₂OCO₂CCH₂), 3.64 (3 H, s, CH₃), 7.32–8.34 (9 H, m, Ar H); ¹³C NMR (see Table I); UV (anhydrous C₂H₅OH) λ_max 377 nm (ε 5343), 368 (2306), 357 (6153), 348 (3431), 339 (4499), 325 (2778), 313 (1462), 255 (251852), 247 (107407).

Anal. Calcd for C₂₀H₂₀O₂: C, 82.16; H, 6.90. Found: C, 81.78, H, 7.10.

Methyl 7-(2-Anthryl)heptanoate (14). Ester 7 (0.440 g, 1.4 mmol) was hydrogenated (atmospheric pressure) over 10% Pd/C (60 mg) in anhydrous C₂H₅OH and the product obtained was boiled with o-chloranil (Aldrich, 0.350 g, 1.4 mmol) in benzene (15 mL) for 3 h under N₂. Workup of the reaction mixture afforded 0.240 g (54%) of ester 14: mp 93–95 °C (C₂H₅OH); IR (KBr) ν_{max} 1725 cm⁻¹ (C=O); ¹H NMR (DCCl₃) δ 3.64 (3 H, s, CH₃), 2.7–2.86 (2 H, t, CH₂), 2.12–2.37 (2 H, t, CH₂), 1.38–1.7 (8 H, m, (CH₂)₄, 7.32–8.34 (9 H, m, Ar H); ¹³C NMR (see Table I); UV (anhydrous C₂H₅OH) λ_max 377 nm (ε 5031), 368 (2201), 357 (5786), 348 (3459), 339 (4402), 325 (2956), 313 (2201), 255 (265000), 247 (128750).

Anal. Calcd for C₂₂H₂₄O₂: C, 82.46; H, 7.55. Found: C, 82.57; H, 7.62.

3-(2-Anthryl)propanoic Acid (15). Ester 5 (0.552 g, 2 mmol) in anhydrous C₂H₅OH (50 mL) was hydrogenated over 10% Pd/C (60 mg), and the product obtained was boiled with o-chloranil (0.545 g, 1.2 mmol) in C₆H₆ for 3 h under N₂. Hydrolysis of the crude product from the above reaction with 10% alcoholic KOH

(50 mL) afforded 0.400 g (80%) of 15: mp 249–250 °C (C₂H₅OH); IR (KBr) ν_{max} 1709, 1600 cm⁻¹; ¹H NMR (Me₂SO-d₆) δ 2.68 (2 H, t, CH₂), 3.04 (2 H, t, H₂CCO₂H), 7.34–7.56 (3 H, m, Ar H), 7.86 (1 H, s, Ar H), 7.96–8.12 (3 H, m, Ar H), 8.50 (2 H, d, Ar H); UV (anhydrous C₂H₅OH) λ_{max} 376 nm (ε 3800), 357 (4400), 340 (3200), 325 (1900), 255 (200 000), 247 (90 000).

Anal. Calcd for C₁₇H₁₄O₂: C, 81.60; H, 5.60. Found: C, 81.33; H, 5.84.

5-(2-Anthryl)pentanoic Acid (16). Ester 6 (0.548 g, 2 mmol) was hydrogenated over 10% Pd/C in anhydrous C₂H₅OH (50 mL), and the product obtained was boiled with o-chloranil (0.590 g, 1.2 mmol) for 3 h under N₂. Hydrolysis of the product from the above reaction with 10 alcoholic KOH solution (20 mL) afforded 0.410 g (71%) of acid 16: mp 191–192 °C (C₂H₅OH); IR (KBr) ν_{max} 1695, 1575 cm⁻¹; ¹H NMR (DCCl₃) δ 1.6 (4 H, m, CH₂) 2.2–2.3 (2 H, m, CH₂), 2.82 (2 H, m, CH₂), 7.3–7.5 (3 H, m, Ar H), 7.72 (1 H, m, Ar H), 7.88 (3 H, m, Ar H), 8.00–8.32 (2 H, m, Ar H); UV (anhydrous C₂H₅OH) λ_{max} 377 nm (ε 5400), 358 (6100), 341 (4400), 327 (2500), 291 (700), 254 (237 000), 249 (88 900).

Anal. Calcd for C₁₉H₁₈O₂: C, 82.01; H, 6.44. Found: C, 82.13; H, 6.56.

3-(9-Anthryl)propanoic Acid (22).[20] Hydrogenation of acid 20 (0.496 g, 2 mmol) over 10% Pd/C (50 mg) in anhydrous C₂H₅OH (20 mL) afforded 0.450 g (90%) of acid 22: mp 188–190 °C (C₂H₅OH–H₂O, lit.[20] mp 191–192 °C); IR (KBr) 1695, 1600 cm⁻¹; ¹H NMR (DCCl₃) δ 2.78–2.96 (2 H, br t, CH₂), 3.8–4.0 (2 H, br t, CH₂), 7.40–7.55 (5 H, m, Ar H); 7.9–8.1 (2 H, m, Ar H),

8.2–8.4 (2 H, m, Ar H); UV (anhydrous C₂H₅OH) λ_{max} 336 nm (ε 5000), 361 (5180), 347 (380), 332 (1450), 256 (95 700).

5-(9-Anthryl)pentanoic Acid (23). Hydrogenation of acid 21 (0.556 g, 2 mmol) in anhydrous C₂H₅OH (30 mL) over 10% Pd/C (70 mg) afforded 0.440 g (79%) of acid 23: mp 112–113 °C (ether–petroleum ether); IR (KBr) ν_{max} 1695, 1613 cm⁻¹; ¹H NMR (DCCl₃) δ 1.70–1.98 (4 H, d, CH₂), 2.42 (2 H, m, CH₂), 3.58 (2 H, m, CH₂), 7.16 (1 H, s, Ar H), 7.26–7.60 (4 H, m, Ar H), 7.94–8.20 (2 H, m, Ar H), 8.10–8.32 (1 H, m, Ar H), 11.14 (1 H, s, CO₂H); UV (anhydrous C₂H₅OH) λ_{max} 387 nm (ε 8830), 382 (4640), 367 (8990), 348 (5420), 331 (2490), 318 (1020), 257 (169 000), 250 (80 900), 236 (21 600), 223 (6700).

Anal. Calcd for C₁₉H₁₈O₂: C, 82.01; H, 6.44. Found: C, 81.87; H, 6.65.

THE ACTIVATION ENERGY OF INCORPORATION OF EXTRINSIC PROBES IN MODEL VESICLES

MARK G. ROCKLEY and DADA S. NAJJAR

Department of Chemistry, Oklahoma State University, Stillwater, OK 74078 (U.S.A.)

Time dependence of fluorescence enhancement of probes after addition to lipid vesicles has been used to investigate the position of chromophores in the lipid bilayer. Incorporation studies of a series of n-(9-anthroyloxy) fatty acids ($n = 2, 2, 12$ and 16) and 1,6-diphenylhexatriene in dipalmitoyl phosphatidylcholine vesicles are described. The activation energies for incorporation of these several lipid-mimic type fluorescent probes have been measured. Results show that the activation energy is a function of the distance of the anthracene moiety (chromophore) from the polar end of the probe and the length of the acyl portion of the probe. An average insertion energy of 0.6 kcal/carbon is seen for these fatty acid probes. The activation energy of 1,6-diphenylhexatriene, a factor of 2 greater than that of 16-(9-anthroyloxy)palmitic acid, is consistent with locating 1,6-diphenylhexatriene in the middle of the bilayer.

Introduction

The incorporation of extrinsic fluorescent probes by model or real membranes is an ill-defined process. It is known that the final location of the probe within the bilayer is often dictated by the hydrophobic or hydrophilic character of the probe. This has been established by careful analysis of fluorescence emission and time-resolved fluorescence techniques. Some work has also been carried out on the measurement of the rate of incorporation of the probe. For example, interaction of 1-anilino-8-naphthalene sulfonate with erythrocyte membranes has been extensively studied in the last several years. A biphasic interaction was attributed to the presence of 'fast' and 'slow' sets of binding sites in erythrocyte membranes. That corresponded to interactions at the outside and diffusions into the membrane. However, only the fast

phase was observed with sonicated membranes and membrane proteins. The interaction was observed to be strongly pH-dependent and was sensitive to changes in ionic strength brought about by addition of NaCl [1].

Further investigations [2] were concerned with the fluorescent enhancement of 1-anilino-8-naphthalene sulfonate added to erythrocyte ghosts, at room temperature, in terms of 'fast', 'medium' and 'slow' phases. It was suggested that most 1-anilino-8-naphthalene sulfonate binding sites are similar on the molecular level. However, the sites on the outer side of the membrane always give a fast 1-anilino-8-naphthalene sulfonate response, whereas the response from sites within the permeability barrier may be fast, medium or slow depending on the state of the membrane.

Later work by Fortes and Hoffman [3] on 1-anilino-8-naphthalene sulfonate, showed that the slower process had a half-time of about 8 min, independent of 1-anilino-8-naphthalene sulfonate concentration, in contrast with the rate of interaction of 1-anilino-8-naphthalene sulfonate with erythrocyte ghosts under

---

Abbreviations: 2-AP, 2-(9-anthroyloxy)palmitic acid; 16-AP, 16-(9-anthroyloxy)palmitic acid; 2-AS, 2-(9-anthroyloxy)stearic acid; 12-AS, 12-(9-anthroyloxy)stearic acid; DPH, 1,6-diphenylhexatriene.

similar conditions where equilibrium was reached within a few seconds [1,2]. Fortes et al. [3] found that 1-anilino-8-naphthalene sulfonate was a permeant anion and a potent inhibitor of anion permeability in red cells. The inhibitory effects, regardless of the actual mechanisms involved, indicated that 1-anilino-8-naphthalene sulfonate and related compounds are not inert in their interactions with membranes. Hence, care must be excercised when interpreting observations made in the presence of a probe where the probe itself alters the characteristics of the membrane.

In a study of the microsomal drug metabolism and the interaction of fluorescent probes with microsomes at different temperatures, Lang et al. [4] observed that the fluorescent enhancement lasted about 4 min at 38°C in the case of 12-(9-anthroyloxy)stearic acid in microsomal suspensions as opposed to at least 35 min at 10°C.

Another probe that has been used extensively in labelling membranes is 1,6-diphenylhexatriene. Esko et al. [5] reported a rapid increase in fluorescence intensity as the dye was incorporated into the membrane. The uptake of the dye into the cells appeared to saturate after about 20 min. They reported apparent activation energies for membranes from choline and ethanolamine-supplemented cells of 7.7 and 8.7 kcal/mol, respectively.

Quenching studies of aromatic hydrocarbons have also been exploited to obtain information about the permeability of membrane-like systems [6—9]. Tsong [10] reported an apparent activation energy of 1-anilino-8-naphthalene sulfonate transport in dimyristoyl phosphatidylcholine of 240 kcal/mol in the first half of the transition and —96 kcal/mol at the second half. The time scale used was up to 60 s. The negative activation energy seems to be strange. However the author attributed that to the nonreproducibility of the results due to the slow fusion of the vesicles.

Pyrene binding to dimyristoyl phosphatidylcholine bilayers has been studied by Tsong [10]. Although the kinetics were complex, the half-time of the binding showed no abnormalities in the phase transition temperature of the phospholipid vesicles.

To gain more insight into the process of incorporation, the activation energies for incorporation of several lipid-mimic type fluorescent probes into dipalmitoyl phosphatidylcholine vesicles have been

measured. The results of this study are presented here.

Experimental

Dipalmitoyl phosphatidylcholine was obtained from Sigma Chemical Co. The fluorescent probes, 12-(9-anthroyloxy)stearic acid, 2-(9-anthroyloxy)-stearic acid, 16-(9-anthroyloxy)palmitic acid and 2-(9-anthroyloxy)palmitic acid were obtained from Molecular Probes, Inc. and used as received. 1,6-diphenylhexatriene was obtained from Aldrich Chemical Co. Water for the buffer solutions was deionized and then distilled over $KMnO_4$ to remove any traces of fluorescent impurities and millipore filtered. The structures of the probes are shown for clarity in Fig. 1.

The vesicles (minimum size) were prepared by the injection method [11] and were characterized by transmission electron microscopy. The vesicle diameters were found to range from 200 to 700 Å. All vesicle preparations were made immediately prior to the fluorescent measurement. The final vesicle suspension consisted of $1.7 \cdot 10^{-4}$ M phospholipid in a phosphate buffer with an acid salt concentration (NaH_2PO_4) of 0.012 M and pH 7.4.

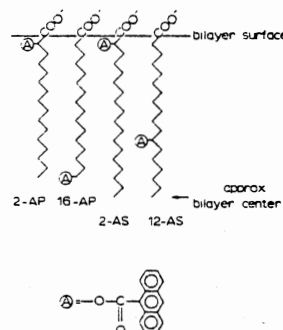The vesicle suspension in the phosphate buffer was stirred at approx. 5 Hz with a teflon coated stir-

Fig. 1. The n-anthroyloxy fluorophore structures as located in a biological membrane. The format is similar to that in Ref. 17 because of the clarity provided by such a presentation.

rer within a thermostatically controlled housing in the sample compartment of the fluorometer over the course of each experiment. Stirring of the suspension was found to be essential to the measurement of reproducible incorporation curves. A Bailey Instrument Co. thermocouple thermometer was used for temperature measurement. The jacket was thermostatically controlled sufficiently well that the maximum temperature excursion of the sample over the course of an individual incorporation measurement did not exceed ±0.1 °C.

Fluorescence measurements were made on a homebuilt fluorescence spectrometer with 0.45 meter excitation and emission monochromators (16 Å/mm reciprocal dispersion). The excitation source was a 500 watt xenon arc lamp and the detection system included a single photon counting apparatus. The entire fluorometer was automated using an Apple II Plus microcomputer.

The wavelength settings of the excitation and emission monochromators are given in Table I. These wavelengths were chosen such that the maximum intensity of the fluorescence was obtained with little or no interference from Raman bands associated with the H_2O solvent or the vesicles themselves. Raman emission proved to be of considerable relative strength at the low total emission intensities obtained. It was soon apparent, therefore, that emission filters would not be nearly selective enough. The band pass of the emission monochromator was typically 3.2 nm while that of the excitation monochromator was typically 2.4 nm.

The total emission intensity of the chromophore emission relative to the Raman scattering intensity was low primarily because the probes were used at a low total concentration. This concentration was

TABLE I

WAVELENGTH SETTINGS OF FLUOROMETER FOR DIFFERENT PROBES

Probe	Excitation (nm)	Emission (nm)
2-AP	363.5	442.5
16-AP	366	439
2-AS	362	446
12-AS	367	458
DPH	355	450

chosen so that the overall solution optical density at the λ_{max} of the probe was less than 0.04 per cm to eliminate problems associated with the inner filter effect. For example, the molar ratio of the probe to lipid concentration in case of 2-(9-anthroyloxy)palmitic acid was 0.035.

To monitor the rate of incorporation of the probe by the vesicles, a small amount (1.5 μl) of a concentrated solution of the probe in tetrahydrofuran was injected into 2.5 ml of vesicle suspension. The increase in the fluorescence intensity was then recorded by the photon-counting system as a function of time with a strip chart recorder. Some typical incorporation curves are shown in Fig. 2. The intensity is seen to increase exponentially and level off at long times or approach a slightly increasing but linear intensity with time. The linear long-time plot was extrapolated back to earlier times. From this straight line, a fluorescence intensity difference (extrapolated minus observed) was plotted against time to obtain the logarithmic incorporation curves shown in Fig. 3. Since these are so clearly logarithmic in functional form, it is clear that the incorporation process on this scale (i.e. $t \geqslant 1$ min) is first order. Fig. 3 does not
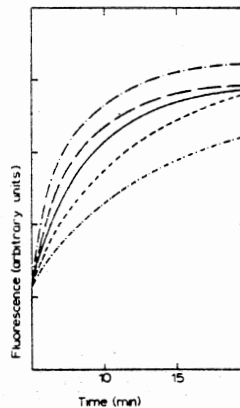

Fig. 2. The relative fluorescence intensity of 12-(9-anthroyloxy)stearic acid, measured at different temperatures of incorporation into dipalmitoyl phosphatidylcholine vesicles, as a function of incorporation time. ········, temp. 20°C; -----, temp. 25°C; ———, temp 35°C; – – –, temp. 38.5°C; – · –, temp. 40.5°C.
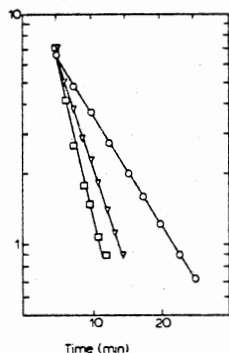
Fig. 3. Semi-logarithmic plots of the fluorescence intensity difference in the case of 12-(9-anthroyloxy)stearic acid incorporated into dipalmitoyl phosphatidylcholine vesicles at different temperatures, as a function of incorporation time. o————o, temp. 20°C; ▽————▽, temp. 35°C; □————□, temp. 40.5°C.

Fig. 4. Arrhenius plots of the rate constants for incorporation of 2-(9-anthroyloxy)palmitic acid (□————□); 12-(9-anthroyloxy)stearic acid (o————o); 1,6-diphenylhexatriene (△————△) into dipalmitoyl phosphatidylcholine vesicles.

show the data for times less than 5 min. The data was unreliable over the first 1–2 min because of turbulence in the mixing of the injected 1.5 μl of probe in tetrahydrofuran into the bulk solution. It should be noted that control studies in which the experiments were repeated but without vesicles present resulted in Arrhenius plots with slopes of approx. 0 K (no activation energies).

Results and Discussion

Arrhenius plots of the rate constants for incorporation of three different probes (for example purposes) are shown in Fig. 4. The activation energies for the incorporation process for the five probes studied is summarized in Table II. The data reveal much about the energetics of the incorporation process at temperatures below the gel-to-liquid crystal phase transition. At temperatures above the phase transition, the incorporation was essentially instantaneous for the time scale of these experiments.

Examination of the data shown in Table II reveal the following. The insertion energy is lowest when the anthracene moiety (the chromophore) is nearest the polar end of the probe. Thus, the insertion energies for 2-(9-anthroyloxy)stearic acid and 2-(9-an-
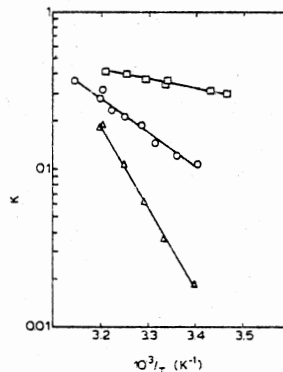
throyloxy)palmitic acid (5 and 2.6 kcal, respectively) are much lower than the insertion energies for probes in which the chromophore is well removed from the polar head group, as in 16-(9-anthroyloxy)palmitic acid and 12-(9-anthroyloxy)stearic acid (insertion energies of 12 and 10 kcal, respectively). This gives implicit credibility to the accepted idea that these probes align themselves with the lipids in the bilayer (as opposed to resting on the surface, for example). As further confirmation of the above, it is noteworthy that the insertion energy for 12-(9-anthroyloxy)stearic acid is lower than that for 16-(9-anthroyloxy)palmitic acid, although by only 2 kcal.

From this data it can be concluded that moving the chromophore 14 carbons down the lipid chain (16 vs. 2)-(9-anthroyloxy)palmitic acids increases the

TABLE II

CALCULATED ACTIVATION ENERGIES

Probe	E_{act} (kcal)
2-AP	2.6 ± 0.3
16-AP	12 ± 1
2-AS	5 ± 1
12-AS	10 ± 1
DPH	23 ± 2

100

insertion energy by about 0.7 kcal per carbon. A similar trend is seen when the insertion energies for 12 and 2-(9-anthroyloxy)stearic acids are compared. In that case, the energy increases by about 0.5 kcal per carbon. These two figures are well within experimental error of each other.

There remains, however, one discrepancy to be explained. That is the difference in insertion energies between 2-(9-anthroyloxy)palmitic acid (2.6 kcal) and 2-(9-anthroyloxy)stearic acid (5 kcal). 2-(9-anthroyloxy)stearic acid has a lipid chain two carbons longer than 2-(9-anthroyloxy)palmitic acid. This fact must account for at least some of the difference. Such a comparison of chain lengths cannot be made between the 12-(9-anthroyloxy)stearic acid and the 16-(9-anthroyloxy)palmitic acid because clearly the position of the chromophore is the dominant cause of the high or low insertion energy.

Finally, the above conditions shed some light on the result obtained for 1,6-diphenylhexatriene. The insertion energy for 1,6-diphenylhexatriene is a factor of 2 greater than that for 16-(9-anthroyloxy)palmitic acid. This is consistent with locating 1,6-diphenylhexatriene in the middle of the bilayer. It is tempting to conclude that 1,6-diphenylhexatriene must end up parallel to the plane of the bilayer since it requires only about 12 kcal to move an anthracene moiety to the vicinity of the middle of the bilayer (i.e. the case of 16-(9-anthroyloxy)palmitic acid) and 1,6-diphenylhexatriene is not so much larger than anthracene.

These results are tedious to obtain with any degree of reproducibility but provide data not available by any other methods. To wit, these results are now being used to obtain data on the occlusion of membrane surfaces by glycoproteins (Carraway, K., Rockley, M.G. and Najjar, D.S., unpublished results). This is information that cannot be obtained by fluorescence depolarization studies, for instance. Further-

more, the results reported here verify the binding constant efficiency data obtained in separate studies of the uptake and fluorescence quenching of n-(9-anthroyloxy) fatty acid probes [12,13].

Acknowledgements

References

1 Freedman, R.B. and Radda, G.K. (1969) FEBS Lett. 3, 150−152
2 Radda, G.K. and Smith, D.S. (1973) Biochim. Biophys. Acta 318, 197−204
3 Fortes, G.P.A. and Hoffman, J.F. (1974) J. Membrane. Biol. 16, 79−100
4 Lang, M., Koivusaari, U. and Hietanen, E. (1978) Biochim. Biophys. Acta 539, 195−208
5 Esko, J.D., Gilmore, J.R. and Glaser, M. (1977) Biochemistry 16, 1881−1890
6 Gratzel, M. and Thomas, J.K. (1973) J. Am. Chem. Soc. 95, 6885−6889
7 Infelta, P.P., Gratzel, M. and Thomas, J.K. (1974) J. Phys. Chem. 78, 190−195
8 Chen, M., Gratzel, M. and Thomas, J.K. (1974) Chem. Phys. Lett. 24, 65−68
9 Pownall, H. and Smith, L. (1974) Biochemistry 13, 2594−2597
10 Tsong, T.Y. (1975) Biochemistry 14, 5409−5414
11 Kremer, J.M.H., Van den Esker, M.W.J., Pathmamanoharan, C. and Wiersema, H. (1977) Biochemistry 16, 3932−3935
12 Haigh, E.A., Thulborn, K.R., Nichol, L.W. and Sawyer, W.H. (1978) Aust. J. Biol. Sci. 31, 447−457
13 Thulborn, K.R. and Sawyer, W.H. (1978) Biochim. Biophys. Acta 511, 125−140

VITA [2]

Dada Salim Najjar

Candidate for the Degree of

Doctor of Philosophy

Thesis: A PHOTODYNAMIC CHARACTERIZATION OF EXTRINSIC
          MEMBRANE PROBES

Major Field: Chemistry

Biographical:

   Personal Data: Born in Bishmezzine, El-Koura, North
       Lebanon, on February 11, 1956.   One of four
       children of Salim Mitri Najjar and Wahibie
       Shaheen Najjar.

   Education: Graduated from Bishmezzine High School,
       Bishmezzine, Lebanon in 1972;   attended National
       Protestant College, Beirut, in 1973; and the
       American University of Beirut, Beirut 1973-1975;
       received Bachelor of Science degree in Chemistry
       from Oklahoma State University in May, 1977;
       completed requirements for the Doctor of Philosophy
       degree at Oklahoma State University in July, 1981.

   Professional Experience: Graduate Teaching Assistant,
       Oklahoma State University, 1976-1980; National
       Institute of Health Research Assistant, Oklahoma
       State University, 1978-1981; Gulf Fellow and
       Du-pont Fellow, Oklahoma State University, summer
       1978; Oklahoma State University research support,
       summer 1980.

   Membership in Honorary and Professional Societies:
       Member of Phi Lambda Upsilon, Honorary Chemical
       Society; member of the American Chemical Society.